In presenting this dissertation as a partial fulfillment of the requirements for an advanced degree from Emory University, I agree that the Library of the University shall make it available for inspection and circulation in accordance with its regulations governing materials of this type. I agree that permission to copy from, or to publish, this dissertation may be granted by the professor under whose direction it was written, in his/her absence, by the Dean of the Graduate School when such copying or publication is solely for scholarly purposes and does not involve potential financial gain. It is understood that any copying from, or publication of, this dissertation which involves potential financial gain will not be allowed without written permission.

_____

John H. Shugart

Properties and Synthesis of Red-Ox Active Proline Mimics By

John H. Shugart

Doctor of Philosophy

Department of Chemistry

Vincent P. Conticello

Adviser

P. Barry Ryan

Committee Member

Dale Edmondson

Committee Member

Accepted:

Lisa A. Tedesco, Ph.D.

Dean of the Graduate School

Date

Properties and Synthesis of Red-Ox Active Proline Mimics

By

John H. Shugart

B.S., Berry College, 2000

M.S., Emory University, 2003

Adviser: Vincent P. Conticello, Ph.D.

An Abstract of

A dissertation submitted to the Faculty of the Graduate

School of Emory University in partial fulfillment

of the requirements for the degree of

Doctor of Philosophy

Department of Chemistry

2008

ABSTRACT

A balance of factors composed of sterics, nonbonded interactions, and stereoelectronics account for the structural preferences seen in individual amino acids, and subsequently in the global structure of peptides and proteins. These factors in the amino acid proline present a method to potentially control macromolecular structure. Thiazolidine-4-carboxylic acid presents a pseudoproline with Red-Ox potential that can be stereoselectively oxidized. In this study the conformational dynamics of the stereoselective oxidation of molecular systems containing thiazolidine-4-carboxylic acid are explored and evaluated for their potential utility as a Red-Ox switch for the self assembly of peptides. Ultimately, it was determined that through stereoselective oxidation the conformational properties of the proline-like thiazolidine-4-carboxylic acid can be modulated to select for different conformational preferences.

Properties and Synthesis of Red-Ox Active Proline Mimics

By

John H. Shugart

B.S., Berry College, 2000

M.S., Emory University, 2003

Adviser: Vincent P. Conticello, Ph.D.

A dissertation submitted to the Faculty of the Graduate

School of Emory University in partial fulfillment

of the requirements for the degree of

Doctor of Philosophy

Department of Chemistry

2008

ACKNOWLEDGEMENT

First, I would like to thank my adviser, Dr. Vincent Paul Conticello, for his support and guidance, particularly in navigating the bureaucratic juggernaut that is the Emory chemistry department. Without his support this science and thesis would not have come to be, and I would not have had the opportunity to finish what I started many years ago. Thank you.

I also would like to thank my committee members, Dr. Edmondson and Dr. Ryan, for their support, insight, and interest in my career. I have found their suggestions to be both insightful and helpful. Also I would like to thank all my lab members, both past and present, for their friendships and fellowship; specifically Holly Carpenter, Steven Dublin, Wookhyun Kim, Melissa Patterson as well as old friends Marty Jacquez and Shannon Coleman.

Additionally I would like to thank the support staff at Emory including Dr. Shaoxiong Wu and Dr. Bing Wang in the Emory University NMR Research Center. Both Shaoxiong and Bing have been very supportive in setting up experiments and obtaining NMR data, and also with helping me with my Chinese. I also would like to thank Dr. Kenneth Hardcastle for his work in obtaining X-ray crystallographic data. Ken's contribution to this thesis adds another level of insight to this science. I would also like to acknowledge Dr. Robert P. Apkarian as we all grieved at his passing, and the reminder at how fleeting life is.

On a personal level I would like to make note of several people who have helped me on my journey through life. To “Coach”, Dr. E. Pierce Arant, his life affected mine for years before I even realized it. I count myself luck to have known the man, and to have sung at his funeral. Coach’s massive influence upon countless lives is a testament to the power that educators can have on their students. Additionally I would like to acknowledge my teachers Dr. Gary Breton and Dr. Larry McRae; who are now both my friends and colleagues.

To Jason M. Martin and Scott Love Percy, many people do not have one lifelong friend. I have been blessed with two. Thank you for opening your homes to me and making me part of y’all’s families. Thank you for your friendship.

To my darling wife Beth: I love you. Finally, to my mother, Julia Merrie Ball Shugart, and my grandmother, Edith Gardener Ball, their lives shaped the boy that I was, and their deaths made me the man that I am.

Table of Contents

List of Figures

CHAPTER 1.

CHAPTER 2.

CHAPTER 3.

List of Tables

List of Schemes

Chapter 1

Introduction

Introduction

The first isolation of proline was performed by Emil Fischer in 1901 via a complex isolation procedure from the natural source casein.[1] Although reported as a minor constituent of the various compounds isolated by Fischer from casein, proline has been shown to have a major impact upon both peptide and protein structure.[2] The presence of proline in an amino acid sequence often precludes a change in secondary structure as well as the fact that certain structural components of peptides and proteins contain significant amounts of proline.[3, 4] However, due to its imino acid structure proline is limited in its ability to participate in both alpha helix and beta sheet secondary structures.[5] Thus the presence of proline, as well as its absence in a primary sequence, can provide insight into peptide and protein structure.[2, 4, 6] These empirical results can be explained by the fact that proline has several unique structural properties compared to other amino acids. Due to the presence of a secondary amine, as compared to the primary amines present in all other amino acids, proline's main chain torsion angles are extremely limited. Of particular interest is the fact that 99.95 % of amino acids exist in the trans amide bond configuration while the imino acid proline exists in a 94 % trans/ 6 % cis amide bond configuration in peptides and proteins.[7] The trans/ cis rotameric isomerization of proline can be seen in Figure 1, with the atoms of the pyrrolidine rings labeled appropriately in greek letters. The pyrrolidine ring plays an important role in proline's conformation considerations. Five membered rings traditionally adopt an envelope confirmation to relieve steric and torsional strain. In the case of proline this envelope confirmation can exist in a C^{γ} exo ring pucker, where the envelope confirmation

has the C^{γ} carbon puckered away (trans) from the carboxylate group of the C^{α} carbon as seen in Figure 2. Conversely, the C^{γ} endo ring pucker configuration exists with the C^{γ} carbon puckered toward (cis) to the carboxylate group of the C^{α} carbon. Figure 2 shows the interchange between the two ring pucker forms. Additionally, proline is extremely limited in its ability to form hydrogen bonds due to the pyrrolidine nitrogen being tertiary when involved in main chain peptide bonds. These unique properties account for proline's prevalence in such biochemical structures as collagen's polyproline II (PPII) triple helical strands[8], elastin's type II beta turns[9], alpha helix kinks[5] and are integral to their structure and function.

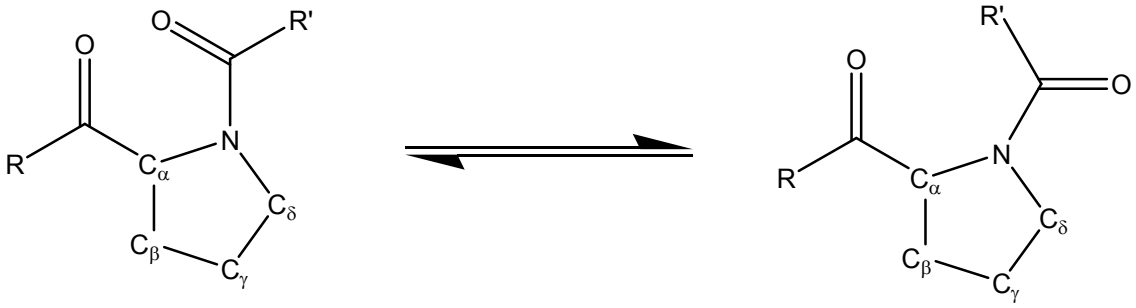

Trans Cis

Figure 1. Cis-Trans amide bond isomerization of the imino acid proline with appropriately labeled pyrrolidine ring carbons.

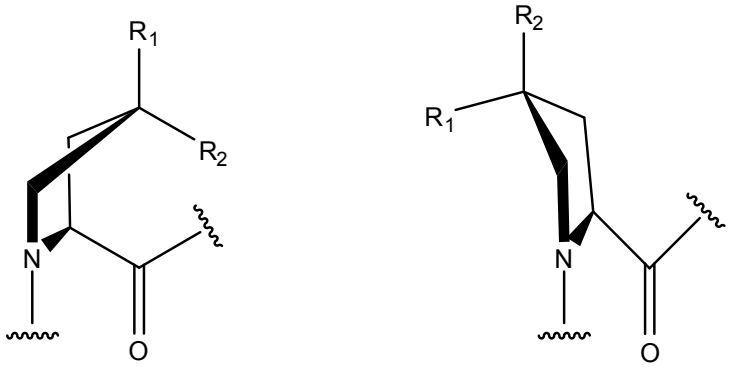

C^{γ}-endo C^{γ}-exo

Figure 2. Structures of C^{γ}-endo and C^{γ}-exo pyrrolidine ring puckers.

The cis form of most amino acids is disfavored because of steric interactions of the alpha carbon's hydrogen and the loss of the favorable electrostatic interactions between the carbonyl O_i and C'_{i+1}. In proline these unfavorable interactions are present in both the cis and trans form and there is a change in the electrostatic interactions of the O_i--- C'_{i+1} bond that makes it less favorable.[10] In small peptides an equivalent mixture of the cis and trans form of the Xaa-Pro peptide bond are found because they are almost isoenergetic with a slight favoring of the trans form.[11] However, in proteins the cis or the trans form of the Xaa-Pro peptide bond is set by the overwhelming interactions with neighboring groups such that only the cis or only the trans form is found. The cis/trans isomerization of proline during protein folding is an important rate determining step. There is a high energy barrier (~20kcal/mol) limiting the rate of the interconversion.[12] This can be seen in the well studied RNAse A. When an essential cysteine Cys93 was mutated to an alanine (Ala93), the mutant RNAse still had the Tyr92-Ala93 peptide group in the cis form in the folded protein[13] which is surprising when less then 1% of normal amino acids adopt this orientation.[10] This indicates that the correct orientation of the peptide bond (ω) often dictates the secondary structure.

In order to accommodate the phi and psi angles of the restricted proline in many important biochemical structures there is a pairing between proline and glycine in the amino acid sequence. This pairing between the highly restricted proline and the conformationally promiscuous glycine enables confirmations outside of the range of other amino acids. A prime example of the Pro-Gly cooperativity is in the presence of type II beta turns as seen in Figure 3. The confirmation of the type II beta turn is made possible by the favored ϕ and ψ dihedral angles of the proline (normally ϕ= -60, ψ =

120) and the flexibility of the glycine.[14] Another important Pro-Gly structure is the polyproline II helix (PPII) formed when neighboring residues adopt the phi psi dihedral angles of roughly (-75 and 150) with the trans isomer of the peptide bond (ω).[15] Such structures play an imperative role in many proteins allowing them to fold into compact shapes and driving their three dimensional structure.

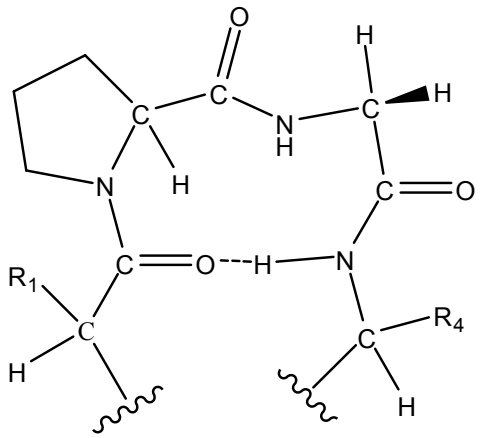

Figure 3. Structure and hydrogen bonding pattern of a prolyl type II Beta turn

The beta turn and PPII discussed previously are types of structures in native peptides and proteins that contain the Pro-Gly sequence motif. In Table 1 is a list of modular domains of fibrous proteins that contain the repeat sequences of the Pro-Gly pattern. All of these proteins are proline rich as their modular domains are potentially repeated several hundred times with beta turns and PPII conformations contained in the protein structure; hence, the importance of prolines configurational contribution to the function and structure of each domain. Elastin is the most prevalent of the proteins in Table 1 as the elastic properties of the protein make it an integral part of mammalian connective tissue particularly at such sites as the aorta, nuchal ligament, and lungs.[16] In each of the repeats of elastin proline, and subsequently pro-gly, make up a large portion

of the repeat domain. This is also the case in glutenin HMW subunits which are responsible for the viscoelastic properties of wheat dough due to their propensity to form high molecular mass aggregates. [17] Also, the same properties exist in flagelliform silk, dragline silk[18], mussel byssus, as well as resilin. Resilin, found in arthropods, was reported to be the most efficient elastic protein isolated.[19] All of these peptides have possible applications in drug delivery, protein isolation, as well as biomedical engineering, but all of them rely heavily upon proline for their unique physical properties and structure. [20, 21]

Collagen

However, of all of the native substances containing the pro-gly sequence motif arguably the most important is that of collagen. Collagen is the major proteinaceous component of the extracellular matrix (ECM) of vertebrates, and plays a major role in the composition of bones, skin, liver, teeth, and cartilage.[22] The fibrous collagen protein has a very high tensile strength. This property coupled with its ubiquitous presence in biological systems makes collagen an extremely interesting target of study. In the 1950's the three dimensional structure of collagen was determined to be a right handed triple helix consisting of the parallel coiling of three left handed polyproline II-type (PPII) strands around a common axis.[23, 24] Subsequently, many different classes and types of collagen have been discovered with all containing a typical triple-helical domain formed by the three independent peptide strands with most of the different classes being fiber-forming. Several different types of collagen have a lengthy uninterrupted repeat domain

Protein	Repeat Units
Elastin	Val-**Pro-Gly**-Gly Val-**Pro-Gly**-Val-Gly Ala-**Pro-Gly**-Val-Gly-Val Val-**Pro-Gly**-Phe-Gly-Val-Gly-Ala-Gly
Flagelliform Silk	Gly-**Pro-Gly**-Gly-Xaa (Xaa = Ser, Tyr, Ala, Val)
Dragline Silk	Gly-**Pro-Gly**-Gln-Gln Gly-**Pro-Gly**-Gly-Tyr Gly-Gly-Tyr-Gly-**Pro-Gly**-Ser
Glutenin HMW subunits	Gln-**Pro-Gly**-Gln-Gly-Gln
Resilin	Gly-Gly-Arg-Pro-Ser-Asp-Ser-Tyr-Gly-Ala-**Pro-Gly**-Gly-Gly-Asn Gly-Tyr-Ser-Gly-Gly-Arg-**Pro-Gly**-Gly-Gln-Asp-Leu-Gly
Mussel Byssus	Gly-**Pro-Gly**-Gly-Gly

Table 1. Repeat sequences of native protein-based elastomeric materials containing the "Pro-Gly" sequence motif.[25]

that in addition to forming a triplex helix also form a large globular domain at the C and N-terminus.[20] In most native collagens every third amino acid residue is the conformationally flexible glycine who's small size is integral to the tight packing of the collagen triple helix. The other amino acid components in the collagen triple helix consist of a triad repeat of 'Xaa-Yaa-Gly' with glycine being conserved throughout the sequence. The Xaa and Yaa positions of the triad repeat are initially both held by proline; however, the proline in the Yaa position is subjected to a post translational modification by the enzyme prolyl-4-hydroxylase (P4H). This stereoselective oxidation of proline by prolyl-4-hydroxylase installs a hydroxyl group on the C^{γ} carbon of the pyrrolidine ring forms (2S, 4R)-4-hydroxyproline (Hyp) which is essential to the stability of the collagen structure.[26]

The amino acid (2S, 4R)-4-hydroxyproline was isolated shortly after the discovery of proline. In 1902 Emil Fischer published a paper announcing the discovery of the amino acid oxypyrrolidine-alpha-carboxylic acid from the hydrolysate of gelatin. A short time later Fischer changed the name of the designation of his earlier discovery pyrrolidine-alpha-carboxylic acid to the now common name proline, and correspondingly changed the name of oxypyrrolidine-alpha-carboxylic acid to hydroxyproline. [27] It was not until 1913 that Leuchs and Brewster determined the location of the hydroxyl group on the pyrrolidine ring to occur at the C4 position.[28] Subsequent experiments investigating hydroxyproline produced interesting results such as the embryonic morbidity of mice and *Caenorhabditis elegans* (roundworm) due to the lack of the P4H enzyme, as well as a deficiency in the production of 4-hydroxyproline leading to scurvy. The inability to generate hydroxyproline in the collagen matrix weakens the collagen superstructure

rendering the extracellular matrix unstable, and subsequently compromising the cellular structure of biological organisms.

Of corresponding interest is why (2S, 4R)-4-hydroxyproline is essential in forming a stable extracellular matrix in fibular collagen. Initially it was thought that the importance of 4-hydroxyproline to collagen stability was due to its role in a series of complex intermolecular and intramolecular hydrogen bonding patters, where 4-hydroxyproline acted as a mediator between both water molecules and the individual strands of the collagen triple helix.[29, 30] Raines and coworkers went on to prove that stereoelectronic effects play an immensely important role in explaining the stability imparted by 4-hydroxyproline upon collagen. In a classic experiment Raines studied the differences in physical properties between a collagen repeat containing a native (Pro-Hyp-Gly) amino acid triad and a synthetic collagen that replaced the 4-hydroxyproline with 4-fluoroproline (Flp) to produce a (Pro-Flp-Gly) triad repeat. The results of the study showed that the presence of the electronegative fluorine in the same stereochemical configuration as that of native 4-hydroxyproline enhanced the overall stability of the synthetic collagen over that of the native collagen. Due to fluorine's inability to accommodate a hydrogen bond and its extreme electronegativity it was concluded that the stereoelectronic effect from the presence of the fluorine was responsible for the stability of the synthetic collagen. Thus proving that the electronegativity of the oxygen in the hydroxyl group of 4-hydroxyproline plays a major role in the stability of native collagen, while the hydrogen bonding capability of 4-hydroxyproline played a lesser role than previously thought. [31] As initial steps in these fascinating experiments Raines and coworkers synthesized model compounds of proline and pseudoprolines in order to better

study their possible role in native and synthetic collagen. The prolyl model compounds produced efficient results, and provided insight into the conformational preferences of the amide bond as well as the pyrrolidine ring pucker of the proline analogues, and thus provided a quick and efficient route toward exploring the behavior of proline and pseudoproline in peptides and proteins.[32, 33]

Model Studies of Proline, 4-Hydroxyproline, and 4-Fluoroproline

Investigations of N-acetylproline methyl esters derivatives have proven an effective model system to assess and determine conformational preferences of pyrrolidine rings in proline and pseudoprolines.[32-35] A number of studies of compounds of this type have been explored, and given insight into preferences for cis-trans amide bond isomerization through the study of crystal structures as well as a variety of nuclear magnetic resonance studies. Proline's cis-trans amide bond rotameric isomerization plays an important role in the rate determining steps of protein folding as well as global protein structure. Reviewed in [13] Correspondingly information from these studies can also give insight in to the C^{γ} endo or C^{γ} exo pyrrolidine ring pucker in the context of the observation of the gauche effect. The gauche effect is an electrostatic phenomenon that occurs when a gauche confirmer is more stable and thus preferred over the traditionally more stable anti configuration. The gauche effect is most frequently observed when two electronegative groups exist in a vicinal orientation to one another. The classic example of the gauche effect is that of 1, 2 difluoroethane with the gauche confirmer (2.4 kJ/mole) being more stable than anti confirmer (3.4 kJ/mole) due to the electronic effect of

hyperconjugation. In these cases, such as 1,2-difluoroethane, electronic considerations take precedence over steric effects.

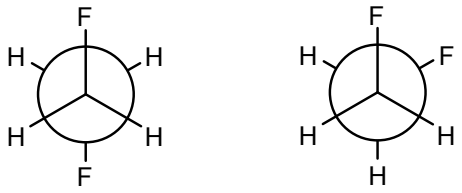

Anti Gauche

Figure 4. Newman projections of the Anti and Gauche configurations of 1,2-Difluoroethane

It is these subtle stereoelectronic effects that dictate the confirmations of the pyrrolidine ring in proline, and thus the cumulative effects of many of these interactions working in concert facilitate protein folding, structure, and function. The appeal of studying a simple model compound that can produce results similar to those seen in large peptides and protein is quite advantageous. Initial studies of N-acetylproline methyl esters derivatives, in the context of possible use in collagen related peptides, were performed by Raines and coworkers in 1994.[33] In this study native proline was fitted with an acetyl group on the prolyl nitrogen as well as a methyl ester functionality on the carboxyl group to produce compound **1**. The methyl ester moiety was used to eliminate intramolecular hydrogen bonding as the free acid of proline, as well as the carboxy amide, are prone to alter molecular structure to accommodate hydrogen bonds.[36-38] Results from these free acid and carboxy-amide model systems can give a skewed picture of molecules structure rather than how it would appear in peptides. [36-38] The acetyl group on the prolyl nitrogen closely mimics the natural amino acid glycine, but offers easier

synthetic access as well as simplified spectra. A crystal structure of the compound was obtained and showed the structure to form a cis amide bond. This was observed in conjunction with a C^{γ}-endo configuration of the pyrrolidine ring, in this configuration the C^{γ} carbon lies above the plane of the amide bond as seen in Figure 2. These results were consistent with those observed for proline, since proline is known to adopt a cis amide bond structure in certain biochemical structures.[13, 39] This structure was used as a reference point for further experimentation in this first publication as well as in subsequent ones.

To continue the exploration of stereoelectronic effects on pseudoprolines Raines synthesized the N-acetyl/ methyl ester model compounds of both (2S, 4R)-hydroxyproline (**2**) and (2S, 4R)-fluoroproline (**3**). Both compounds were studied in the same manner as the N-acetylproline methyl ester (**1**). Crystal structures of the two compounds show that in contrast to the native proline (**1**) they both possess trans amide bonds and a C^{γ} exo pyrrolidine configurations. In the C^{γ} exo pyrrolidine configuration the C^{γ} carbon lies below the plane of the amide bond as seen in Figure 2. Both of the electronegative groups in **2** and **3** adopt an axial orientation in the pyrrolidine ring. This result is consistent with the most stable configuration of polar groups in the ribose rings of nucleosides. [40] Additionally the structure of the pyrrolidine ring is affected by the electronegative group by decreasing the bond lengths between the C^{γ}–C^{β}-carbons and C^{γ}–C^{δ}-carbons from the values observed in native proline model with the largest decrease in the C^{γ}–C^{β} bond. In the fluoroproline derivative there was also a shortening of the C^{β}–C^{α}-carbon bond; however, this was not observed in the prolyl or hydroxyproline model compound.[33] Of additional interest both structures of the compounds **2** and **3** are

consistent with an increase in pyramidalization in the pyrrolidine nitrogen SP^3 character compared to that of proline (**1**). This decrease in tetrahedral character of the pyrrolidine nitrogen is presumably due to presence of the electron withdrawing character of the hydroxyl and fluorine groups. The degree of pyramidalization of the nitrogen was consistent with the inductive effects of the corresponding groups with a trend of **3** > **2** > **1** for each respective compound. This effect presumably reduces the barrier to cis-trans amide bond isomerization allowing for easier conversion between the two forms.[33]

In following publications Raines explores the dynamics of the three compounds via a variety of spectroscopic methods as well as pK_a measurements. The observed pK_a's of proline (pK_a = 10.8), 4-hydroxyproline (pK_a = 9.68), and 4-fluoroproline (pK_a = 9.23) [32] produce the anticipated trend from the corresponding electronegativity values of atoms hydrogen, oxygen, and fluorine found at the C^{γ} position. That the trend of increasing acidity in accordance with increasing electronegativity shows the inductive effects of the electronegative atom at the C^{γ} position of the pyrrolidine ring can be sensed through the σ-bond scaffold of the molecule to increase the acidity of the carboxylic acid. This indicates that the electronegativity of atoms on the ring can have a profound effect throughout the molecule. The electronegativity effect was also observed in infrared spectra via amide vibrational modes where the molecules had a bond order of **1** < **2** < **3** with respective values of 1658.99, 1660.92, and 1664.78 cm^{-1} in dioxane. [32] Additionally spectroscopic study of 1D proton and 2D NOE NMR were used to identify and assign peaks observed from the rotameric effect of the prolyl amide bond. These experiments revealed the dynamic cis-trans ratio of the prolyl amide of each of the model compounds with their values respectively being **1** (Pro, $K_{trans/cis}$ = 3.0), **3** (Flp, $K_{trans/cis}$ =

4.0), **12 (**flp, $K_{trans/cis}$ = 1.2). [34, 41, 42] These values show a preference in each of the prolyl compounds for the trans form of amide bond in solution with an electronegative group in the R configuration at the C^{γ} position of the ring enhancing the preference for the trans amide bond. These results also introduce for the first time an electronegative substituent in the S configuration at the C^{γ} position as seen in (2S, 4S)-fluoroproline (**12**).[41] While electronegative groups in the R configuration at the C^{γ} position select for the pyrrolidine exo ring pucker; conversely electronegative groups in the S configuration of the C^{γ} position select for the endo ring pucker. Concurrently, the endo ring pucker also lessens the preference for the trans amide bond in prolyl groups hence the low selectivity seen in the $K_{trans/cis}$ value for (2S, 4S)-fluoroproline. The native proline analogue **1** had a mild preferences for the endo configuration with all of the results from these dynamic studies determined via coupling constants from 1D proton NMR.[34] These findings were also supported by computational data from exploring the energetic preference of the configurations of the prolyl analogues in the gas phase. Most intriguing from these findings was that hyperconjugation aids in the perturbation of the structure of the fluorinated proline models with an increase in the C^{γ} - F bond due to hyperconjugation. The most pronounced effects are seen in **3** (4R-Flp) in the exo configuration with a calculated bond value of 1.4121 Å, and 1.4036 Å in the endo ring pucker. Conversely, in **12** (4S-flp) the bond lengths are reversed with the exo value being calculated at 1.4003 Å and the longer endo value 1.4105 Å. Thus a mild energetic release in steric conflict is observed due the bond elongation in the fluorinated proline's favored configuration due to hyperconjugation.[34]

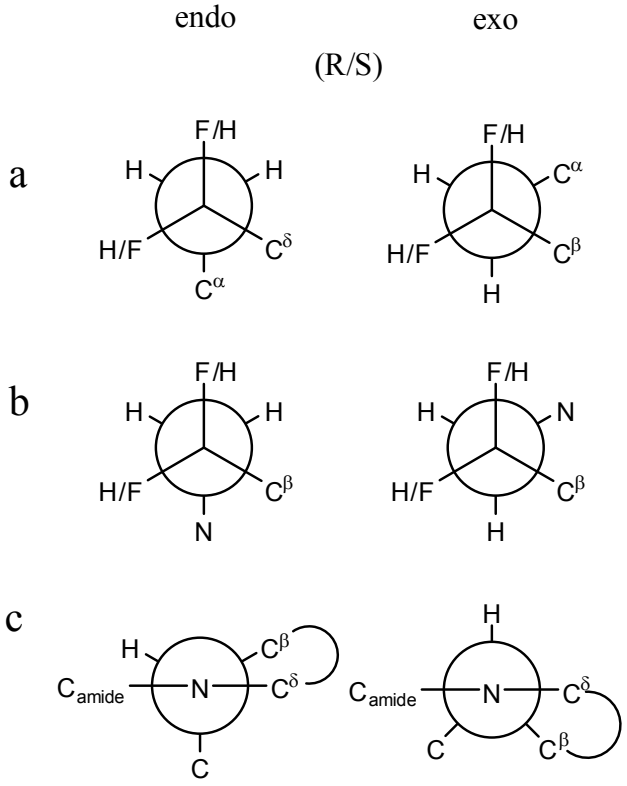

Figure 5. Newman projection of the endo and exo conformations of the proline containing model compounds (4R-Flp/4S-Flp) about the (a) C^{γ}-C^{β}, (b) C^{γ}-C^{δ} and (c) N-C^{α} bond axis. Each dihedral angle is shown in the fully staggered conformation.[34]

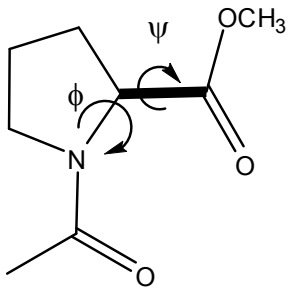

Figure 6. Structure of proline showing the phi and psi bonds. [34]

All of these configurational preferences (endo vs. exo) of the proline model systems ultimately are dictated by subtle stereoelectronic effects regarding an atoms orientation and electronegativity. Specifically the pyrrolidine ring pucker is determined by the gauche effect, or the tendency of molecules to adopt the confirmation with the maximum number of gauche orientations between vicinal electronegative atoms. In Figure 5 are Newman projections of three bond axis (a: C^{γ} - C^{β}; b: C^{γ} - C^{δ}; c: N - C^{α}) with each correspond configuration under a heading for the endo or exo pyrrolidine ring pucker of the epimeric pair of 4-fluoroproline. In each of the preferred configurations the electronegative atom (Fluorine or Nitrogen) orients itself anti to a hydrogen atom to be closer to a more electronegative atom such as carbon. A secondary effect alluded to earlier is that the anti configuration of the C^{γ} - F bond provides better orbital overlap between the anti C – H bond and the antibonding orbital of the C^{γ} - F bond. Although an idealized version of these bond angles is portrayed in Figure 6 the real bond angles, such as ϕ and ψ bond angels in Table 2, are substantially affected by such stereoelectronic effects. Although steric effects do play a role in the confirmation of the prolyl analogues the main structure is determined by stereoelectronic effects. As can be seen for the values of the ϕ and ψ bond angels in Table 2 compounds **2** and **3** have an exo ring pucker preference, and correspondingly a relatively small ϕ value compared to the native proline model. Molecules with the exo ring pucker also have a less negative ψ bond angel than its endo counterparts. Thus, it should be remembered that the interplay between the different stereoelectronic parameters is responsible for the structure of individual prolyl groups, and consequently the global conformational stability of peptide and protein structure. The ϕ and ψ bond angels are of particular importance as they play a major role

Compound	C^{γ} Ring Pucker	Amide bond	ϕ	ψ
1 (Pro)	Endo	Cis	-78.9	176.7
2 (Hyp)	Exo	Trans	-56.9	150.8
3 (Flp)	Exo	Trans	-55.0	140.5
4R (HypAc)	Exo	Trans	-58.2	142.0
5S (HypAc)	Endo	Cis	-73.9	-170.8
6 (Clp)	Exo	Trans	-56.0	147.5
7(Mop)	Exo	Trans	-58.1	147.7
8 (3-Hyp)	C^{β} exo/ twist	Trans	-79.5	163.7
9 (Azp)	Exo	Trans	--	--
10 (3-Flp) R	Exo (C^{β} endo)	Trans	-56.4	151.5
11 (3-flp) S	Endo (C^{β} exo)	Trans	-71.2	158.4

Table 2. Data from crystal structures of various proline and pseudoproline model compounds.

in the 'backbone' of proteins, and can give insight into the suitability of the model compounds potential use in synthetic peptides and proteins such as elastin or to be uses to create beta turns. In the case of these compounds they were being examined as possible replacements for the Yaa repeat in the collagen amino acid triad 'Xaa-Yaa-Gly' where the Yaa position is natively held by (2S, 4R)-4-hydroxyproline. Thus the model studies of the epimeric pair of fluoroprolines showed that **3** (4R-Flp) would be an intriguing replacement due to its similar configuration and properties to that of the native hydroxyproline (exo ring pucker, trans amide bond). While the epimeric form **12** (4S-flp) had properties that were opposite of those desired in a hydroxyproline isomer (endo ring pucker, cis amide bond). This was supported by the synthesis of three different synthetic collagen triads: $(Pro\text{-}Pro\text{-}Gly)_{10}$; $(Pro\text{-}Hyp\text{-}Gly)_{10}$; and $(Pro\text{-}Flp\text{-}Gly)_{10}$, and their subsequent study.[31] In a 1998 Nature paper the studies from the prolyl model

systems **1**, **2**, and **3** proved correct with the synthetic collagens showing an order of stability: $(Pro\text{-}Pro\text{-}Gly)_{10} < (Pro\text{-}Hyp\text{-}Gly)_{10} < (Pro\text{-}Flp\text{-}Gly)_{10}$ [31]. This experiment provided conclusive proof of the importance of stereoelectronic effects upon proline residues and their correlation to protein structure. It also proved the N-acetylprolyl methyl ester model systems as a viable method to probe proline structure, dynamics, electronics, and suitability toward specific roles in peptide structure. It should also be noted that although these were the first studies on such compounds in the prolyl model systems, that subsequent experiments continued with a variety of different substituents in the C^{γ} position of the pyrrolidine ring to probe proline structure.

C^{γ}-Oxygen substituted prolines

With these previous experiments in mind Raines continued similar studies on a variety of pseudoprolines with the next in the series being the acetylation of the hydroxyl group of 4-hydroxyproline. The experiments explored both R (**4**) and S (**5**) isomers of O-acetylated-4-hydroxyproline model compounds similar to those previously examined. Crystal structures for both compounds **4** and **5** were obtained with crystalline **4** having a C^{γ} exo pyrrolidine ring pucker and a trans amide bond configuration. [23] The epimeric form **5** had the inverse results with an endo C^{γ} configuration and cis amide bond. These results are consistent with the gauche effects as observed with previous epimeric pairs of prolyl model compounds (**3**, Flp and **12**, flp). The dihedral angles of **4** were found to be between the values of the hydroxyproline model compound **2** and those of the fluorinated proline **3** as seen in Table 2. Additionally, NMR studies were conducted upon both

compounds with insightful ^{13}C data gathered from each of the compounds. The chemical shift of ^{13}C NMR is greatly dependent upon electron density, and therefore an excellent measure of the how much electron density is being draw away from the C^{γ} carbon, subsequently providing an insightful assay as to the electronic properties needed to form the desired pyrrolidine ring pucker. A summary of this ^{13}C NMR data can be seen in Table 3.

Compound	δ
1	21.9 ppm
2	70.4 ppm
4	73.7 ppm
5	73.7 ppm

Table 3. $^{13}C^{\gamma}$ Chemical Shift (δ) of AcProOMe and proline derivatives[23]

The ^{13}C NMR values for **4** and **5** were found to be identical, and were comparable to that of 4-fluoroproline which had a chemical shift of 70.4. These values when compared to that of the native proline model, which has a chemical shift of 21.9, provide an efficient assay to determine if the electronegative substituent provides a sufficient dipole moment to create an endo/ exo ring pucker. Other proton NMR studies revealed the $K_{trans/cis} = 3.3$ for the R isomer **4**, and a $K_{trans/cis} = 1.6$ for the S isomer **5**.[23] These values are also consistent with those for native hydroxyproline and the S isomer of 4-fluoroproline **12**. [34, 41, 42] These values and properties point toward the R epimer as being an excellent candidate for incorporation into the Yaa position of the collagen triad to form a (Pro-AcHyp-Gly) repeat. The synthetic collagen in question was synthesized; however, its ability to form a hyperstable synthetic collagen, as in the case with fluoroproline **3**, was limited due to the steric considerations from the O-Acetyl group. It

should also be noted that attempts at measuring the bond order of the N-acetyl carbonyl group provided no discernable difference between the two isomers that were studied.

In an attempt to lessen the steric hindrance of the O-acetylation but still preserve the electronegativity of the hydroxy group in native 4-hydroxyproline a new model compound was synthesized. N-acetyl-(4R)-methoxyproline methyl ester (**7**, Mop) would preserve the stereoelectronics, but considerably reduce the steric bulk from the previously studied O-acetylated compound. The compound was crystallized and an X-ray structure was determined with the structure containing a C^{γ} exo ring pucker from gauche interactions between the pyrrolidine nitrogen and the methoxy oxygen. Also, the values for the ϕ and ψ bond angles, -58.1^{o} and 147.7^{o} respectively, are analogous to those seen in the model compounds of hydroxyproline and fluoroproline. The methoxy proline analogue has additional stereoelectronic considerations where there is interaction between the methoxy oxygen and the ester carbonyl carbon. The distance between the two atoms is 2.84 Angstroms with an angle of 94.6^{o}.[43] These values are indicative of a Burgi-Dunitz trajectory seen in nucleophilic attack of carbonyl group; however, this effect is also known to have properties of stabilization due to a favorable n to π^{*} interactions between the two groups. This type of effect typically leads to a trans amide bond, and that is what is observed in both the crystal structure as well as the solution phase proton NMR ($K_{trans/cis} = 6.7$ at 37 ^{o}C).[43] Upon incorporation into the collagen triad repeat at the Yaa position it was show that the collagen triad repeat with Mop (**7**) observed a slight increase in triple helical stability from that of native collagen.[43] This study was attempted to further clarify whether hydrogen bonding or stereoelectronics dictate the triple helical structure of collagen, and supports the theory

that stereoelectronics play a larger role in collagen stability. Analogous to the previous work are the studies of epimeric pair of 4-methyl proline (mep, **13,** 2S, 4R; Mep, **14,** 2S, 4S) where the ether linkage of Mop (**7**) had been removed to leave just the methyl groups in the 4 positions. In previous studies stereoelectronics were used to manipulate the pyrrolidine ring pucker and select for pseudoprolines that would be structurally advantageous to formation and stability of the collagen triple helix. The use of 4-methyl prolines was an attempt to manipulate the pyrrolidine ring pucker using steric considerations. This was indeed the case with computational results from (2S, 4R)-4-methyl proline (mep, **13**) adopting a C^{γ} endo ring pucker while (2S, 4S)-4-methyl proline (Mep, **14**) adopts a C^{γ} exo ring pucker.[44, 45] The results of these ring puckers is the opposite of those found with pseudoprolines that have the same stereochemical configuration. The steric effects of the methyl group can also select for the ring pucker of proline. In both cases the methyl group of both compounds adopts a pseudoequatorial conformation in the pyrrolidine ring to relive steric strain, and produce the observed ring pucker. Ultimately these steric effects had a negative effect upon the synthetic collagens that contained both mep (**13**) and Mep (**14**) by destabilizing the triple helix; and thus steric manipulation of the prolyl ring ultimately proved problematic when placed in the larger contest of a peptide structure.[44]

Polar groups at the C^{γ} position

Returning to the stereoelectronic effects that provided success with the fluorinated proline derivatives (2S, 4S)-4-chloroproline (clp, **15**), and (2S, 4R)-4-chloroproline (Clp, **6**) model compounds were explored. These compounds would have similar inductive effects to those observed in covalently bound fluorine ($F_F = 0.45$; $F_{OH} = 0.33$; $F_{Cl} = 0.42$)[46], and subsequently impart similar effects upon the structure of the pyrrolidine ring. Although Chlorine atoms are larger than Fluorine the steric effects should not approach those seen in the methylated or acetylated proline derivatives. Additionally, covalently bound chlorine has the ability to form hydrogen bonds, but it has only a slight capacity for the interaction and was attributed to be a nominal factor.[46] Attempts to crystallize clp **15** were unsuccessful; however, a crystal structure for Clp (**6**) was obtained showing a C^{γ} exo ring pucker as well as dihedral bond angles of $\phi = -56.0^{o}$ and $\psi = 147.5^{o}$.[47] These values are consistent with those seen in the stereochemically similar (2S, 4R)-4-fluoroproline (Flp, **3**) which also had properties that preorganized the prolyl structure for use in the Yaa position of synthetic collagens. This preorganization arises again from the stereochemistry of the R configuration of the chlorine on the proline ring, enabling the gauche effect to dictate the pyrroline ring pucker as well as the backbone dihedral angles. Clp (**6**) also has a high preference for the trans amide bond configuration due to a strong n to π^{*} interaction between the amide oxygen and the ester carbonyl carbon. The distance between the two atoms is 2.80 Angstroms with an angle of 94.1^{o}.[47] These values are consistent with a Burgi-Dunitz trajectory, and are know to stabilize trans amide bonds through n to π^{*} interactions. [34, 48-51] Proton NMR supported these results with a $K_{trans/cis}$

= 5.4 for Clp (**6**), while the value for clp (**15**) $K_{trans/cis}$ = 2.2. It should also be noted that these NMR results supported evidence that clp has a C^{γ} endo ring configuration which is consistent with stereochemical isosteres. These results suggest that clp (**15**) has a preferred configuration that would impart stability to polyproline I-type strands, where as (2S, 4R)-4-chloroproline (Clp, **6**) would be better suited to stabilize PPII strands.[52, 53]

A rather unusual study was done upon the (2S, 4R)-4-azidoproline model compound in order to study the azido gauche effect. Epimeric forms of 4-azidoproline were synthesized then converted to the methyl ester and acetylated at the pyrrolidine nitrogen. A crystal structure was only obtained for the (2S, 4R)-4-azidoproline model with the structure possessing a C^{γ} exo ring configuration, and a preference for the trans amide bond. Unusually no bond angles for the crystal structure were reported; however, there were extensive NMR studies done upon the two epimers. The NMR results produced similar configurations to those seen in the respective R and S isomers of 4-subsitiuted proline analogues of fluorine, chlorine, and oxygen. The 4R isomer (**9**) possessed a C^{γ} exo ring pucker due to gauche interactions from the azido group orienting itself away from vicinal hydrogens as seen in previous electronic isosteres. Additionally, the 4S isomer possessed a C^{γ} endo ring configuration due to corresponding gauche orientations. [50] Both epimers and their respective endo and exo ring puckers. as well as the observed gauche effects in Newman projection form can be seen in Figure 7. As in previous experiments the R isomer (**9,** $K_{trans/cis}$ = 4.2) had a much higher preference for the trans form of the amide bond than the S isomer ($K_{trans/cis}$ = 2.0). Computational data also supported the crystallographic and NMR results. This data points to the azido gauche effect being stereochemically similar to that of the fluoro gauche effect in its

ability to dictate and preorganize 4-substituted proline analogues. Furthermore, the high reactivity of the azido group makes this a particularly curious study, and in the case of these azido-prolines the study was conducted to better understand their reactivity toward the formation of diketopiperazines and cyclotriprolines rather than in the previously seen traditional studies of peptide structure.[50]

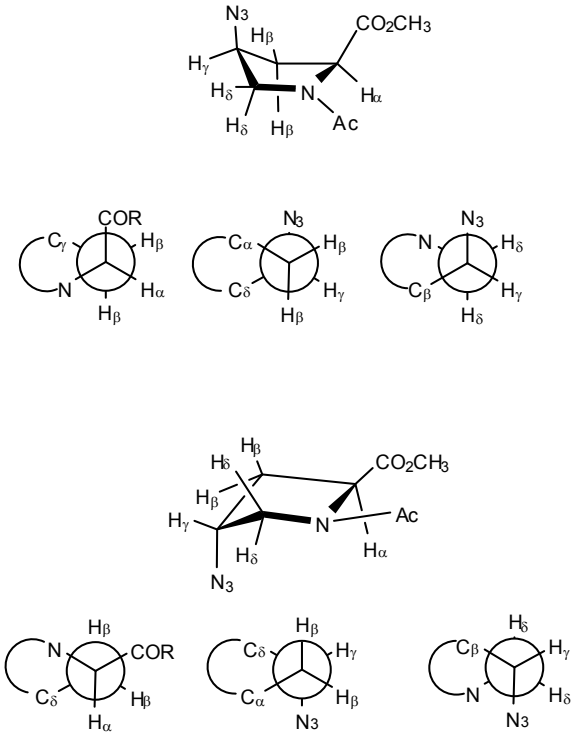

Figure 7. Structures and Newman projections of both epimeric forms of 4-Azidoproline.

C^{β} Substituted Compounds

Having conducted a myriad of studies upon the conformational outcomes of the steric and electronic consequences of different substituents at the C^{γ} position of pyrrolidine ring a new series of studies were conducted at the C^{β} position. These experiments were initially begun by Raines with the exploration of (2S, 3S)-3-hydroxyproline. This constitutional isomer of native 4-hydroxyproline was the natural choice for a primary study of the effect of electronegative atoms at the C^{β} or C3 position as it has a small natural occurrence in native collagen. [54] The synthesis of 3-hydroxy proline (**8,** 3-Hyp) was easily achieved and a subsequent crystal structure was obtained of the model compound **8**. The crystal structure reveals that rather than the accepted C^{γ} endo or exo configuration, 3-hydroxyproline possessed a slight C^{β} exo ring pucker with a twisted confirmation of the pyrrolidine ring.[55] This in conjunction with main chain bond angles of ϕ = -79.5 and ψ = 163.7 preorganized the residue be better suited toward stabilizing the collagen triad repeat in the Xaa position rather than in the Yaa position as previous studied compounds had done. 3-hydroxyproline also has a $K_{trans/cis}$ = 4.6, which is very similar to that of native proline, $K_{trans/cis}$ = 4.9. Additional steric and hydrogen bonding considerations made 3-hydroxy proline **8** less attractive as a means of stabilization of synthetic collagen, and these results were corroborated in the stability studies performed on synthetic collagens containing the 3-hydroxy proline amino acid.[35]

A more intriguing study of 3-substituted prolines was performed on the epimeric pair of 3-fluoroproline **10** (R) and **11** (S). The N-acetyl/ methyl ester analogues of each compound were synthesized and crystal structures were obtained for both compounds.

Both compounds crystallized in the trans amide bond configuration, however there were significant difference in the pyrrolidine ring structure of the two isomers. In the (2R, 3R)-3-fluoroproline (**10**) derivative a pyrrolidine ring structure with a C^{β} exo/ C^{γ} endo configuration was observed, while in the epimeric form **11** a ring pucker configuration of C^{β} endo/ C^{γ} exo was observed. These unusual configurations are attributed toward gauche interactions, and the attempt at relief of torsional strain. The N-C^{α}-C^{β}-F torsion angle produced values of 90.7° for **10** and -87.4° for **11** as seen in Figure 8.[56]

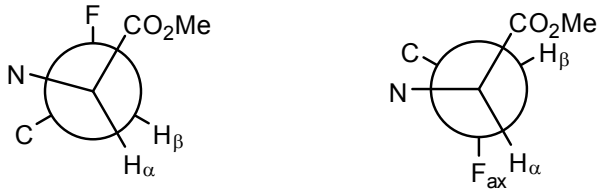

Figure 8. Newman projections along the C^{α}—C^{β} bond vector depicting the *gauche* relation between the amide and fluorine substituents. [56]

The opposite torsion angles give rise to the opposed pyrrolidine ring puckers due to fluorine's strong preference for gauche interactions through hyperconjugation. The ring puckers were not as pronounced as those previously observed, but manipulation of the pyrrolidine ring pucker at the C^{γ} position via fluoro-gauche interactions is previously unfounded. These results were also corroborated via computational models, but with the corresponding ring preferences observed at a lesser degree than those from crystal structures. As seen in the previous model compounds the pyrrolidine ring pucker can have an effect upon the main chain dihedral angles. In the case of the 3-fluoroproline epimers the ψ angles are fairly similar with values of 151.5 for R isomer **10** and 158.4 for S isomer **11**. However, the ϕ values for **10** and **11** are -56.4 and -71.2 respectively. The

values for **10** are similar to those seen previously corresponding to endo pyrrolidine ring puckers; however, **10** possesses an exo ring pucker. The same 'flip-flop' arrangement exists for the S isomer **11** with these results occurring from gauche effect from fluorination at the C^{β} position. Additional stereoelectronic effects that have an impact upon ring structure are n to π^{*} interactions between the amide oxygen atom, and the antibonding orbital of the ester carbonyl group. These two atoms are separated by a distance of 2.81 Å with an angle of incidence between the two of 91^{o}.[56] These values are consistent with those previously attributed to a Burgi-Dunitz trajectory, and have been show previously by Raines[57-60] to have a stabilizing impact upon the trans amide bond. These stereoelectronic effects all produce an unusual epimeric set of compounds that have an inverse ring confirmation preference to those previously studied. These properties made the 3-fluoroproline uniquely suited for use as probes to study peptide structure, and the isomers were subsequently analyzed for their effect upon β turn structure in elastin biopolymers.

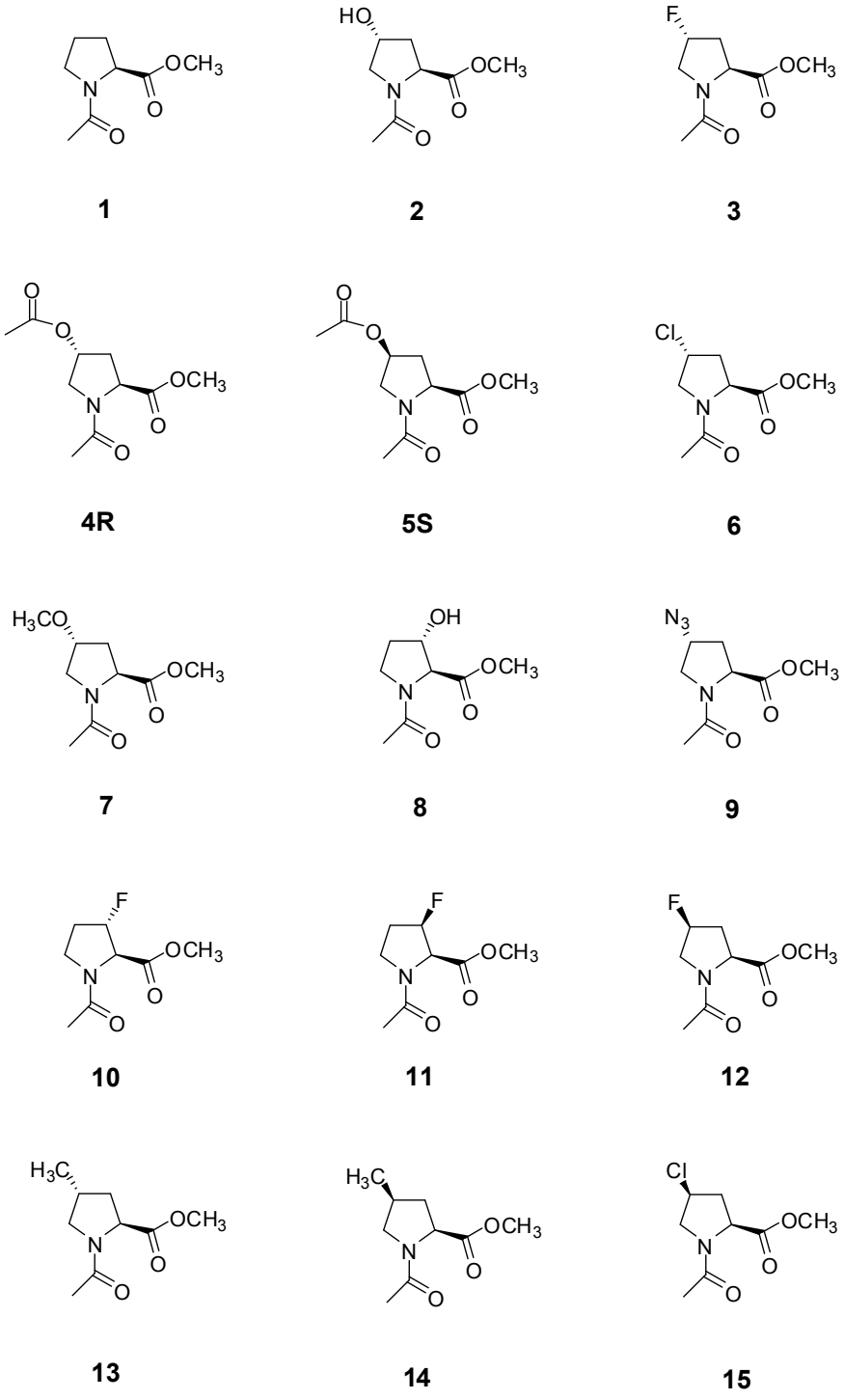

Figure 9. Structures of model compounds of proline and pseudoprolines.

Conclusion

The study of individual components of peptides and proteins is an integral part of understanding and pursuing the rational design of de novo protein structure. The ability to understanding the affects that govern these structures is of paramount importance due the utility and physiological impact of biopolymers upon everyday lives. Determining an efficient and accurate method to probe and predicts these structures was achieved through the use of small molecule studies, specifically in prolines and pseudoproline model systems. In these model systems there was a definite general trend observed that an electronegative atom in the C^{γ} with a stereochemical orientation trans (4R) to that of the pyrrolidine α-carbon produced a C^{γ}-exo ring pucker. Conversely, a stereochemical orientation cis (4S) to that of the pyrrolidine α-carbon at the C^{γ} carbon produced a C^{γ}-endo ring pucker. Also, a preference for the C^{γ}-exo ring pucker precludes a penchant for the trans amide bond just as a C^{γ}-endo ring pucker precludes a cis amide bond preference. These orientations also help to preorganize ϕ and ψ main chain dihedral angles toward the proline's designated role in peptide and protein structure. Additionally, these stereoelectronic effects seen at the C^{γ}-carbon can be 'flip-flopped' by moving the electronegative atom to the C^{β}-carbon of the pyrrolidine ring. A summary of the configurations and dihedral torsion angles for the crystal structures of proline and pseudoproline model compounds can be seen in Table 2.

As additional evidence toward the utility of the study of N-acetyl/ methyl ester prolyl compounds toward predicting ring structure in peptides can be seen in a study by Chacko. Where analysis of the 4-hydroxy proline model compound **2** along side that of

native 4-hydroxy proline in collagen found the pyrrolidine rings to be essentially superimposable.[61] Indicating that the pyrrolidine ring pucker is dependent upon the same factors that determine the structure of the small molecule model compounds. Ultimately, smaller model compounds provide a pure area for the assessment of subtle stereoelectronic effects upon the prolyl structure. In these compounds stereoelectronics, such as the gauche effect, can be easily assessed via NMR and crystal structures or the lack of a crystal structure. Curiously, throughout all of the studies crystal structures with a 4S stereochemical configuration at the C^{γ}-carbon were absent from the literature; however, crystal structures with a 4R configuration were easily obtained. This is presumably due to the dynamic nature of the compounds with a 4S prolyl configuration not having a predominately preferred conformation.

Finally, the study of proline is immensely important to the study of peptide and protein structure, function, and folding. By expanding and exploring various pseudoprolines the do novo design of peptides and proteins can be refined to tune structure for potential use in drug design and delivery, as well as potential biomedical engineering applications. N-acetyl / methyl ester prolyl model compounds provide a quick and efficient method for the evaluation of pseudoprolines for their potential use in a variety of immeasurably valuable fields.

References

[1] Fischer, E.; Skita, A., *z. physiol Chem* **1901**, (33), 177.

[2] Vanhoof, G.; Goossens, F.; De Meester, I.; Hendriks, D.; Scharpe, S., *Faseb J* **1995,** 9, (9), 736-44.

[3] Williams, K. A.; Deber, C. M., *Biochemistry* **1991,** 30, (37), 8919-23.

[4] Williamson, M. P., *Biochem J* **1994,** 297 (Pt 2), 249-60.

[5] Barlow, D. J.; Thornton, J. M., *J Mol Biol* **1988,** 201, (3), 601-19.

[6] MacArthur, M. W.; Thornton, J. M., *J Mol Biol* **1991,** 218, (2), 397-412.

[7] Taylor, C. M.; Hardre, R.; Edwards, P. J.; Park, J. H., *Org Lett* **2003,** 5, (23), 4413-6.

[8] Jenkins, C. L.; Raines, R. T., *Nat. Prod. Rep.* **2002,** 19, 49-59.

[9] Metzler, D. E., Biochemistry the Chemical Reactions of living cells. In 2nd ed.; Harcourt Academic Press: San Diego, 2001; Vol. 1, pp 72-73.

[10] Zimmerman, S. S.; Scheraga, H. A., *Macromolecules* **1976,** 9, (3), 408-16.

[11] Wuthrich, K.; Grathwohl, D.; Schwyzer, R., In *Peptides Polypeptides and Proteins* Blout, E. R.; Bovey, f. A.; Goodman, M.; Lotan, N. E., Eds. Wiley: New York, 1974; pp 300-307.

[12] Corey, R. B.; Pauling, L., *Proc. R. Soc. London, Ser. B* **1953,** 141, 10-20.

[13] Wedemeyer, W. J.; Welker, E.; Scheraga, H. A., *Biochemistry* **2002,** 41, 14637-14644.

[14] Lewis, P. N.; Momany, F. A.; Scheraga, H. A., *Biochim Biophys Acta* **1973,** 303, (2), 211-29.

[15] Adzhubei, A. A.; Sternberg, M. J., *J Mol Biol* **1993,** 229, (2), 472-93.

[16] Kietly, C. M.; Sherratt, M. J.; Shuttleworth, A. C., *Journal of Cell Science* **2002,** 115, 2817-2828.

[17] Van Dijk, A. A.; De Boef, E.; Bekkers, A.; Van Wijk, L. L.; Van Swieten, E.; Hamer, R. J.; Robillard, G. T., *Protein Sci* **1997,** 6, (3), 649-56.

[18] Tatham, A. S.; Shewry, P. R., *Trends Biochem Sci* **2000,** 25, (11), 567-71.

[19] Elvin, C. M.; Carr, A. G.; Huson, M. G.; Maxwell, J. M.; Pearson, R. D.; Vuocolo, T.; Liyou, N. E.; Wong, D. C.; Merritt, D. J.; Dixon, N. E., *Nature* **2005,** 437, (7061), 999-1002.

[20] Smith, A. D., *Oxford Dictionary of Biochemistry and Molecular Biology*. Oxford University Press: Oxford, UK, 2003.

[21] Urry, D. W., In *Protein-Based Materials.*, McGrath, K. P. K., D. , Ed. Birkhauser, Boston,, 1997; pp 133-177.

[22] Myllyharju, J.; Kivirikko, K. I., *Ann Med* **2001**, (33), 7-21.

[23] Jenkins, C. L.; McCloskey, A. I.; Guzei, I. A.; Eberhardt, E. S.; Raines, R. T., *Biopolymers* **2005,** 80, (1), 1-8.

[24] Raines, R. T., *Protein Sci* **2006,** 15, (5), 1219-25.

[25] Tatham, A. S.; Shewry, P. R., *Trends Biochem. Sci.* **2000** 25 (11), 567-571.

[26] Berg, R. A.; Prockop, D. J., *Biochem Biophys Res Commun* **1973,** 52, (1), 115-20.

[27] Fischer, E.; Suzuki, U., *Ber.* **1905,** 37, 2843.

[28] Leuchs, H.; Brewster, J. F., *Ber.* **1913,** 46, 986.

[29] Bella, J.; Brodsky, B.; Berman, H. M., *Structure* **1995,** 3, (9), 893-906.

[30] Bella, J.; Eaton, M.; Brodsky, B.; Berman, H. M., *Science* **1994,** 266, (5182), 75-81.

[31] Holmgren, S. K.; Taylor, K. M.; Bretscher, L. E.; Raines, R. T., *Nature* **1998,** 392, (6677), 666-7.

[32] Eberhardt, E. S.; Panasik, N., Jr.; Raines, R. T., *J Am Chem Soc* **1996,** 118, 12261-12266.

[33] Panasik, N., Jr.; Eberhardt, E. S.; Edison, A. S.; Powell, D. R.; Raines, R. T., *Int J Pept Protein Res* **1994,** 44, (3), 262-9.

[34] DeRider, M. L.; Wilkens, S. J.; Waddell, M. J.; Bretscher, L. E.; Weinhold, F.; Raines, R. T.; Markley, J. L., *J Am Chem Soc* **2002,** 124, (11), 2497-505.

[35] Jenkins, C. L.; Bretscher, L. E.; Guzei, I. A.; Raines, R. T., *J Am Chem Soc* **2003,** 125, (21), 6422-7.

[36] De Tar, D. F.; Luthra, N. P., *J Am Chem Soc* **1977,** 99, (4), 1232-44.

[37] Matsuzaki, T.; Iitaka, Y., *Acta Crystallogr.* **1971,** Sect. B, (27), 507-516.

[38] Liang, G. B.; Rito, C. J.; Gellman, S. H., *Biopolymers* **1992,** 32, (3), 293-301.

[39] Wlodawer, A.; Svensson, L. A.; Sjolin, L.; Gilliland, G. L., *Biochemistry* **1988,** 27, (8), 2705-17.

[40] Cushley, R.; Codington, J. F.; Fox, J. J., *Can.J. Chem* **1968,** 46, 1131-1140.

[41] Bretscher, L. E.; Jenkins, C. L.; Taylor, K. M.; DeRider, M. L.; Raines, R. T., *J Am Chem Soc* **2001,** 123, (4), 777-8.

[42] Raines, R. T.; Bretscher, L. E.; Holmgren, S. K.; Taylor, K. M., In *Peptides for the New Millennium:Proceedings of the Sizteenth American Peptide Symposium*, Kluwer Academic: Dordrecht, The Netherlands, 2000; pp 344-346.

[43] Kotch, F. W.; Guzei, I. A.; Raines, R. T., *J Am Chem Soc* **2008,** 130, (10), 2952-3.

[44] Shoulders, M. D.; Hodges, J. A.; Raines, R. T., *J Am Chem Soc* **2006,** 128, (25), 8112-3.

[45] Flippen-Anderson, J. L.; Gilardi, R.; Karle, I. L.; Frey, M. H.; Opella, S. J.; Gierasch, L. M.; Goodman, M.; Madison, V.; Delaney, N. G., *J Am Chem Soc* **1983,** 105, 6609-6614.

[46] Hansch, C.; Leo, A.; Taft, R. W., *Chem Rev* **1991,** 91, 165-195.

[47] Shoulders, M. D.; Guzei, I. A.; Raines, R. T., *Biopolymers* **2008,** 89, (5), 443-54.

[48] Hinderaker, M. P.; Raines, R. T., *Protein Sci* **2003,** 12, (6), 1188-94.

[49] Hodges, J. A.; Raines, R. T., *Org Lett* **2006,** 8, (21), 4695-7.

[50] Sonntag, L. S.; Schweizer, S.; Ochsenfeld, C.; Wennemers, H., *J Am Chem Soc* **2006,** 128, (45), 14697-703.

[51] Gorske, B. C.; Bastian, B. L.; Geske, G. D.; Blackwell, H. E., *J Am Chem Soc* **2007,** 129, (29), 8928-9.

[52] Horng, J. C.; Raines, R. T., *Protein Sci* **2006,** 15, (1), 74-83.

[53] Ruzza, P.; Siligardi, G.; Donella-Deana, A.; Calderan, A.; Hussain, R.; Rubini, C.; Cesaro, L.; Osler, A.; Guiotto, A.; Pinna, L. A.; Borin, G., *J Pept Sci* **2006,** 12, (7), 462-71.

[54] Gryder, R. M.; Lamon, M.; Adams, E., *J Biol Chem* **1975,** 250, 2470-2474.

[55] Giacovazzo, C.; Monaco, H. L.; Artioli, G.; Viterbo, D.; Ferraris, G.; Gilli, G.; Zanotti, G.; Catti, M., Oxford University Press: Oxford, UK,, 2002.

[56] Kim, W.; Hardcastle, K. I.; Conticello, V. P., *Angew Chem Int Ed Engl* **2006,** 45, (48), 8141-5.

[57] Burgi, H. B.; Dunitz, J.; Shefter, E., *Acta Crystallogr. Sect. B* **1974,** 30, 1517-1527.

[58] Burgi, H. B.; Dunitz, J. D.; Lehn, J. M.; Wipff, G., *Tetrahedron* **1974,** 30, 1563-1572.

[59] Burgi, H. B.; Dunitz, J. D.; Shefter, E., *J Am Chem Soc* **1973,** 95, 5065-5067.

[60] Burgi, H. B.; Lehn, J. M.; Wipff, g., *J Am Chem Soc* **1974**, (96), 1965-1966.

[61] Chacko, K. K.; Swaminathan, S.; Veena, K. R., *Curr. Sci.* **1983**, (52), 660-663.

Chapter 2

Synthesis, analysis, and crystal structures of epimeric S-oxo-Thiazolidine-(R)-Carboxylic Acid Derivatives

Introduction

The function and structure of peptides and proteins arises from the complex conformational preferences of the individual amino acid components that make up a proteins primary sequence. A balance of factors composed of steric, nonbonded interactions, and stereoelectronics account for the structural preferences seen in individual amino acids, and subsequently in the global structure of peptides and proteins. The balance of these factors in the amino acid proline is particularly intriguing due to proline's unique structural character. Proline plays a major role in protein structural units such as the prolyl type II Beta turn[1, 2] and the polyproline type II helix (PPII)[3, 4], as well as in the major component of the extracellular matrix of vertebrates, collagen.[4, 5] The collagen structure consists of three polypeptide chains formed into a right handed triple helix with each peptide chain made up of a triad repeat of 'Xaa-Yaa-Gly'. In this repeat the Xaa position is most often held by proline; while the Yaa position frequently contains the proline derivative (2S, 4R)-4-hydroxyproline (Hyp).[4-6] Thus native collagen is comprised of roughly 25 % proline and 4-hydroxyproline. Recent advances in collagen research have shown a great dependence upon 4-hydroxyproline as a major factor in the global stability of collagen structure.[7] Extensive studies have shown that the introduction of electronegative substituents at both the C^{γ} and C^{β} position upon the proline ring can increase peptide stability.[4, 8] Work done by our lab and others has established the use of 'proline monomers' as a tool for determining conformational preferences of proline analogues, and subsequently the analogues potential impact upon the structural properties of peptides.[4, 5, 9-11] Studies of N-acetyl prolyl methyl esters have

proven to be the most efficient monomeric model compounds for the observation of defining stereoelectronic effects such as the gauche effect, as well as providing a preview of the analogues potential repercussions for peptide function and structure.[4-8, 11-15]

With these factors under consideration our lab explored the possibility of a 4-hydroxylproline isostere that would have oxidation-reduction capabilities. The Red-Ox capability would present a novel method for the control of peptide and protein structure in the context of a chemically induced self-assembly control. To explore this possibility thiazolidine-4-carbonxylic acid (Thz) was chosen as a central focus of study due to its pseudoproline structure as well as its Red-Ox potential. The introduction of a sulfur atom at the γ position in the pyrrolidine ring presents an internal Red-Ox switch would be at a structurally critical position of the pseudoproline. There by presenting a method to potentially catalyze the reversible self-assembly of peptides. The synthesis and study of thiazolidine-4carbonxylic acid model compounds would present an ideal environment to test stereoselective oxidation methods, as well as observe the subtle stereoelectronic effects that dictate prolyl conformation and subsequently peptide structure.

The stereoselective oxidation of the thiazolidine sulfur atom is a key issue as the stereochemistry of the γ position of prolyl compounds is integral to defining conformational preferences such as endo/ exo prolyl ring pucker.[10] These two configurations are seen in the context of the unoxidized thiazolidine ring in Figure 1. Additionally, the stereochemistry at the prolyl γ position has been know to effect trans/ cis amide bond preference, and consequently the folding rate of proteins as well as the global structure of proteins.[4, 16] These two major structural configurations as well as the main chain torsional angles of the model compounds are of primary interest as they are

often dictated by subtle stereoelectronic effects in the prolyl ring. Our study will ascertain their ability to be manipulated via stereoselective oxidation of the thiazolidine sulfur atom with the hope of future use in potential applications such as biomedical engineering and novel protein design.

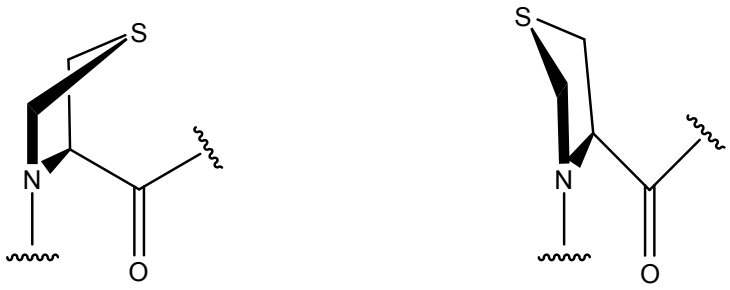

γ -endo γ -exo

Figure 1. Thiazolidine ring of thiazolidine-4-carboxylic acid in the respective γ–endo and γ–exo ring pucker configurations.

Results and Discussion

The synthesis of sulfoxides *N*-Acetyl-1(R_s)-oxo-thiazolidine-4-(R)-carboxylic acid Methyl Ester (**2**) and *N*-Acetyl-1(S_s)-oxo-thiazolidine-4-(R)-carboxylic acid methyl ester (**3**) as well as the preceding unoxidized parent compound *N*-acetyl-4-thiazolidine-R-carboxylic acid methyl ester (**1**) was completed followed by computational, NMR, and crystal structure analysis. These experiments were intended to evaluate the various stereoelectronic interactions of each monomeric model compound, and to assess their cumulative effect upon the thiazolidine ring structure specifically in the context of trans/ cis amide bond structure and γ–endo/ exo ring pucker configuration.

Synthesis

The stereoselective synthesis of sulfoxides has been widely explored, and have been shown to possess a very large synthetic utility.[17-19] However, the oxidation of thiazolidine has received extremely limited attention despite the presence of the thiazolidine ring in important structures such as the penicillins.[20, 21] We set forth to synthesize both the cis and trans sulfoxide epimers of thiazolidine-4-carboxylic acid. Initial synthesis of N-acetyl-4-thiazolidine-R-carboxylic acid methyl ester (**1**) proceeded in a straight forward manner utilizing acetyl chloride in methanol to form the methyl ester, and acetic anhydride with triethylamine to install the N-acetal functionality in excellent yields as seen in Scheme 1. Subsequent oxidation of **1** using mCPBA at low temperature afforded the trans sulfoxide isomer **2** with no detectible amount of the cis sulfoxide isomer **3**. The high stereoselectivity of this reaction proceeds in part from the sterics of the ester groups blocking oxidation from occurring in an cis fashion. Additional selectivity was presumably imparted via unfavorable interactions between the aromatic ring of mCPBA and the polar amide and ester groups forcing the mCPBA to the trans side of the thiazolidine ring helping to produce the trans sulfoxide stereoisomer **2** as the only observed product.

Synthesis of the cis sulfoxide isomer **3** proved more difficult than the synthesis of **2** as no methods for the stereoselective synthesis of **3** could be determined; however, the use of sodium periodate at high temperatures in polar protic solvents produced a diastereomeric mixture of the sulfoxides. The relatively small structure and high reactivity of sodium periodate coupled with high temperatures and a water/ methanol

solvent system combined to produce a maximum amount of the cis isomer **3** in a 54:46 ratio between **2** and **3** respectively. Lower reaction temperatures and aprotic solvents caused a higher degree of selectivity of the trans isomer **2** as well as a decrease in overall yield. The diastereomers, despite being similar in polarity, were separated via silica gel chromatography to produce each diastereomer in high purity.

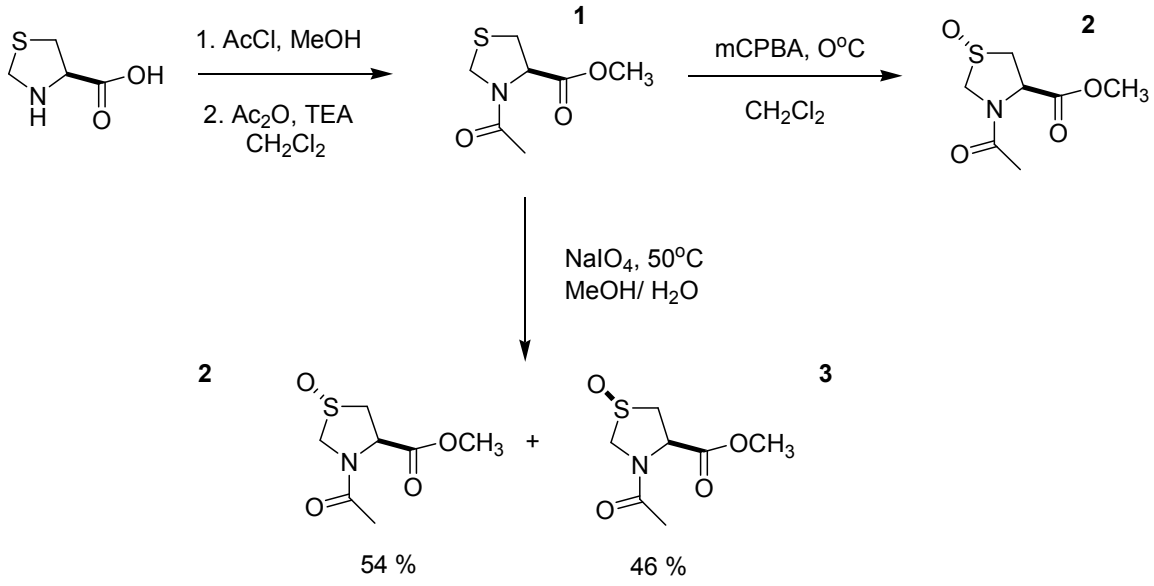

Scheme 1. Synthesis of *N*-acetyl-4-thiazolidine-R-carboxylic acid methyl ester (1) and the corresponding sulfoxides *N*-Acetyl-1(R_s)-oxo-thiazolidine-4-(R)-carboxylic acid Methyl Ester (2) and *N*-Acetyl-1(S_s)-oxo-thiazolidine-4-(R)-carboxylic acid Methyl Ester (3).

Confirmation Analysis of X-Ray Structures

Once synthesized and purified the epimeric pair of sulfoxides were crystallized and their structures determined via single-crystal X-ray diffraction analysis. The crystal structure of N-acetyl-4(R)-oxide-thiazolidine-(R)-carboxylic acid methyl ester **2** is seen in Figure 2, and the crystal structure for N-acetyl-4(S)-oxide-thiazolidine-(R)-carboxylic acid methyl ester is seen in Figure 3. Both structures possessed an inherent deviation from that of traditional proline in that bonds between the C^{γ} carbon and the neighboring carbons of proline are approximately 1.47 Å; however, the carbon-sulfur bonds observed in both sulfoxide isomers have a value of 1.8 Å. The trans sulfoxide **2** has a slight elongation of the carbon-sulfur bonds of 0.2 Å beyond the carbon-sulfur bond seen in the cis sulfoxide **3**. Furthermore, the distance between the nitrogen and sulfur atoms is 2.6 Å, while the value for the distance between nitrogen and the C^{γ} carbon in the pyrrolidine ring of proline is 2.3 Å. Despite the observed bond elongations there is still an observed gauche effect seen in the torsional configuration of the pyrrolidine ring around the sulfoxide bond. In previous studies in our group as well as others the gauche effect has been observed as a major determining factor in the pyrrolidine ring structure of proline and pseudoprolines.[4, 8] The Newman projections in Figure 2 A, B, and C and Figure 3 A, B, and C show the gauche confirmers that are observed in the crystal structures of each respective compound. Newman projection A in Figures 2 and 3 show the view along the C^{α}-C^{β} bond where the pyrrolidine nitrogen and sulfur atom are orientated in a gauche fashion to each other. This occurs so that constructive electrostatic overlap can be maximized between the two groups in both epimers. The most pronounced gauche

effects take place between the sulfoxide oxygen and the pyrrolidine nitrogen with this confirmation seen in both diastereoisomers. In the trans sulfoxide **2** a torsion angle of 68.09^{o} is observed in the O_s-S_γ-C_δ-N bond array which is seen in the corresponding Newman projection in Figure 2C. While in the cis sulfoxide isomer **3** the O_s-S_γ-C_δ-N bond array possesses a torsional angle of 73.63^{o} with a configuration seen in Figure 3C. In both cases the observed torsional angle is slightly greater than that of the ideal gauche torsional angle value; however, in the case of diastereomer **3** this confirmer has unique stereoelectronic interactions that will be addressed later that cause the variance in torsional values. The other Newman projections of **2** in Figure 2 provide further evidence for the gauche effect directing the conformational arrangement of the thiazolidine ring with additional gauche interactions depicted in Figure 3B, as well as in Figure 2B, between the sulfoxide oxygen and the pyrrolidine C^{α} carbon. Of additional interest when looking at Figure 2B is the anti configuration between the sulfoxide oxygen and the β hydrogen which have a torsional angle of 163.22^{o}. A similar configuration is present in Figure 2C where the anti configuration between the sulfoxide oxygen and δ hydrogen occurs again with a torsional angle of 172.43^{o}. These anti-periplanar configurations are suitable for orbital overlap between the anti C – H bond and the antibonding orbital of the sulfoxide moiety, and thus reinforce the observed thiazolidine ring arrangements as the preferred confirmation. These hyperconjugation effects are also seen in Figure 3B and Figure 3C where the sulfoxide oxygen in isomer **3** possesses an anti configuration with both β and δ hydrogens possessing torsional angles of 176.63^{o} (B) and 166.27^{o} (C) respectively. The combination of these effects help to lead to an S_γ-exo

thiazolidine ring pucker for the trans sulfoxide isomer **2** seen in Figure 2, as well as a S_{γ}-endo ring pucker for the cis sulfoxide **3** seen in Figure 3.

The direction of the pyrrolidine ring pucker is often seen to occur in the direction of the dipole moment of the polar bond in the γ position of the proline ring as is seen in fluoroproline and hydroxyproline derivatives.[22] This is also the case for both thiazolidine epimers **2** and **3** with the stereochemistry of the sulfoxide dictating the ring pucker confirmation and both sulfoxide oxygens adopting a pseudoaxial position. As a consequence of this orientation in the cis isomer **3** the sulfoxide oxygen is in close proximity to the ester carbonyl carbon. The pseudoaxial arrangement of the two atoms locates both functionalities in close proximity to one another, with the carbon and oxygen atoms being 2.91 Å apart and possessing a 91.48^{o} angle of incidence. These values are consistent with those seen in the Burgi-Dunitz trajectory of nucleophilic attack upon carbonyl groups. Orientations of this type are known to have properties of stabilization due to a favorable n to π^{*} interactions between the oxygen and carbonyl carbon respectively. This interaction accounts for the pronounced ring pucker seen in the cis stereoisomer **3**, and the deviation of gauche torsional angles in the thiazolidine ring structure. Diaxial interactions of this kind are not unprecedented,[23, 24] and n to π^{*} interactions are know to influence molecular structure in amino acids.[25, 26]

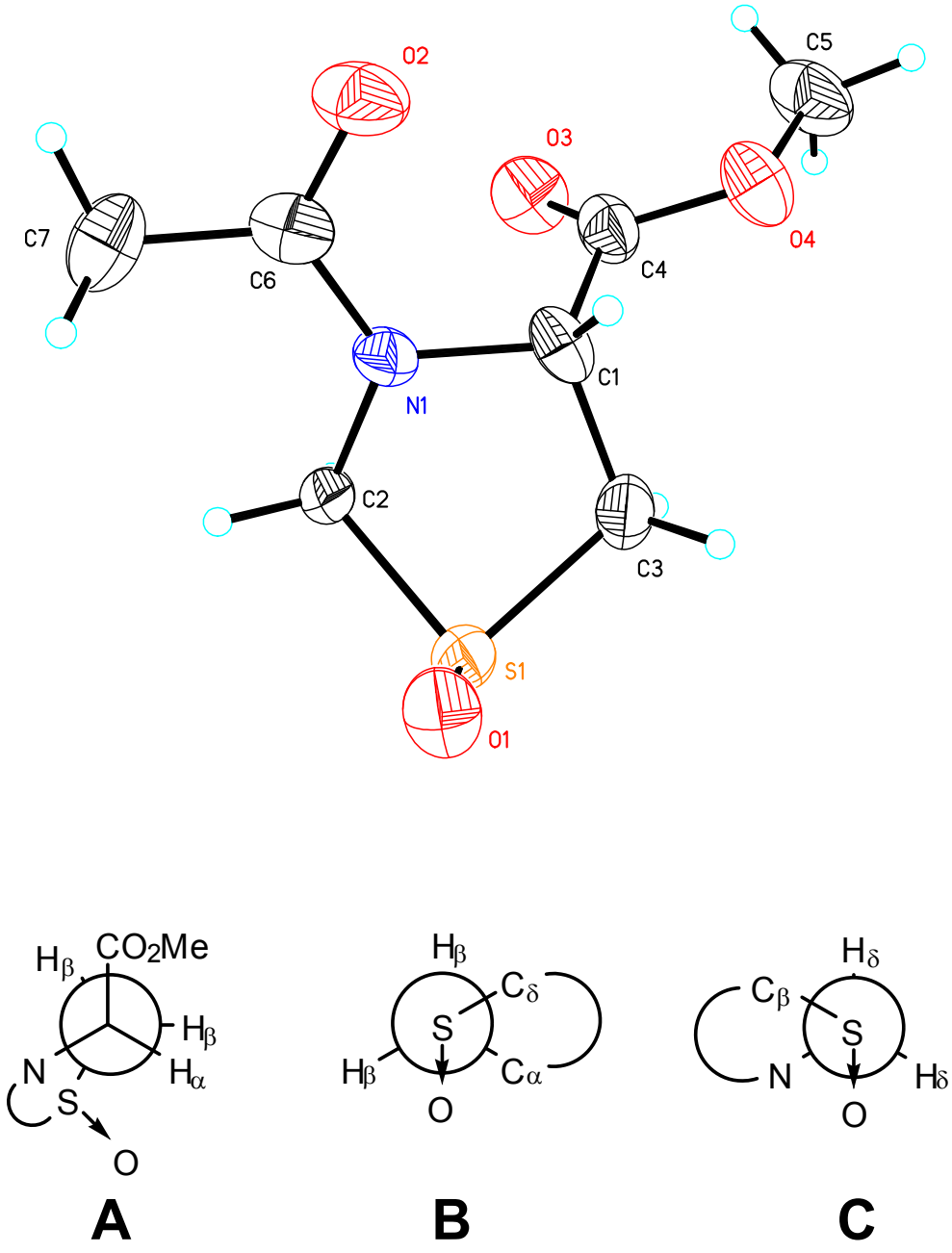

Figure 2. X-Ray crystal structure of N-Acetyl-4(R)-oxide-Thiazolidine-(R)-Carboxylic Acid Methyl Ester **2**. A) Newman projection from C^{α} Carbon to C^{β} Carbon. B) Newman projection from Sulfur to C^{β} Carbon. C) Newman projection from Sulfur to C^{δ} Carbon.

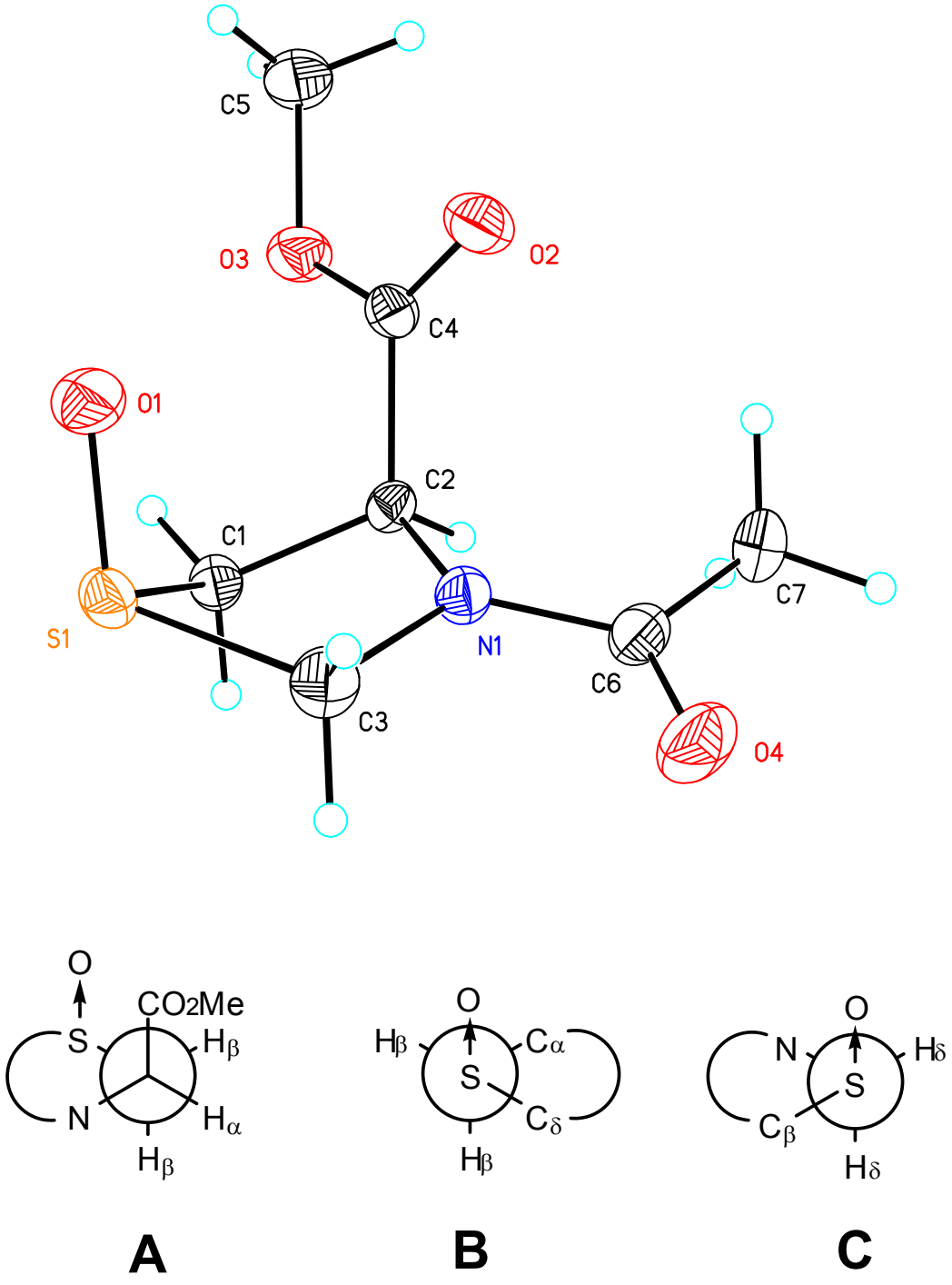

Figure 3. X-Ray crystal structure of N-Acetyl-4(S)-oxide-Thiazolidine-(R)-Carboxylic Acid Methyl Ester **3**. A) Newman projection from C^{α} Carbon to C^{β} Carbon. B) Newman projection from Sulfur to C^{β} Carbon. C) Newman projection from Sulfur to C^{δ} Carbon.

In a vast majority of prolyl analogues the n to π^* interaction between an oxygen and carbonyl carbon is often ascribed to causing the preference of the trans amide bond orientation as seen in crystal structure of sulfoxide **2**.[7, 11, 14, 25-27] In the trans amide bond configuration of sulfoxide **2** the amide oxygen is 3.0 Å away from the ester carbonyl carbon, and the direction between the two atoms is also consistent with a Burgi-Dunitz trajectory. However, this is not the case for the cis sulfoxide **3**, which possesses a cis amide bond configuration. Presumably this is due to the more readily available sulfoxide oxygen providing n to π^* interactions, and thus preempting the opportunity for the amide oxygen to participate in this stabilization. Hence, the cis amide bond is observed in the crystal structure of sulfoxide **3**. It should also be noted that in the crystal structures of both epimers the thiazolidine nitrogen of the amide bond exists in a trigonal planer geometry. All nitrogen bond angles are close to 120^o with the acetal group oriented in the same plane as the nitrogen with each isomer having its respective cis/ trans configuration. All of these conformational subtleties help to influence the main chain torsion angles of both compounds with sulfoxide **2** possessing a $\phi = -71.13^o$ and $\psi = 161.83^o$. The trans diastereomer **3** was found to have dihedral angles of $\phi = -87.33^o$ and $\psi = 18.65^o$ in the crystal structure seen in Figure 3. A summary of the major structural elements of both diastereomers can be seen in Table 1 along with structural elements of other prominent prolyl model compounds. It should also be noted that multiple attempts were made to crystallize the unoxidized model compound **1**, but no suitable crystals were obtained presumably due to the conformational flux of the unoxidized thiazolidine ring.

Compound	γ Ring Pucker	Amide bond	ϕ	ψ
Pro	Endo	Cis	-78.9	176.7
Hyp	Exo	Trans	-56.9	150.8
Flp	Exo	Trans	-55.0	140.5
2	Exo	Trans	-71.13	161.83
3	Endo	Cis	-87.33	18.65

Table 1. Data from crystal structures of various N-acetyl/ methyl ester proline and pseudoproline model compounds.[9]

Amide Vibrational Modes

Infrared Spectroscopy has been used as a measure of the inductive effects of the vibrational modes of amide bonds in prolyl model compounds. Raines and coworkers reported values of 1658, 1660, and 1664 cm^{-1} respectively for N-acetyl methyl ester model compounds proline (Pro), hydroxyproline (Hyp), and fluoroproline (Flp). These values show an increase in bond order according to the electron withdrawing ability of the atom at the γ position of the proline ring. For the unoxidized thiazolidine prolyl model compound a value of 1654 cm^{-1} was observed while for the trans sulfoxide (**2**) and cis sulfoxide (**3**) values of 1658 and 1654 cm^{-1} were observed respectively. These values imply the possibility that the vibrational mode of the amide bond could be a function of the stereochemistry of the electron withdrawing substituent in addition to the electron withdrawing capability of the group at the γ position of the proline ring.

Computational Chemistry and NMR Studies

The major structural motifs of the endo/ exo thiazolidine ring pucker and cis/ trans amide bond isomerization of the thioproline analogues **1**, **2**, and **3** were varied and analyzed via computational chemistry. These calculations produced insightful results with the 4-hydroxyproline isostere **2** possessing a computational configuration very similar to that observed in the crystal structure. The most stable computational structure of **2** possesses the γ-exo ring pucker with the sulfoxide oxygen in a pseudoaxial position as observed in the crystal structure. Additionally, the trans amide bond configuration was also preferred due to an n to π^* interaction between the amide oxygen and the ester carbonyl carbon. This same arrangement was observed in the crystal structure with both values in agreement that a Burgi-Dunitz trajectory exists between the two atoms, thus causing the preference for the trans amide bond. A propensity for the trans amide bond was also observed in the NMR studies of compound **2** with a $K_{trans/\ cis} = 3.43$, as well as *J* couplings that are consistent with the bond angles observed in the computational and crystal data to indicate a structure with a γ-exo ring pucker. Additionally, NOE studies via the irradiation of trans sulfoxide **2** at 2.18 ppm shows an enhancement at 4.79 ppm. This result is consistent with NOE interactions that would occur between the γ hydrogens and the acetyl methyl group in the trans amide bond configuration. This irradiation of the 'major' rotomeric acetyl peak, along with integration values, enabled the assignment the NMR peaks for the cis and trans rotomers of the trans sulfoxide **2**.

For the cis sulfoxide diastereomer **3** the computational results also produced a trans amide bond as being the most stable amide bond configuration; however the cis

amide bond was observed in the crystal structure. In the crystal structure the predominant n to π^* interaction in the molecule was between the sulfoxide oxygen and the ester carbonyl carbon leaving the amide bond free to rotate without the stabilizing force of the n to π^* interaction. In the computational scenario the n to π^* interaction between the amide oxygen and ester carbonyl was attributed priority for this interaction, and thus the amide bond assumed the trans configuration as seen in several other model compounds of this type.[10, 14, 28] Empirical results from NMR studies show that indeed the trans amide bond of sulfoxide **3** predominates with a ratio of $K_{trans/\ cis} = 2.01$. Thus it can be deduced that in solution the amide-ester n to π^* interaction is dominant, but that there is still a significant interaction between the ester and sulfoxide oxygen helping cause the relatively low preference for the trans amide bond. NMR data from the *J* couplings of compound **3** indicate a γ-endo ring pucker configuration similar to that seen in the crystal structure of **3**. Additionally, the computational results for sulfoxide **3** in the γ-endo ring pucker configuration show that the sulfoxide adopts a pseudoequatorial position rather than the axial configuration seen in the crystal structure. This pseudoequatorial position greatly increases the distance between the sulfoxide oxygen and the ester carbonyl carbon, and removes the possibility of n to π^* interaction between the two. This attempt at the relief of steric considerations enables the n to π^* interaction between the amide and the ester to predominate, and dictate the variance in computational structure of compound **3**. Peak assignments for NMR spectra of the cis sulfoxide **3** were aided by NOE studies. Irradiation of **3** at 5.44 ppm shows a mild enhancement at 2.16 ppm to indicate a cis amide bond configuration due to the interaction between the α carbon proton and the methyl group of the acetyl. This

interaction between the two environments in the minor rotomeric for along with integration values allowed for the assignment of the cis and trans amide isomers of compound **3** supporting the high occurrence of the cis amide rotomeric form. Further, calculations of the unoxidized parent thioproline **1** also produced a trans amide bond configuration that arose from n to π^* interactions between the amide and ester groups having an orientation similar to a Burgi-Dunitz trajectory. Proton NMR data supports these findings with a $K_{trans/\ cis} = 2.68$. Additionally, NOE studies were performed to assign cis and trans rotomeric form of unoxidized model compound **1**. In these experiments an unusual observation in the NOE spectra of parent compound **1** is the constant enhancement seen in the β hydrogens in all of the NOE spectra even when the acetyl methyl group is irradiated. However, irradiation at 5.22 ppm showed a mild enhancement at 2.06 ppm. These results are consistent with an NOE between the α hydrogen and the acetyl methyl group. Thus, the minor set of peaks in the proton spectra of **1** were assigned to the cis amide isomer, while the major set of rotomeric peaks were attributed to the trans amide form. Additional, previous studies by Tinant and coworkers presented evidence for a slight γ-endo thiazolidine ring pucker in a crystal structure of the N-methyl amide analogue of the unoxidized model compound **1**.[29] This observation is also in agreement with NMR data of bond angles derived from *J* couplings and computational findings for a γ-endo ring pucker configuration for thioproline **1**.

Conclusion

The most interesting dynamic found in these experiments is between the sulfoxide oxygen and the ester carbonyl carbon of sulfoxide **3** in the results of the three studies. While the crystal structure supports a strong n to π^* interaction between the two resulting in a cis amide bond the computational and NMR studies show a greater preference for the trans amide bond due to traditional prolyl n to π^* interactions. 1, 3 diaxial interactions of this type have been seen before in six-membered thioester rings where a sulfoxide oxygen and a carbonyl carbon were found in close proximity.[24] This n to π^* interaction is able to work in the context of the other stereoelectronic interactions seen in the Newman configurations in Figure 3 to lessen the preference for the trans amide bond and produce the γ-endo thiazolidine ring pucker that is observed in each study. Ultimately, the sulfoxide diastereomer **3** possesses a relatively high propensity for the cis amide bond configuration due to cooperative diaxial interactions between the ester and sulfoxide resulting in a low $K_{trans/\ cis}$ value.

Conversely, trans sulfoxide **2** possesses analogous properties to those previously explored as seen in the summary of data in Table 2. Sulfoxide **2** has the same major structural preferences as (2S, 4R)-4-fluoroproline (Flp) and (2S, 4R)-4-hydroxyproline (Hyp). 4-fluoroproline and 4-hydroxyproline both play an integral role in the stability of synthetic collagen and native collagen, respectively.[22] Additionally, all experimental results are in agreement for diastereomer **2** possessing γ-exo thiazolidine ring pucker with a large preference for the trans amide bond configuration. These properties in conjunction with the ability to produce diastereomer **2** exclusively using mCPBA in high

yield makes it an ideal candidate for use as a Red-Ox switch for self assembly of peptide structure given the desirable properties of the compound.

Studies of the unoxidized model compound **1** presented evidence for a slight γ-endo thiazolidine ring pucker, which is consistent with the structure of native proline. Thus the pair of the unoxidized thioproline **1** and the trans sulfoxide **2** present a Red-Ox duo that produce dissimilar structural preferences. With **1** presenting proline like properties and configurations, which can be stereoselectively oxidized to a native 4-hydroxyproline isostere of the trans sulfoxide **2**. The different properties of the two oxidation states of the two compounds presents an ideal system for use of thiazolidine-4-carboxylic acid as a synthetic amino acid Red-Ox switch for the self-assembly of peptide structure. As the oxidized form would impart added stability to the global peptide structure through conformational preferences brought on by stereoelectronic interactions from generation of the trans sulfoxide diastereomer *in situ*. This Red-Ox pair could have extended potential uses in biomedical engineering as well as novel protein design due to the change in prolyl structure from stereoselective oxidation. Finally, by use of N-acetyl prolyl methyl esters as a model system for the evaluation of the Red-Ox potential of pseudoprolines a Red-Ox pair with properties advantageous for chemically induced self-assembly was discovered.

Materials and Methods

All chemical reagents were purchased from either Fisher Scientific, Inc. (Pittsburgh, PA) or Sigma-Aldrich Chemical Co. (St. Louis, MO) unless otherwise noted. ^{1}H, ^{19}F and ^{13}C NMR spectra were recorded on a Varian Mercury-300 spectrometer (300MHz for ^{1}H, 75 MHz for ^{13}C), on an Inova-400 spectrometer (400 MHz for ^{1}H, 384 MHz for ^{19}F NMR, 100 MHz for ^{13}C), or an INOVA-600 spectrometer (600 MHz for ^{1}H, 150 MHz for ^{13}C). NMR spectra were recorded on solutions in deuterated chloroform ($CDCl_3$) with residual chloroform (7.26 ppm for ^{1}H NMR and 77.23 ppm for ^{13}C NMR) taken as the internal standard, as well as hexafluorobenzene (-164.9 for ^{19}F NMR) and were reported in parts per million (ppm). Abbreviations for signal coupling are as follows s, singlet; d, doublet; t, triplet; q, quartet; m, multiplet. Trans/ cis prolyl rotameric studies were conducted in d^{8}-dioxane at 24^{o} C. Electrospray ionization mass spectra were recoded on a JEOL JMS-SX102/SX102A/E mass spectrometer. Analytical Thin Layer Chromatography (TLC) was performed on precoated glass backed plates purchased from Whitman (silica gel 60 F254; 0.25mm thickness). Flash chromatography was carried out with silica gel 60 (230-400 mesh ASTM) from EM Science.

X-Ray Crystallography

The crystals of N-Acetyl-1(R_s)-oxo-thiazolidine-4-(R)-carboxylic acid Methyl Ester (2) and *N*-Acetyl-1(S_s)-oxo-thiazolidine-4-(R)-carboxylic acid Methyl Ester (3) used for X-ray structure determination were obtained by dissolving a small amount of white solid in a minimal amount of methanol and allowing the dissolved solutions to equilibrate in a reservoir of hexanes. Crystals suitable for X-ray crystallography grew slowly over the course of two and three weeks time respectively. The tables of atomic coordinates, bond lengths, bond angles, and torsion angles are provided in the appendix 3.

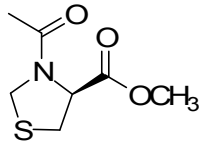

***N*-Acetyl-4-Thiazolidine-R-Carboxylic Acid Methyl Ester (1).** 1 g (7.21 mmole) of 4-Thiazolidine-(R)-Carboxylic Acid was dissolved in 50 mL of fresh methanol and cooled to 0^{o}C under a slow argon purge. Thionyl chloride (1.5 mL, 7.9 mmol) was then added slowly to the reaction mixture, and then allowed to warm to room temperature over night with stirring under argon. The solvent was then removed *in vacuo* to yield a white solid, which was then taken up in 60 mL of fresh methylene chloride and cooled to 0^{o}C under argon. Triethyl amine (2.5 mL, 34.3mmol) was then added slowly to the reaction followed by the slow addition of neat acetic anhydride (1.4 mL, 12.7 mmol), and the reaction was allowed to warm to room temperature overnight with stirring under static argon. The reaction mixture was then worked up by the washing the reaction mixture with 2 x 50 mL of 1M HCl. The organic extract was then dried over sodium sulfate, and

the solvent removed *in vacuo* to yield an oil that was further purified by eluting the crude product down a plug of silica gel (app. 10 g) with ethyl acetate to give a pure final product as an oil in 98 % yield (1.35 g, 7.14 mmol). Rf = 0.5 (1:1 hexanes/ ethyl acetate). ^{1}H NMR (600MHz, $CDCl_3$) δ 5.08 (q, 1H; J = 3.6 Hz; $^{\alpha}$H; minor isomer at 4.72), 4.55 (q, 2H; J = 5.7, 8 Hz; $^{\delta}$H'; minor isomer at 4.74), 3.71 (s, 3H; OCH_3; minor isomer at 3.77), 3.23 (dd, 1H; J = 7; $^{\beta}$H; minor isomer at 3.31), 3.16 (dd, 1H; J = 3.6; $^{\beta}$H'; minor isomer at 3.31), 2.15 (s, 3H; $COCH_3$ minor isomer at 2.06). ^{13}C NMR (150 MHz, $CDCl_3$): δ 21.8 (minor isomer at 22.4), 32.5 (minor isomer at 34.0), 48.4, 51.8 (minor isomer at 52.1), 170.2, 167.7 (minor isomer at 168.1). FT–IR (dioxane): 1004, 1172, 1200, 1409, 1654, 1744, 2847, 2925, 2953, 3011. ESI-MS, Calc. for $C_7H_{11}NO_3S$ [M + H]: 190.0532; found 190.0531.

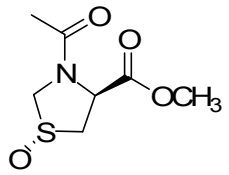

***N*-Acetyl-1(R_s)-oxo-thiazolidine-4-(R)-carboxylic acid Methyl Ester (2). 1**, (0.3 g, 1.58 mmol) was dissolved in 15 mL of methylene chloride, and cooled in an ice bath open to atmosphere. Then 0.39 g (1.74 mmol) of mCPBA were added in one portion, and the reaction was allowed to stir overnight while warming to room temperature. The reaction was then worked up by washing the crude reaction mixture with 3 x 75 mL of sat. aq. sodium bicarbonate. The organic layer was then dried over sodium sulfate and the solvent removed *in vacuo*. The crude product was then purified by silica gel chromatography using 5 % methanol/ chloroform to yield 0.23 g (1.12 mmol) of oxidized

product in a 77 % yield. Rf = 0.3 (10 % methanol/ chloroform). ^{1}H NMR (600MHz, $CDCl_3$): δ 5.36 (t, 1H; J = 8 Hz; $^{\alpha}$H; minor isomer at 5.10), 4.77 (m, 1H; $^{\delta}$H; minor isomer at 5.51), 4.31 (d, 1H; J = 12 Hz $^{\delta}$H'; minor isomer at 3.92), 3.75 (s, 3H; OCH_3; minor isomer at 3.80), 3.41 (dd, 1H; J = 14 Hz; $^{\beta}$H; minor isomer at 3.55), 2.93 (dd, 1H; J = 14 Hz;$^{\beta}$H'; minor isomer at 3.09), 2.18 (s, 3H; $COCH_3$ minor isomer at 2.14). ^{13}C NMR (150 MHz, $CDCl_3$): δ 22.58 (minor isomer at 21.95), 53.24, 53.66 (minor isomer at 55.53), 58.00 (minor isomer at 58.99), 70.01 (minor isomer at 68.17), 170.08 (minor isomer at 170.73), 170.97 (minor isomer at 170.76). FT–IR (dioxane): 3007, 2937, 1658, 1740, 1397, 1298, 1278, 1078, 1045. ESI-MS, Calc. for $C_7H_{11}NO_4S$ [M + H]: 206.0409; found 206.0479

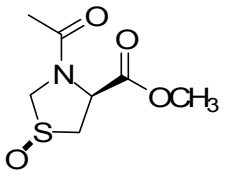

***N*-Acetyl-1(S_s)-oxo-thiazolidine-4-(R)-carboxylic acid Methyl Ester (3). 1**, (0.3 g, 1.58 mmol) was dissolved in 3 mL methanol in a round bottom flask. Then 0.37 g (1.74 mmol) sodium periodate was dissolved in 1.5 mL water, and added to the reaction mixture. The reaction was heated to 50 ^{o}C for 3 hours until all starting material was consumed by TLC. Reaction was then worked up by removing excess solvent *in vacuo*, and then partitioning the reaction mixture between water and methylene chloride. The aqueous layer was then extracted two additional times with 20 mL methylene chloride, dried over sodium sulfate, and the solvent removed *in vacuo*. The crude reaction product was then purified by silica gel chromatography using 10 % methanol/ chloroform to yield 53.8 % major isomer (**2**, 0.11g, 0.53 mmol) and 46.2 % minor isomer (**3**, 0.096 g, 0.46

mmol) in a 65 % overall yield (total: 0.21 g, 1.02 mmol) Rf = 0.25 (10 % methanol/ chloroform). ^{1}H NMR (600MHz, $CDCl_3$) δ 5.42 (dd, 1H; J = 2.3, 8.6 Hz; $^{\alpha}$H; minor isomer at 5.87), 4.89 (d, 1H; J = 11.6; $^{\delta}$H; minor isomer at 4.95), 4.41 (d, 1H; J = 11.6 Hz $^{\delta}$H'; minor isomer at 4.87), 3.75 (s, 3H; OCH_3; minor isomer at 3.79), 3.47 (dd, 1H; J = 13.6 Hz; $^{\beta}$H; minor isomer at 4.47), 3.17 (dd, 1H; J = 13.6; Hz $^{\beta}$H'; minor isomer at 3.10), 2.17 (s, 3H; $COCH_3$ minor isomer at 2.15). ^{13}C NMR (150 MHz, $CDCl_3$): δ 22.65 (minor isomer at 22.72), 53.26 (minor isomer at 53.60), 54.60, 57.90 (minor isomer at 59.70), 70.23 (minor isomer at 69.95), 165.09 (minor isomer at 169.42), 169.36 (minor isomer at 169.82). FT–IR (dioxane): 2953, 2921, 2847, 1740, 1654, 1392, 1348, 1278, 1213, 1037. ESI-MS, Calc. for $C_7H_{11}NO_4S$ [M + H]: 206.0409; found 206.0478.

References

[1] Venkatachalem, C. M., *Biopolymers* **1968,** 6, (1425-1436).

[2] Metzler, D. E., Biochemistry the Chemical Reactions of living cells. In 2nd ed.; Harcourt Academic Press: San Diego, 2001; Vol. 1, pp 72-73.

[3] Steinberg, I. Z.; Harrington, W. F.; Berger, A.; Stela, M.; Katchalski, E., *J Am Chem Soc* **1960,** 82, 5263-5279.

[4] Raines, R. T., *Protein Sci* **2006,** 15, (5), 1219-25.

[5] Shoulders, M. D.; Guzei, I. A.; Raines, R. T., *Biopolymers* **2008,** 89, (5), 443-54.

[6] Jenkins, C. L.; Bretscher, L. E.; Guzei, I. A.; Raines, R. T., *J Am Chem Soc* **2003,** 125, (21), 6422-7.

[7] DeRider, M. L.; Wilkens, S. J.; Waddell, M. J.; Bretscher, L. E.; Weinhold, F.; Raines, R. T.; Markley, J. L., *J Am Chem Soc* **2002,** 124, (11), 2497-505.

[8] Kim, W.; Hardcastle, K. I.; Conticello, V. P., *Angew Chem Int Ed Engl* **2006,** 45, (48), 8141-5.

[9] Panasik, N., Jr.; Eberhardt, E. S.; Edison, A. S.; Powell, D. R.; Raines, R. T., *Int J Pept Protein Res* **1994,** 44, (3), 262-9.

[10] Shoulders, M. D.; Hodges, J. A.; Raines, R. T., *J Am Chem Soc* **2006,** 128, (25), 8112-3.

[11] Sonntag, L. S.; Schweizer, S.; Ochsenfeld, C.; Wennemers, H., *J Am Chem Soc* **2006,** 128, (45), 14697-703.

[12] Holmgren, S. K.; Taylor, K. M.; Bretscher, L. E.; Raines, R. T., *Nature* **1998,** 392, (6677), 666-7.

[13] Jenkins, C. L.; McCloskey, A. I.; Guzei, I. A.; Eberhardt, E. S.; Raines, R. T., *Biopolymers* **2005,** 80, (1), 1-8.

[14] Kotch, F. W.; Guzei, I. A.; Raines, R. T., *J Am Chem Soc* **2008,** 130, (10), 2952-3.

[15] Ruzza, P.; Siligardi, G.; Donella-Deana, A.; Calderan, A.; Hussain, R.; Rubini, C.; Cesaro, L.; Osler, A.; Guiotto, A.; Pinna, L. A.; Borin, G., *J Pept Sci* **2006,** 12, (7), 462-71.

[16] Wedemeyer, W. J.; Welker, E.; Scheraga, H. A., *Biochemistry* **2002,** 41, 14637-14644.

[17] Mikolajczk, M.; Drabowicz, J.; Kielbasinski, P., *Chiral Sulfur Reagents: Applications in Asymmetric and Stereoselective Synthesis*. CRC Press: Boca Raton NY, 1997.

[18] Davis, F. A.; Yang, B.; Deng, J.; Zhang, J., Asymmetric synthesis of heterocycles using sulfinimines (N-sulfinyl imines). In *Arkivoc part 7*, 2006; pp 120-128.

[19] Zhou, P.; Chen, B. C.; Davis, F. A., Synthesis and Reactions of Sulfinimines Advances in Sulfur Chemistry. In Rayner, C. M., Ed. JAI Press Inc.: Stamford, CT 2000; Vol. 2, pp 249-282.

[20] Betts, M.; Pritchard, R. G.; Schofield, A.; Stoodley, R.; Vohra, S., *Journal of the Chemical Society, Perkin Transations 1: Organic and Bio-Organic Chemistry* **1999,** 8, 1067-1072.

[21] Kanai, K.; Podanyi, B.; Bokotey, S.; Hajdu, F.; Hermecz, I., *Tetrahedron: Asymmetry* **2002,** 13, 491-495.

[22] Eberhardt, E. S.; Panasik, N., Jr.; Raines, R. T., *J Am Chem Soc* **1996,** 118, 12261-12266.

[23] Lambert, J. B.; R.G., K., *Journal of Organic Chemistry* **1966,** 31, (10), 3429-3431.

[24] Antennis, M. J., *Acta Crystallogr.* **1985,** C41, 1818-1821.

[25] Hodges, J. A.; Raines, R. T., *Org Lett* **2006,** 8, (21), 4695-7.

[26] Gorske, B. C.; Bastian, B. L.; Geske, G. D.; Blackwell, H. E., *J Am Chem Soc* **2007,** 129, (29), 8928-9.

[27] Hinderaker, M. P.; Raines, R. T., *Protein Sci* **2003,** 12, (6), 1188-94.

[28] Hodges, J. A.; Raines, R. T., *J AM CHEM SOC* **2003,** 125, 9262-9263.

[29] Tinant, B.; Declercq, J. P.; Germain, G.; van Meerssche, M., *Bull Soc Chim Belg* **1982,** 91, 57-61.

Chapter 3

Amino Acid Triad Synthesis and Analysis

Introduction

Stereoelectronic stabilizing interactions play a major role in protein structure, folding, and function. All of these characteristics rely upon the individual properties of specific amino acids to achieve a cooperative and functional protein.[1] Of particular importance is the amino acid proline because of its large role in the conformational stability of proteins in prolyl type II β turns, polyproline II helixes, as well as the in the rate of protein folding.[2, 3] Proline also plays a predominant role in the major proteinaceous component of the extra cellular matrix (ECM) of vertebrates, specifically in the protein collagen where proline can compose up to a third of collagens total structure.[4] Collagen possesses a triad repeat of amino acids in the form 'Xaa-Yaa-Gly' with the small achiral amino acid glycine being the lone amino acid conserved in the collagen sequence. The constant repeat of glycine in the sequence is required for the tight packing of the collage triple helix.[5-9] However; it is frequently the case that both the Xaa and Yaa amino acid repeat in the collagen sequence are occupied by proline. Posttranslational modifications of the triad repeat of collagen by the enzyme prolyl-4-hydrozylase (P4H) convert the proline in the Yaa position into (2S, 4R)-4-hydroxyproline (Hyp).[10] The introduction of the hydroxyl groups is done stereospecifically with the presence of 4-hydroxyproline playing an important role in collagen stability.[11, 12] The presence of 4-hydroxyproline is essential to collagen function and stability as both *Caenorhabditis elegans* and mice lacking 4-hydroxyproline in their collagen structure experienced a destabilization of their extracellular matrix (ECM) and consequently suffered high morbidity rates in the embryonic stages of development.[13, 14]

Recent developments by Raines and coworkers have shown that collagen stability is highly dependant upon stereoelectronic effects, specifically those concerning the stabilizing interactions within the conformation of the pyrrolidine ring in 4-hydroxyproline.[1, 15, 16] Previously it was assumed that the importance of 4-hydroxyproline to collagen stability was due to a series of complex intermolecular and intramolecular hydrogen bonding patterns, where 4-hydroxyproline acted as a mediator between both water molecules and other portions of the collagen triple helix.[9, 17-20] However, experiments by Conticello as well as Raines have reinforced the fact that the collagen triple helix, and thus global collagen structure, is not dictated solely by hydrogen bonding but rather by subtle stereoelectronic effects.[21, 22] In its native form collagen relies upon (2S, 4R)-4-hydroxyproline (Hyp) to stabilize the triple helix via the dipole moment created from the 4 hydroxyl group. This causes the pyrrolidine ring to adopt an γ-exo ring pucker configuration.[23] The exo pyrrolidine ring configuration seen in Hyp is principally due to the inherent preference for Hyp to adopt a trans amide bond configuration concurrent with the exo ring confirmer. These two effects are related due to the gauche effect from the stereoelectronic preference for vicinal polar groups to be next to each other.[24-26] Just as the exo ring pucker stabilizes collagen by giving Hyp a preference for the trans amide bond configuration an endo pyrrolidine ring configuration causes destabilization of the collagen superstructure.[23] The γ-exo ring configuration can be selected for by the installation of an electronegative atom covalently bound to the carbon in the γ position of the pyrrolidine ring with an R stereochemical configuration.[21, 23-26] This is the configuration seen in (2S, 4R)-4-hydroxyproline in the Yaa position of native collagen.[27, 28]

In the de novo design of peptides and proteins careful detail should be given to the stereochemistry and stereoelectronics of the amino acid in the Yaa position of the triad repeat when developing synthetic collagens. Recent developments by Conticello and Shugart have shown that the pseudoproline thiazolidine-2-(R)-carboxylic acid (Thz) has the potential to act as a red-ox active switch for the self assembly of collagen related peptides.[29] Model compounds of thiazolidine-2-(R)-carboxylic acid have shown very high stereoselectivity when oxidized by mCPBA resulting in the corresponding sulfoxide which is stereoelectronically analogous to (2S, 4R)-4-hydroxyproline. Both the sulfoxide in Figure 1 and native hydroxyproline have dipole moments in the gamma position of the pyrrolidine ring that produce the desired exo ring pucker, as well as a preference for the trans amide bond configuration.[29] Using our previously successful red-ox chemistry as a base we continue our progress toward the synthesis of novel collagen analogue in which red-ox activity of the sulfur atom in Thz would govern the conformational stability of the pseudoproline Thz, and subsequently influence the structure of synthetic collagen. Having done work on model systems of single amino acid units we hope to expand our study to both synthesizing and analyzing the structure of a Xaa-Yaa-Gly triad repeat using Pro-Thz-Gly as the triad scaffold. Study of these larger model systems will provide a more accurate analysis of the ability of thiazolidine carboxylic acid, in both its oxidized and unoxidized form, to function in a cooperative manner in the Xaa-Yaa-Gly triad collagen repeat. As well as provide a possible gateway toward the synthesis of a red-ox active synthetic collagen with the hope of future applications of the red-ox active synthetic collagen in wide variety of biomedical applications such as stents and artificial skins.[1, 30]

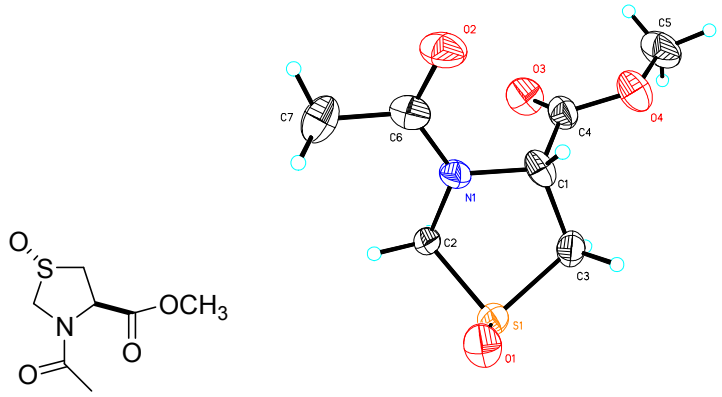

Figure 1. Structure and X-Ray crystal structure of N-Acetyl-4(R)-oxide-Thiazolidine-(R)-Carboxylic Acid Methyl Ester.

Results and Discussion

The use of oxidation to protect sulfur atoms during chemical ligation of peptides is a common practice; however the stereoselective oxidation of thiazolidine containing amino acids has received very little attention.[31, 32] Subsequently we report the synthesis of both the unoxidized and stereoselectively oxidized synthetic collagen triad of Pro-Thz-Gly, as well as the preparation of the triads for use in automated peptide synthesis. Additionally, the X-ray crystal structure of the stereoselectively oxidized amino acid triad Boc-Pro-Thz(O)-Gly-OBn was obtained and analyzed.

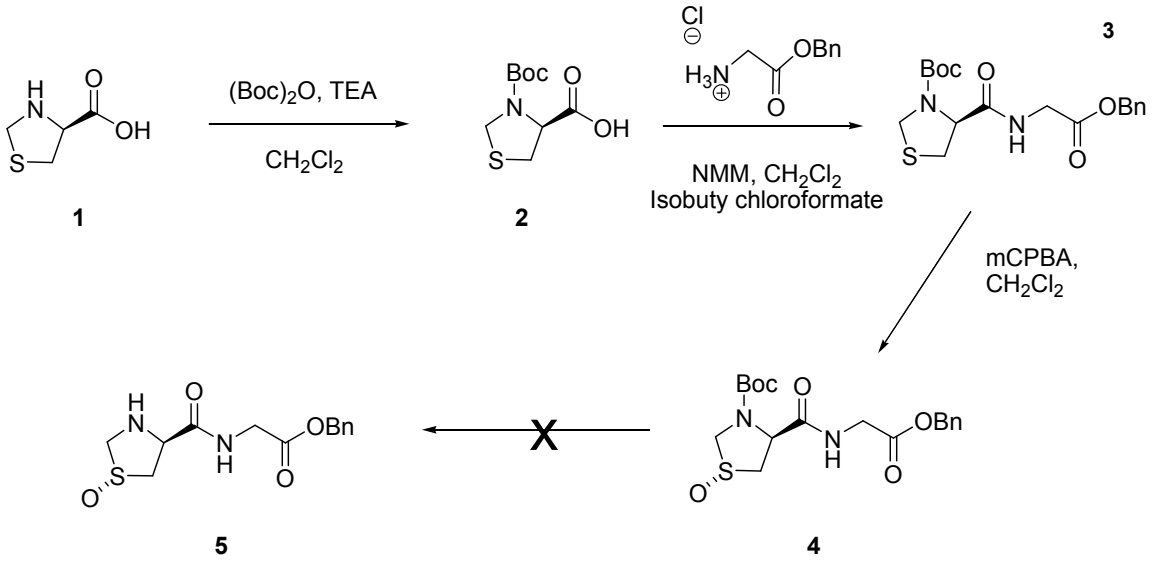

Scheme 1. Attempted approach toward the stereoselective synthesis of amino acid triad N-tert-butoxycarbonyl-prolyl-thiazolidine-2-(R)-carboxylic acid-glycine benzyl ester (7, Pro-Thz-Gly).

Formation of building block core

The synthesis of CRP building block 'Pro-Thz-Gly' triad was initialized by Boc protection of thiazolidine-2-(R)-carboxylic acid with Boc anhydride and TEA in methylene chloride which proceeded in excellent yield (98 %), which allowed for ease in drying the hydrophilic product **2**.[33] The protection of the free amine was required due to the reactivity of the thiazolidine ring systems, and the ring systems propensity for decomposition/ ring opening when left as the unprotected amine.[34, 35] The Boc protected thiazolidine (**2**) was then coupled to glycine benzyl ester via a mixed anhydride coupling using isobutyl chloroformate and NMM to yield (**3**) in a 94 % yield. Initial attempts at this coupling using DCC/HBTU and DIC/HBTU proved less effective (45 % yield), and required longer reaction times as well as more extensive purification than the preferred mixed anhydride coupling. The mixed anhydride coupling required anhydrous reaction

conditions; however this method proved superior due to the high yield and purity of the product as well as shortened reaction times.

The Thz-Gly diamino acid **3** was then oxidized stereoselectively as demonstrated previously,[29] using mCPBA to produce **4** as the desired trans sulfoxide. Subsequent removal of the Boc group of **4** resulted in decomposition of the reactant with no product formation and no starting material recovered. Both TFA and HCl at room temperature and at low temperature produced a nominal amount of the desired product upon attempted removal of the Boc group of the newly formed sulfoxide with no recovery of starting material. The decomposition of the starting material proceeds presumably via an acidolysis, such as that shown in the reversible protection/ deprotection of cystine. However in this case decomposition occurs more rapidly due to the possibility of the extrusion of sulfur dioxide in addition to formaldehyde.[34-36]

The synthesis was then redesigned employing the oxidation step at a later stage in the synthesis such as after the creation of a permanent amide bond between the nitrogen on the thiazolidine ring and the N-terminal proline when the triamino acid building block core was formed. Thus deprotection of the unoxidized product (**3**) was attempted due to the stability of the unoxidized thiazolidine ring system to acidolysis.[34-37] Deprotection of **3** with 4M HCl in dioxane was immediately successful to produce amine hydrochloride **6** which was purified via precipitation at low temperature with hexanes to produce a white solid that was isolated by filtration in good yield (92 %). The white solid (**6**) was stable for long periods of time and did not display many of the hydrophilic properties exhibited by several of the other compounds synthesized. To complete the triamino acid building block Boc protected proline was coupled to the amine salt **6.**

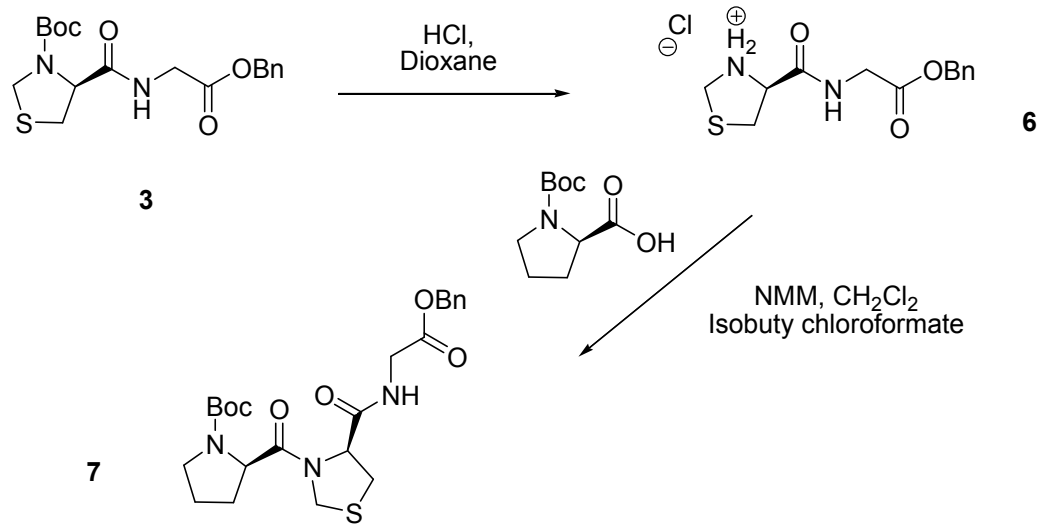

Scheme 2. Completions of scaleable synthesis of N-tert-butoxycarbonyl-prolyl-thiazolidine-2-(R)-carboxylic acid-glycine benzyl ester (7, Pro-Thz-Gly).

Initial attempts using traditional coupling reagents such as mixture of DCC/ DIC and HBTU/ HOBt produced long reaction times and mediocre results at best. Subsequent endeavors at coupling the thiazolidine ring to Boc protected proline were attempted via the mixed anhydride method previously used in the Thz-Gly coupling proved more effective. Aqueous work up of the crude reaction product produced excellent yields (90 %) without need of further purification.

Stereoselective Oxidation

With the Pro-Thz-Gly core of the building block now formed investigation of the stereoselective oxidation of the thiazolidine sulfur atom was pursued. With results from our previous study on the oxidation of monomeric model systems of the thiazolidine sulfur atom[29] the same reaction conditions that produced N-Acetyl-4,R-oxide-Thiazolidine-R-Carboxylic Acid Methyl Ester were pursued to achieve the stereoselective synthesis of Boc-Pro-Thz(O)-Gly-OBn (**8**). Curiously, when the reaction was run with the exact same conditions both yield suffered and reaction times increased. This is presumably due to both the starting material (**7**) and product's (**8**) affinity to aggregate, and mask the thiazolidine sulfur atom that is in the center of the triamino acid building block from the mCPBA reactant thus preventing oxidation. However, increasing the dilution of the reaction starting material by two fold produced the oxidized product (**8**) using the same reaction conditions that were successful upon the monomeric model systems of the sulfur atom of thiazolidine ring without further need of purification and in excellent yields (97 %).

The only observed product from the reaction in scheme 3 is the stereoisomer shown, with the chiral sulfoxide in the trans position relative to the stereochemistry of the thiazolidine alpha carbon as shown in our previous studies, with the crystal structure shown in figure 1 to confirm our findings. Presumably the high stereoselectively of the reaction is from steric preference of the mCPBA to approach the sulfur atom opposite of the carboxyamide moiety on the thiazolidine alpha carbon.[31] The additional presence of steric encumbrance from C(3) and C(4) of the N-terminal proline ring due to the trans

amide bond orientation of proline carboxyamide as well as the use of a polar nonprotic solvent such as methylene chloride aided in the stereospecificity. It has also been hypothesized that the negatively charged oxygen atom of the Thz amino acid could unfavorably interact with the aromatic ring of the mCPBA oxidant, thus driving the reagent to the opposite side of the thiazolidine ring to produce the observed product **8**.[31] These steric and electronic effects add addition tension to those observed in the previously stereoselectively oxidized monomeric model systems, and matching results were obtained in the form of compound **8**.

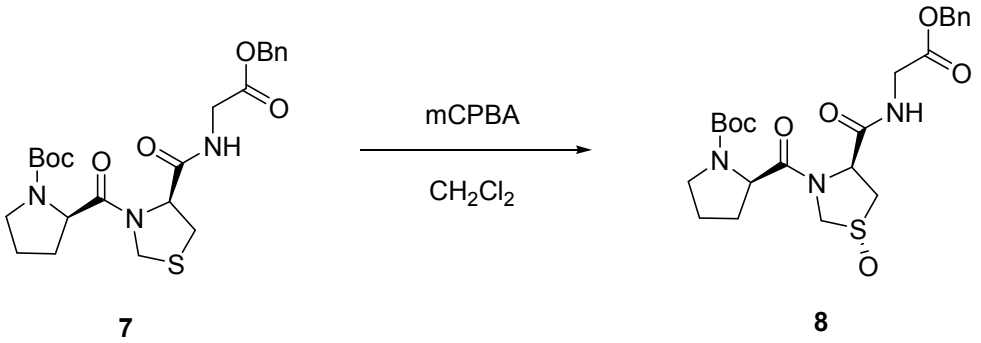

7 **8**

Scheme 3. Stereoselective oxidation of N-tert-butoxycarbonyl-prolyl-thiazolidine-2-(R)-carboxylic acid-glycine benzyl ester (7, Pro-Thz-Gly) triad to N-tert-butoxycarbonyl-prolyl-1(R_s)-oxo-thiazolidine-4-(R)-carboxylic acid-glycine benzyl ester (8, Pro-Thz(O)-Gly) via mCPBA.

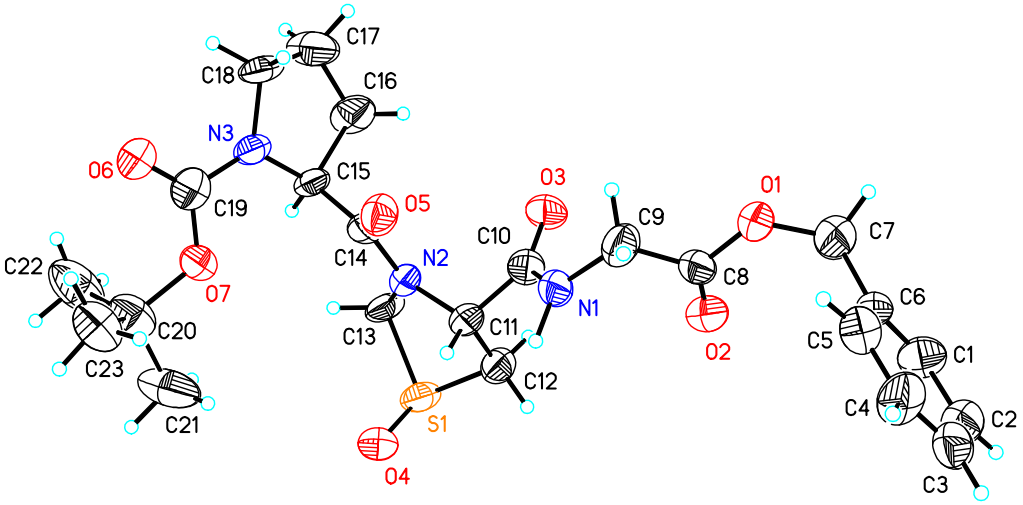

Figure 2. Crystallographically determined structure of N-tert-butoxycarbonyl-prolyl-1(R_s)-oxo-thiazolidine-4(R)-carboxylic acid-glycine benzyl ester (8, Boc-Pro-Thz(O)-Gly-OBn).

Fmoc protection of building blocks

The use of Fmoc protecting groups for automated peptide synthesis has become a widespread technique with a multitude utility.[38, 39] Thus the need to augment the protecting groups of the triamino acid building blocks **7** and **8** for their potential use in automated peptide synthesis. As an initial step attempts were made to remove the C terminal benzyl groups via the traditional method of hydrogenolysis with Palladium on Carbon to produce the free carboxylic acid.[40] Attempts with both the oxidized (**8**) and unoxidized (**7**) triamino acids proved unsuccessful with attrition of a portion of the starting material of both compounds. The presence of sulfur in the thiazolidine ring potentially caused the failed reaction due to sulfur's high affinity for metal binding which could have poisoned the palladium catalyst. Alternative methods for removal of the C terminal benzyl groups were explored, and success was found in a method using a

water/acetonitrile solvent system and a two fold excess of lithium hydroxide to unmask the carboxylic acid moiety on both the oxidized (**8**) and unoxidized (**7**) triamino acids. Subsequently removal of the Boc group from the N terminal proline proved problematic as classic deprotection conditions using TFA provided limited success presumably due to the thiazolidine rings sensitivity to acid hydrolysis.[34, 35, 37, 41, 42] However, hydrochloric acid in dioxane proved capable of removal of the proline Boc group with yields of 98 % for the formation of **10** and 74 % for the formation of **13**. Of particular importance are the purification steps to isolate **10** and **13** as a small amount of methanol is necessary to solvate impurities during the precipitation of both compounds. Without the use of the added methanol an impure brown syrup is isolated; however, a small addition of methanol followed by precipitation with hexanes provided both **10** and **13** in their respective procedures without need of further purification. Finally protection of the N terminal proline was achieved using Fmoc-OSu in aqueous sodium bicarbonate. Initial attempts at Fmoc protection using Fmoc-Chloride proved poor yields; however, the Fmoc-OSu preparation provided the desired products in good yields of both **11** (67 %) and **14** (75 %) in a single step. The overall yields of **11** and **14** were 50 % and 40 % respectively starting from N-tert-butoxycarbonyl-thiazolidine-2-(R)-carboxylic acid (1).

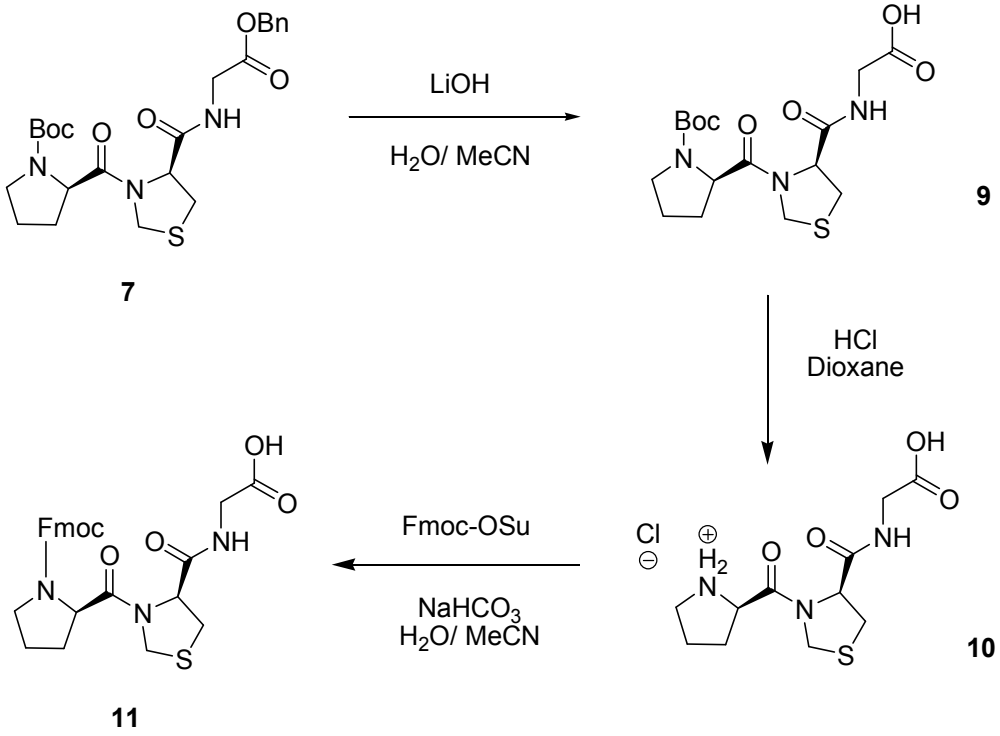

Scheme 4. Protecting group manipulation of unoxidized prolyl-thiazolidine-2-(R)-carboxylic acid-glycine (Pro-Thz-Gly) triad.

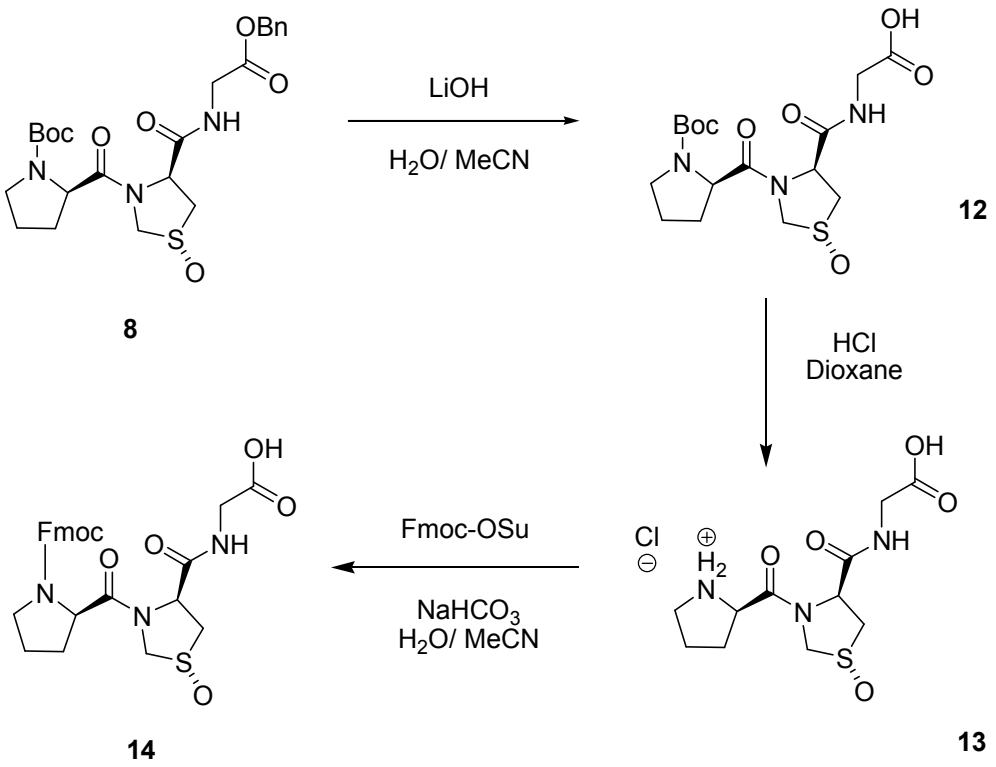

Scheme 5. Protecting group manipulation of N-tert-butoxycarbonyl-prolyl-1(R_s)-oxo-thiazolidine-4-(R)-carboxylic acid-glycine benzyl ester (8, Pro-Thz(O)-Gly).

Analysis of crystal structure of 8

Single crystal X-ray diffraction analysis of **8** produced the crystal structure seen in Figure 2, and confirms the stereochemistry of the sulfoxide group from the oxidation of **7** with mCPBA. The conformation of the thiazolidine ring in compound **8** is remarkably similar to that found in the thiazolidine ring of *N*-acetyl-1(R_s)-oxo-thiazolidine-4-(R)-carboxylic acid methyl ester seen in Figure 1. This is a very encouraging result as the acetyl-methyl ester was made as a model compound to determine the conformational preference of the thiazolidine-R_s-oxide, and in an attempt to predict how the ring conformation would acclimatize to being in an amino acid sequence. The most prominent similarity concerning peptide structure between the model compound and that of the thiazolidine-oxide in the amino acid triad is the trans amide bond. While native proline has a slight preference for the trans amide bond[2] it is often the case that proline can and will adopt a cis amide bond as seen in the crystal structure in Figure 2. This is also the case with the confirmation of the unoxidized thiazolidine carboxylic acid; however, oxidation of the thiazolidine sulfur atom in a stereoselective manner to produce structures shown in Figure 1 and in compound **8** produce qualities similar to those found in native 4-hydroxyproline. These stereoelectronic properties manifest themselves by causing the central thiazolidine in compound **8** to have a distinct preference for the trans amide bond as is observed in the crystal structure in Figure2.

The other predominant property conserved between the model compound in Figure 1 and the thiazolidine ring in Figure 2 is the confirmation of the ring pucker. In both cases the thiazolidine ring has a γ-exo ring pucker, which is the same configuration

seen in native hydroxyproline. [1, 16] The γ-exo ring pucker observed in the central amino acid arises from the same factors that produced the γ-exo ring pucker in the model compound. A series of stereoelectronic effects cause the exo ring pucker with gauche interactions playing a major role in dictating these conformational preferences. The proximity of the sulfur atom to the thiazolidine nitrogen is slightly longer than that observed in native proline (2.59 Å vs. 2.33 Å), but there is still an observable gauche effect between the nitrogen and sulfur atoms with a torsional angle between the two of 40.0°. However, the most pronounced gauche effects are observed between the sulfoxide oxygen and the vicinal δ–carbon as well as the vicinal nitrogen. The torsional angles of the two are 61.77° and 68.04° respectively with the electronegative oxygen siphoning away electron density from both in order to stabilize the molecules overall structure. These two gauche interactions are compounded by additional anti configurations between the sulfoxide oxygen and hydrogens from the δ and β carbons each with anti torsional angles of 178.83° and 172.34 respectively. These anti configurations stabilize the sulfoxide though hyperconjugation thus further reinforcing the γ-exo ring pucker configuration as the most stable. It should also be noted that all of these stereoelectronic effects were seen in the model compound in Figure 1, and that without these stereoelectronic preferences the ring structures becomes more conformationally ambiguous as seen in the proline structure in **8**.

Despite similarities in the major individual structural elements of the thiazolidine moiety there were some divergent values between the model system and compound **8**. In the main chain torsion angle of compound **8** the central thiazolidine amino acid has a

ψ angle value of 138.59. This value is slightly different from those seen in the model compound as well as in other natural amino acids as seen in Table 1. However, the ϕ main chain torsion angle for the Thz amino acid is -55.56, which is very close to the value observed for native hydroxyproline[43]. A summary of this data as well as major conformational preferences of proline and proline analogues provided from crystal structures can be seen in Table 1. It should also be noted that the nitrogens in both proline and the thiazolidine ring in the crystal structure of compound **8** are completely trigonal planar and in conjugation with the corresponding amide bond. Additionally, multiple attempts were made to crystallize the unoxidized triamino acid (**7**) with no success. Among the methods attempted to crystallize **7** were sublimation as well as vapor diffusion and slow evaporation with a variety of polar and nonpolar solvents. Presumably the dynamic nature of the unoxidized form of the thiazolidine amino acid in the triad prevents it from adopting a major preferred conformation needed for crystal growth. Additionally, a Burgi-Dunitz relationship is observed between the amide oxygen and the carboxylate carbon of the central thiazolidine amino acid with an angle of 98.5 ^{o} and a distance between the two atoms of 2.81 angstroms.

Compound	**γ Ring Pucker**	**Amide bond**	**ϕ**	**ψ**
Pro	Endo	Cis	-78.9	176.7
Hyp	Exo	Trans	-56.9	150.8
Thz(O) in **8**	Exo	Trans	-55.56	-138.59
Thz(O)	Exo	Trans	-71.13	161.83

Table 1. Data from crystal structures of proline (pro), native 4-hydroxyproline (hyp), *N*-Acetyl-1(R_s)-oxo-thiazolidine-4-(R)-carboxylic acid Methyl Ester [Thz(O)], and the central thiazolidine-oxide in compound **8**.[43, 44]

Spectral Data

Spectral data for the compounds synthesized confirmed their identity and purity. The chemical shifts for compounds possessing both the unoxidized and oxidized thiazolidine moiety are very similar to those observed from previous studies upon model compounds of the same form. From the similar chemical shifts it can be inferred that the protons exist in similar chemical environments to those observed in the model compounds, as is observed in the similar configurations between the oxidized thiazolidine structure in compound **8** and the corresponding model compound. However, Due to the rotomeric effects from the two prolyl groups as well as the overlap of peaks due to similar chemical shifts the determination of individual coupling constants was impaired in all of the trimeric amino acid compounds. Mass spectral data corresponds with that of the desired compounds, and in many cases the loss of protecting groups can be observed in the fractionation patters of the spectra.

Conclusion

We have shown the ability to synthesize both the unoxidized and oxidized amino acid triad of 'Pro-Thz-Gly'. Oxidation of the sulfur thiazolidine in the triad was accomplished stereoselectively with only one product detected and in good yield. Steric effects from the carbonyl group from the thiazolidine alpha carbon as well as electrostatic considerations from the aryl group of the mCPBA are believed to be the main factors responsible for the high stereoselectivity of this reaction. Additionally, analysis of the

crystal structure of the oxidized triad 'Pro-Thz(O)-Gly' (**8**) provided insight into the structure of the trimeric amino acid repeat and its potential use in synthetic collagens. The crystal structure of the oxidized triad provided support for the use of N-acetyl/ methyl ester amino acids as a viable method for the analysis of the conformational preferences of prolines and pseudoprolines, and for how these structures would perform in a peptide sequence. In both the monomeric model compound as well as the oxidized triad repeat compound **8** the same major configurational elements were observed with each adopting a γ-exo thiazolidine ring pucker and both having a preference for the trans amide bond. These major structural elements arose out of subtle stereoelectronic effects such as the anti configurations observed between the sulfoxide oxygen and vicinal hydrogen atoms. However, the most prominent of these considerations was the gauche effect[24-26] which was observed among the sulfoxide oxygen and vicinal carbons in the thiazolidine ring, as well as between the sulfur and nitrogen atoms in the thiazolidine ring. The gauche interaction observed between the sulfur and nitrogen is slightly unusual due to the fact that the distance between the two atoms is greater than the distance observed in native proline.[45] It is these same gauche interactions that are observed in native 4-hydroxyproline and account for the very similar configurations observed between 4-hydroxyproline and the sulfoxide isostere seen in triad **8**. The similarities between these two compounds enable the possibility of the use of thiazolidine amino acid as a potential Red-Ox active switch for use in biomaterials or as a switch for other proline containing structural motifs. Finally, this study reinforces the importance of exploring the stereoelectronic properties of proline and pseudoprolines due to their immense importance in peptide and protein structures.

Materials and Methods

All chemical reagents were purchased from either Fisher Scientific, Inc. (Pittsburgh, PA) or Sigma-Aldrich Chemical Co. (St. Louis, MO) unless otherwise noted. ^{1}H, ^{19}F and ^{13}C NMR spectra were recorded on a Varian Mercury-300 spectrometer (300MHz for ^{1}H, 75 MHz for ^{13}C), on an Inova-400 spectrometer (400 MHz for ^{1}H, 384 MHz for ^{19}F NMR, 100 MHz for ^{13}C), or an INOVA-600 spectrometer (600 MHz for ^{1}H, 150 MHz for ^{13}C). NMR spectra were recorded on solutions in deuterated chloroform ($CDCl_3$) with residual chloroform (7.26 ppm for ^{1}H NMR and 77.23 ppm for ^{13}C NMR) taken as the internal standard, as well as hexafluorobenzene (-164.9 for ^{19}F NMR) and were reported in parts per million (ppm). Abbreviations for signal coupling are as follows s, singlet; d, doublet; t, triplet; q, quartet; m, multiplet. Electrospray ionization mass spectra were recoded on a JEOL JMS-SX102/SX102A/E mass spectrometer. Analytical Thin Layer Chromatography (TLC) was performed on precoated glass backed plates purchased from Whitman (silica gel 60 F254; 0.25mm thickness). Flash chromatography was carried out with silica gel 60 (230-400 mesh ASTM) from EM Science.

X-Ray Crystallography

The crystals of N-tert-butoxycarbonyl-prolyl-1(R_s)-oxo-thiazolidine-4-(R)-carboxylic acid-glycine benzyl ester (8) used for X-ray structure determination were obtained by dissolving a small amount of white solid in a minimal amount of ethyl acetate followed by a few drops of hexanes. Crystals suitable for X-ray crystallography grew slowly over the course of three weeks time. The tables of atomic coordinates, bond lengths, bond angles, and torsion angles are provided in the appendix 3.

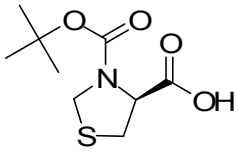

***N-tert*-butoxycarbonyl-thiazolidine-2-(R)-carboxylic acid (1).** A 10g portion of Thiazolidine-2-(S)-carboxylic acid (0.075 moles) in methylene chloride (150 mL) was cooled to 0 ^{o}C open to the atmosphere. Then 18.0 g of di-tert-butyl dicarbonate (0.082 moles) was added to the reaction followed by 11.5 mL of triethylamine (0.082 moles). Reaction was then allowed to warm to room temperature overnight with stirring. Crude reaction mixture was then washed twice with 150 mL portions of aqueous 3M HCl followed by saturated aqueous ammonium chloride. The organic layer was then dried over Na_2SO_4 and the solvent was removed *in vacuo* to yield 17.4 g (0.074 moles) of Boc protected thiocarboxylate as a white solid in 98.6 % yield. mp 129-130 ^{o}C. Rf = 0.6 (ethyl acetate). IR (neat): 2980, 1745, 1635 cm^{-1}. ^{1}H NMR (400 MHz, $CDCl_3$): δ 1.5 (s, 9H), 3.3 (s, 2H), 4.4-4.7 (m, 2H), 4.9 (m, 1H). ESI-MS, Calc. for $C_9H_{15}NO_4S$ [M + H]: 233.0722; found 233.

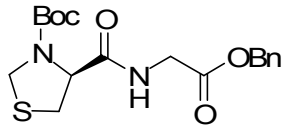

***N-tert*-butoxycarbonyl-thiazolidine-2-(R)-carboxylic acid-glycine-benzyl ester (2).** In 150 mL of anhydrous methylene chloride 19.0 g (81 mmol) of N-tert-butoxycarbonyl-thiazolidine-2-(S)-carboxylic acid (1) was dissolved under argon. The reaction mixture was then cooled to 0 ^{o}C, and 20.4 mL (186 mmol) of N-Methylmorpholine was added to the reaction followed by stirring for 15 min. Then 12.7 mL (97 mmol) of isobutyl chloroformate was then added slowly to the stirring reaction mixture, and the reaction was stirred under argon for 1 hr. Then 17.88 g (89 mmol) of glycine benzyl ester hydrochloride was added to the reaction as a solid in three portions about 5 to 10 minutes apart. The reaction was then allowed to warm to room temperature with stirring for 5 hrs. Reaction is then opened to the atmosphere and washed with 150 mL of 1M aqueous potassium bisulfate solution, and 2 x 100 mL 3M HCl, and the crude reaction mixture is then washed with 2 x 100 mL 3M NaOH. Then methylene chloride layer is then dried over sodium sulfate, filtered, and the solvent was removed *in vacuo* to yield **2** as a yellow oil. The crude oil was the purified by silica gel chromatography using 1:1 hexanes/ ethyl acetate to yield 28.9 g (76 mmol) of purified product in 94 % yield. Rf = 0.6 (1:1 hexanes/ ethyl acetate). ^{1}H NMR (600MHz, $CDCl_3$): δ 1.5 (s, 9H), 3.30 (dd, J = 12 Hz, 6 Hz, 1H), 3.40 (dd, J = 12 Hz, 4 Hz, 1H), 4.05 (d, J = 5.5 Hz, 2H), 4.40 (d, J = 9 Hz, 1H), 4.65 (d, J = 9 Hz, 1H), 4.70 (dd, J = 6 Hz, 4 Hz, 1H), 5.09 (m, 2H), 7.30-7.36 (m, 5H). ^{13}C NMR (150 MHz, $CDCl_3$): δ 26.7, 35.26, 41.38, 66.99, 67.49, 79.5, 126.66, 128.81, 128.88, 135.23, 154.3, 169.83, 171.43. ESI-MS, Calc. for $C_{18}H_{24}N_2O_5S$ [M + H]: 381.1406; found 381.1477

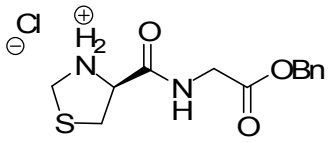

Thiazolidine-2-(R)-carboxylic acid-glycine-benzyl ester amine hydrochloride (3). N-tert-butoxycarbonyl-thiazolidine-2-(S)-carboxylic acid-glycine-benzyl ester (**2**, 27.86 g, 73.3 mmol) is then taken up in approximately 50 mL methylene chloride, and cooled to 0 ^{o}C open to the atmosphere. Then 50 mL of 4M HCl in dioxane is then slowly added to the reaction which is allowed to warm to room temperature overnight. The desired product isolated by cooling the crude reaction mixture to 0 ^{o}C, and then precipitated the product from the crude reaction mixture with hexanes. The resulting white solid was collected by filtration through a medium glass frit. The solid is then washed on the frit with 2 x 15 mL portions of cooled hexanes to yield the desired product (as a white solid without further purification in a 92 % yield (18.74 g, 66.7 mmol). ^{1}H NMR (600MHz, $CDCl_3$): δ 3.07-3.12 (dd, J = 8, 3.4 Hz; 1H), 3.44-3.48 (dd, J = 4, 6.9 Hz; 1H), 3.96-4.24 (m, 5H), 5.10 (m, 2H), 7.32-7.38 (m, 5H), 7.56 (bs, 1H). ^{13}C NMR (150 MHz, $CDCl_3$): δ 35.26, 41.38, 66.99, 67.49, 126.66, 128.81, 128.88, 135.23, 169.83, 171.43. ESI-MS, Calc. for $C_{13}H_{17}ClN_2O_3S$ [M + H]: 316.0648; found 316.

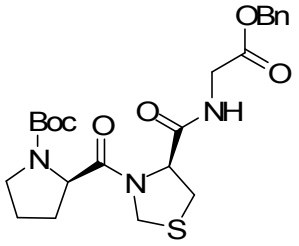

***N-tert*-butoxycarbonyl-prolyl-thiazolidine-2-(R)-carboxylic acid-glycine benzyl ester (7).** *N*-(*tert*-Butoxycarbonyl)-L-proline (9.4 g, 43.7 mmol) was dissolved in 150 mL

anhydrous methylene chloride and cooled to 0 ^{o}C under argon. N-Methylmorpholine (9.6 mL, 86.8 mmol) was then added to the reaction mixture followed by stirring for 15 min. Isobutyl chloroformate (6.12 mL, 46.8 mmol) was then added slowly to the reaction mixture, and the reaction was stirred under argon for 1 hr. **3** (12.48 g, 39.4 mmol) was then added to the reaction mixture in two portions so as not to evoke too vigorous a reaction. The reaction mixture was allowed to warm to room temperature over a 12 hr period with stirring under argon. The crude reaction mixture was then worked up by washing with 150 ml of 1M aqueous potassium bisulfate solution then 2 x 100 mL 3M HCl followed by 2 x 100 mL 3M sodium hydroxide. The methylene chloride layer was then dried over sodium sulfate and the solvent was removed *in vacuo* to yield a clear oil in 90 % yield (18.74 g, 39.3 mmol). ^{1}H NMR (600MHz, $CDCl_3$): δ 1.37 (1.42, s, 9H), 1.53-2.28 (m, 6H), 2.98-3.19 (m, 1H), 3.34-3.53 (m, 2H), 3.69-3.71 (m, 0.5H), 3.86-3.95 (m, 1H), 4.11-4.21 (m, 1H), 4.33-4.52 (m, 1.5H), 4.63-4.78 (m, 1H), 5.08-5.18 (m, 2H), 7.28-7.36 (m, 5H). ^{13}C NMR (150 MHz, $CDCl_3$): δ 25.09 (24.79), 28.55 (29.39), 34.01 (34.94), 42.00 (41.71), 47.25, 49.73 (49.54), 58.70, 63.16, 67.17, 80.55, 128.43, 128.58, 128.81, 135.55, 155.09, 169.37, 169.90, 171.77. ESI-MS, Calc. for $C_{23}H_{31}N_3O_6S$ [M + H]: 478.1934; found 478.1997

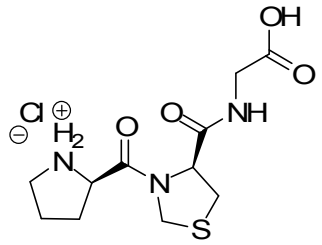

Prolyl amine hydrochloride-thiazolidine-2-(R)-carboxylic acid-glycine (10).

9 (12.06 g, 25 mmol) was taken up in 50 mL acetonitrile and cooled to 0 ^{o}C, and 100 mL of 1M lithium hydroxide was added. The reaction was allowed to stir for 1 hr at low temperature, and then taken out of the ice bath and allowed to stir at room temperature for an additional 4 hours. The crude reaction mixture was then reduced in volume *in vacuo*, and then extracted with 2 x 75 mL of 1:1 hexane/ethyl acetate. The aqueous portion is then acidified with concentrated sulfuric acid, and then extracted 3 x 75 mL methylene chloride. The combined methylene chloride extracts were then dried over sodium sulfate and condensed to yield the free acid as a clear oil. The clear oil was then taken up in 30 mL methylene chloride and cooled to 0 ^{o}C open to the atmosphere. Then 30 mL of 4M HCl in dioxane were then added slowly to the reaction mixture. The reaction is then allowed to stir over night to form a brown oil from which the solvent is decanted. The oil is then taken up in methylene chloride with a small amount of methanol, and precipitated using hexanes to yield a white solid that is then collected via filtration. The solid is then rinsed with hexanes 2 x 50 mL to remove any further impurities. 8.04g (24.8 mmol) of **10** in 98 % yield were isolated, and were without need of further purification. ^{1}H NMR (600MHz, $CDCl_3$): δ 1.55-2.30 (m, 6H), 3.01-3.19 (m, 1H), 3.35-3.57 (m, 2H), 3.70-3.72 (m, 0.5H), 3.88-3.97 (m, 1H), 4.11-4.21 (m, 1H), 4.33-4.52 (m, 1.5H), 4.63-4.78 (m, 1H). ^{13}C NMR (150 MHz, $CDCl_3$): δ 25.09 (24.79), 28.55

(29.39), 34.01 (34.94), 42.00 (41.71), 47.25, 49.73 (49.54), 58.70, 63.16, 67.17, 80.55, 128.43, 128.58, 128.81, 135.55, 155.09, 169.37, 169.90, 171.77. ESI-MS, Calc. for $C_{11}H_{18}ClN_3O_4S$ [M - H]: 322.0707; found 322.0632.

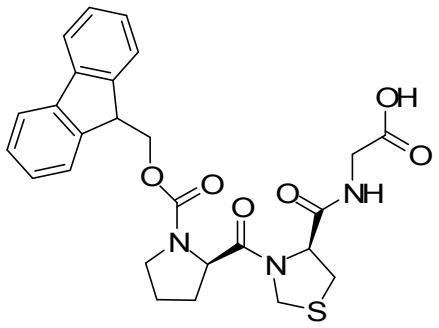

***N*-9-Fluorenylmethoxycarbonyl-prolyl-thiazolidine-2-(R)-carboxylic acid-glycine (11).** The hydrochloride salt **10** (8.04g, 24.8 mmol) was dissolved in 100 mL of a 1M aqueous sodium bicarbonate solution, and solid sodium bicarbonate was added until the solution reached a constant pH of 8. Solid 9-Fluorenylmethyl *N*-succinimidyl carbonate (Fmoc-OSu) was then added in one portion followed by 75 mL of acetonitrile to ensure all reagents were in solution. The reaction was then allowed to stir for 24 hours at room temperature open to the atmosphere. The reaction was then worked up by removing excess solvent *in vacuo*, and the partitioning the reaction mixture between 75 mL of water and 100 mL hexanes. The organic layer was then backextracted with 25 mL water, and then acidified with solid potassium hydrogen sulfate to a pH of 7. The aqueous layers were combined then taken to a pH of 3 using 6M HCl, and then extracted with 3 x 100 mL methylene chloride. The organic layer was then dried over sodium sulfate and the solvent was removed *in vacuo* to yield the desired product **11** (8.25 g, 1.6 mmol) as a white solid in a 67 % yield. ^{1}H NMR (600MHz, $CDCl_3$): δ 1.55-2.30 (m, 6H), 2.98-3.19

(m, 1H), 3.34-3.53 (m, 2H), 3.69-3.71 (m, 0.5H), 3.86-3.95 (m, 1H), 4.11-4.21 (m, 1H), 4.24-4.52 (m, 4.5H), 4.63-4.78 (m, 1H), 7.36-7.89 (m, 8H). ESI-MS, Calc. for $C_{26}H_{27}N_3O_6S$ [M + H]: 510.1621; found 510.1693

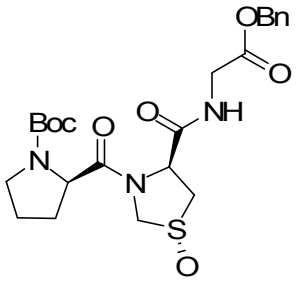

N-*tert*-butoxycarbonyl-prolyl-1(R_s)-oxo-thiazolidine-4-(R)-carboxylic acid-glycine benzyl ester (8). **7** (1 g, 2 mmol) was dissolved in 75 mL methylene chloride and cooled to 0 ^oC open to the atmosphere. 0.51 g of mCPBA (2.3 mmol) was added to the reaction mixture and allowed to warm to room temperature overnight with stirring. The reaction was then worked up by the addition of solid sodium bicarbonate, and the reaction was allowed to stir for one hour. The crude reaction mixture was then extracted 2 x 75 mL of sat. aq. sodium bicarbonate then dried over sodium sulfate and filtered. The solvent was removed *in vacuo* to yield pure **8** which did not require further purification as a white solid (0.92 g, 1.94 mmol) in a 97 % yield. ^1H NMR (600MHz, $CDCl_3$): δ 1.33 (s, 9H), 1.78-2.29 (m, 4H), 3.00-3.30 (m, 0.5H), 3.32-3.80 (m, 4H), 3.89-4.21 (m, 2.5H), 4.49-4.61 (m, 1H), 4.80-4.95 (m, 0.5H), 5.04-5.16 (m, 2.5H), 5.62-5.66 (5.43, m, 1H), 7.27-7.35 (m, 5H). ^{13}C NMR (150 MHz, $CDCl_3$): δ 24.96, 29.65, 34.18, 41.81, 48.52, 49.45, 60.07, 62.61, 70.07, 80.34, 128.53, 128.54, 128.91, 134.45, 154.94, 169.87, 170.09, 175.32. ESI-MS, Calc. for $C_{23}H_{31}N_3O_7S$ [M + H]: 494.1883; found 494.1847.

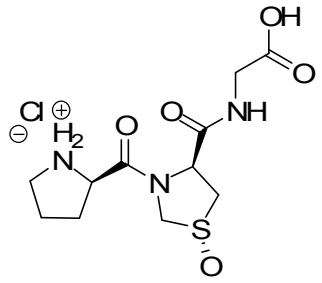

Prolyl amine hydrochloride-1(R_s)-oxo-thiazolidine-4(R)-carboxylic acid-glycine (13). **8** (2.56 g, 5.1 mmol) was taken up in 25 mL acetonitrile and cooled to 0 ^{o}C, and 50 mL of 1M lithium hydroxide was added. The reaction was allowed to stir for 1 hr at low temperature, and then taken out of the ice bath and allowed to stir at room temperature for an additional 4 hours. The crude reaction mixture was then reduced in volume *in vacuo*, and then extracted with 2 x 75 mL of 1:1 hexane/ethyl acetate. The aqueous portion is then acidified with concentrated sulfuric acid, and then extracted 3 x 75 mL methylene chloride. The combined methylene chloride extracts were then dried over sodium sulfate and condensed to yield the free acid as a clear oil. The clear oil was then taken up in 30 mL methylene chloride and cooled to 0 ^{o}C open to the atmosphere. 30 mL of 4M HCl in dioxane were then added slowly to the reaction mixture. The reaction is then allowed to stir over night to form a brown oil from which the solvent is decanted. The oil is then taken up in methylene chloride with a small amount of methanol, and precipitated using hexanes to yield a white solid that is then collected via filtration. The solid is then rinsed with hexanes 2 x 50 mL to remove any further impurities. 1.31 g (3.87 mmol) of **10** in 74 % yield were isolated, and were without need of further purification. ^{1}H NMR (600MHz, $CDCl_3$): δ 1.82-2.32 (m, 4H), 3.10-3.33 (m, 0.5H), 3.42-3.86 (m, 4H), 3.90-4.31 (m, 2.5H), 4.51-4.31 (m, 1H), 4.82-5.00 (m, 0.5H), 5.06-

5.18 (m, 2H), 5.72-5.79 (5.43, m, 1H), 9.68 (bs, 1H). ESI-MS, Calc. for $C_{11}H_{18}ClN_3O_5S$ [M + H]: 340.0656; found 340.0643.

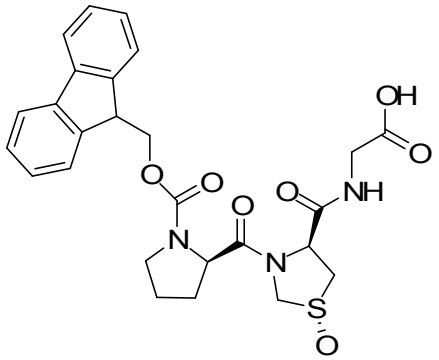

***N*-9-Fluorenylmethoxycarbonyl-prolyl-1(R_s)-oxo-thiazolidine-4(R)-carboxylic acid-glycine (14). 13** (0.52 g, 1.53 mmol) was dissolved in 10 mL of a 1M aqueous sodium bicarbonate solution, and solid sodium bicarbonate was added until the solution reached a constant pH of 8. Solid 9-Fluorenylmethyl *N*-succinimidyl carbonate (Fmoc-OSu) was then added in one portion followed by 7 mL of THF to ensure all reagents were in solution. Reaction was then allowed to stir for 24 hours at room temperature open to the atmosphere. The reaction was then worked up by removing excess solvent *in vacuo*, and the crude reaction mixture was taken up in 40 mL of water, and extracted with 2 x 30 mL hexanes. The aqueous layer was then taken to a pH of 3 using 6M HCl, and then extracted with 3 x 60 mL methylene chloride. The organic layer was then dried over sodium sulfate and the solvent was removed *in vacuo* to yield the desired product **11** (0.61 g, 1.1 mmol) as a white solid in a 75 % yield. ^{1}H NMR (600MHz, $CDCl_3$): δ 1.82-2.32 (m, 4H), 3.10-3.33 (m, 0.5H), 3.42-3.86 (m, 4H), 3.90-4.31 (m, 4.5H), 4.51-4.31 (m, 1H), 4.82-5.00 (m, 0.5H), 5.06-5.18 (m, 2H), 5.72-5.79 (5.43, m, 1H), 7.35-7.91 (m, 8H), 9.68 (bs, 1H). ESI-MS, Calc. for $C_{26}H_{27}N_3O_7S$ [M - H]: 524.1570; found 524.1564.

References

[1] Raines, R. T., *Protein Sci* **2006,** 15, (5), 1219-25.

[2] Wedemeyer, W. J.; Welker, E.; Scheraga, H. A., *Biochemistry* **2002,** 41, 14637-14644.

[3] Vanhoof, G.; Goossens, F.; De Meester, I.; Hendriks, D.; Scharpe, S., *Faseb J* **1995,** 9, (9), 736-44.

[4] Smith, A. D., *Oxford Dictionary of Biochemistry and Molecular Biology*. Oxford University Press: Oxford, UK, 2003.

[5] Ricard-Blum, S.; Ruggiero, F.; van der Rest, M., *Top Curr Chem* **2005,** 247, 35-84.

[6] Veit, G.; Kobbe, B.; Keene, D. R.; Paulsson, M.; Koch, M.; Wagener, R., *J. Biol Chem.* **2006,** 281, 2494-3504.

[7] Jenkins, C. L.; Raines, R. T., *Nat Prod Rep* **2002,** 19, (1), 49-59.

[8] Brodsky, B.; Persikov, A. V., *Adv Protein Chem* **2005,** 70, 301-39.

[9] Bella, J.; Eaton, M.; Brodsky, B.; Berman, H. M., *Science* **1994,** 266, (5182), 75-81.

[10] Myllyharju, J., *Matrix Biol* **2003,** 22, (1), 15-24.

[11] Berg, R. A.; Prockop, D. J., *Biochem Biophys Res Commun* **1973,** 52, (1), 115-20.

[12] Burjanadze, T. V., *Biopolymers* **2000,** 53, (6), 523-8.

[13] Friedman, L.; Higgin, J. J.; Moulder, G.; Barstead, R.; Raines, R. T.; Kimble, J., *Proc Natl Acad Sci U S A* **2000,** 97, (9), 4736-41.

[14] Holster, T.; Pakkanen, O.; Soininen, R.; Sormunen, R.; Nokelainen, M.; Kivirikko, K. I.; Myllyharju, J., *J Biol Chem* **2007,** 282, (4), 2512-9.

[15] Hodges, J. A.; Raines, R. T., *Org Lett* **2006,** 8, (21), 4695-7.

[16] Shoulders, M. D.; Hodges, J. A.; Raines, R. T., *J Am Chem Soc* **2006,** 128, (25), 8112-3.

[17] Bella, J.; Brodsky, B.; Berman, H. M., *Structure* **1995,** 3, (9), 893-906.

[18] Suzuki, E.; Fraser, R. D. B.; MacRae, T. P., *Int. J. Biol. Macromol* **1980,** 2, 54-56.

[19] Nemethy, G., Collagen 1. In Nimni, M. E., Ed. CRCPress: Boca Raton, FL, 1988; pp 79-94.

[20] Ramachandran, G. N.; Bansal, M.; Bhatnagar, R. S., *Biochim. Biophys. Acta.* **1973,** 322, 166-171.

[21] Shoulders, M. D.; Guzei, I. A.; Raines, R. T., *Biopolymers* **2008,** 89, (5), 443-54.

[22] Kim, W.; Hardcastle, K. I.; Conticello, V. P., *Angew Chem Int Ed Engl* **2006,** 45, (48), 8141-5.

[23] Hodges, J. A.; Raines, R. T., *J AM CHEM SOC* **2003,** 125, 9262-9263.

[24] Bretscher, L. E.; Jenkins, C. L.; Taylor, K. M.; DeRider, M. L.; Raines, R. T., *J Am Chem Soc* **2001,** 123, (4), 777-8.

[25] DeRider, M. L.; Wilkens, S. J.; Waddell, M. J.; Bretscher, L. E.; Weinhold, F.; Raines, R. T.; Markley, J. L., *J Am Chem Soc* **2002,** 124, (11), 2497-505.

[26] Doi, M.; Nishi, Y.; Uchiyama, S.; Nishiuchi, Y.; Nakazawa, T.; Ohkubo, T.; Kobayashi, Y., *J Am Chem Soc* **2003,** 125, (9922-9923).

[27] Fietzek, P. P.; Kuhn, K., *Mol Cell Biochem* **1975,** 8, (3), 141-57.

[28] Engel, J.; Bachinger, H. P., *Top Curr Chem* **2005,** 247, 7-33.

[29] Shugart, J.; Hardcastle, K. I.; Conticello, V. P., *unpublished results.*

[30] Holmgren, S. K.; Bretscher, L. E.; Taylor, K. M.; Raines, R. T., *Chemistry & Biology* **1999,** 6, (2), 63-70.

[31] Kanai, K.; Podanyi, B.; Bokotey, S.; Hajdu, F.; Hermecz, I., *Tetrahedron: Asymmetry* **2002,** 13, 491-495.

[32] Betts, M.; Pritchard, R. G.; Schofield, A.; Stoodley, R.; Vohra, S., *Journal of the Chemical Society, Perkin Transations 1: Organic and Bio-Organic Chemistry* **1999,** 8, 1067-1072.

[33] Threadgill, M. D.; Gledhill, J. P., *J. Org. Chem.* **1989,** 54, 2940-2949.

[34] Nachtergaele, W. A.; Anteunis, J. O., *Bull Soc Chim Belg* **1980,** 89, 749-758.

[35] Ratner, s.; Clarke, H. T., *J Am Chem Soc* **1937,** 59, 200-206.

[36] Wohr, R.; Wahl, F.; Nefzi, A.; Rohwedder, B.; Sato, T.; Sun, X.; Mutter, M., *J. Am. Chem.Soc* **1996,** 118, 9218-9227.

[37] Vanwetswinkel, S.; Carlier, V.; Marchand-Brynaert, J.; Fastrez, J., *Tetrahedron letters* **1996,** 37, (16), 2761-2762.

[38] Chan, W. C.; White, P. D., *Fmoc Solid Phase Peptide Synthesis: A Practical Approach*. Oxford University press: Oxford, UK, 2000.

[39] Fukuda, H.; Imajoh-Ohmi, S., *Tanpakushitsu Kakusan Koso* **2004,** 49, (11 Suppl), 1527-33.

[40] Dutton, F. E.; Lee, B. H.; Johnson, S. S.; Coscarelli, E. M.; Lee, P. H., *J Med Chem* **2003,** 46, (11), 2057-73.

[41] Brown, F. C., In *Chemical Reviews*, Washington, DC, 1961; Vol. 61, pp 463-521.

[42] Singh, S. P.; S.S., P.; K., R.; Stenberg, v. I., In *Chemical Reviews*, Washington DC, 1981; Vol. 81 (2), pp 175-203.

[43] Jenkins, C. L.; Bretscher, L. E.; Guzei, I. A.; Raines, R. T., *J Am Chem Soc* **2003,** 125, (21), 6422-7.

[44] Jenkins, C. L.; McCloskey, A. I.; Guzei, I. A.; Eberhardt, E. S.; Raines, R. T., *Biopolymers* **2005,** 80, (1), 1-8.

[45] Panasik, N., Jr.; Eberhardt, E. S.; Edison, A. S.; Powell, D. R.; Raines, R. T., *Int J Pept Protein Res* **1994,** 44, (3), 262-9.

CHAPTER 4

Conclusions

Conclusions

The use of monomeric model compounds as a method for the evaluation of prolyl structures has been shown to be successful by our group as well as others. Crystal structures from such compounds provide access to critical structural data to evaluate the prolyl group's potential impact upon peptide structure. The purpose of these experiments was to find a pseudoproline structure that could act as a Red-Ox switch for the self-assembly of peptides structure through stereoselective oxidation. Specifically, in pursuit of an amino acid to assume the Yaa position of the 'Xaa-Yaa-Gly' triad repeat in collagen that could facilitate self-assembly of collagen structure. The synthetic amino acid replacement would need to possess similar structural characteristics to (2S, 4R)-4-hydroxyproline (Hyp) that occupies the Yaa position in most native collagen, as well as possess a conformationally dynamic structure parallel to proline in its unoxidized form.

The beginning pursuit of such a Red-Ox switch led to experimentation with thiazolidine-4-carboxylic acid (Thz), which possessed a sulfur atom at the structurally critical γ position of the prolyl ring. N-acetyl-4-thiazolidine-R-carboxylic acid methyl ester was synthesized and used as a model system for the determination of diastereoselectivity of various reagents. The use of meta-chloroperoxybenzoic acid offered excellent results providing the trans sulfoxide in high yields, as well as the production of a single diastereomeric product, N-acetyl-1(R_s)-oxo-thiazolidine-4-(R)-carboxylic acid methyl ester. Conversely, oxidation using sodium periodate at elevated temperatures with polar protic solvents produced a mixture of diastereomers. Ultimately, this was the most efficient method to access the cis sulfoxide N-acetyl-1(S_s)-oxo-

thiazolidine-4-(R)-carboxylic acid methyl ester for study. Crystal structures were obtained for the epimeric pair of sulfoxides, while repeated attempts at the crystallization of the unoxidized thioproline were unsuccessful. The crystal structures of both sulfoxides provided insight into the subtle stereoelectronic preferences that govern prolyl ring structure. For the cis sulfoxide gauche effects were observed between the sulfoxide oxygen and both the thiazolidine nitrogen and α-carbon atom. A gauche configuration was also observed between the thiazolidine sulfur and nitrogen atoms. These configurations although not unusual are of interest due to the increased size of the thiazolidine ring compared to that of the pyrrolidine ring of proline. Despite the longer carbon-sulfur bonds gauche effects were still conformationally important in both sulfoxides. The cis sulfoxide's gauche interactions are reinforced due to hyperconjugation from anti configurations between the sulfoxide oxygen and the vicinal hydrogens from the β and δ carbons. Additionally, a Burgi-Dunitz trajectory was observed between the sulfoxide oxygen and the ester carbonyl carbon through a cooperative diaxial interaction. This interaction led to a cis amide bond in the crystal structure of the cis sulfoxide, and to a lessened preference of the trans amide bond in solution. All of these stereoelectronic effects produced a pseudoproline that possessed a γ-endo ring pucker, and main chain dihedral angles that would not be advantageous in a peptide structure. These physical properties as well as the synthetic inaccessibility made the cis sulfoxide a poor choice for peptide incorporation.

The trans sulfoxide was subject to many of the same stereochemical effects that the cis sulfoxide experienced as observed in the crystal structure of the trans compound. Gauche effects between the sulfoxide oxygen and both thiazolidine nitrogen and α-

carbon atom, as well as anti configurations between the sulfoxide oxygen and vicinal hydrogens from the β and δ carbons were also observed. However, the trans sulfoxide possessed torsional angles in these configurations that are very close to ideal values, and led to a pseudoaxial sulfoxide configuration with a γ-exo ring pucker. This thiazolidine ring pucker allowed for the traditional n to π^* interactions that cause a large preference for the trans amide bond. Thus the trans sulfoxide possessed the major structural characteristics of native 4-hydroxyproline with crystal structure, NMR, and computational data all in agreement over the conformation. These results in conjunction with the easy synthetic access from high yields and stereoselectivity of the reaction with meta-chloroperoxybenzoic acid make the trans sulfoxide an ideal candidate for incorporation into synthetic collagen.

The production of a synthetic collagen containing thiazolidines would present a nontrivial task as thiazolidines are known to be prone to decomposition and are highly reactive. To circumvent this problem the collagen triad repeat of 'Pro-Thz-Gly' would be assembled and studied before peptide synthesis was attempted. The synthesis of the amino acid trimer started with the protection of the thiazolidine free amine followed by coupling to benzyl glycine. The subsequent deprotection proved to be very sensitive to decomposition, but was accomplished and followed by coupling to proline forming the amino acid triad. All coupling reaction were achieved via mixed anhydride reactions and the incorporation of thiazolidine-4-carboxylic acid was accomplished in good overall yield. The stereoselectivity of the oxidation of the amino acid trimer was then tested using the previously successful meta-chloroperoxybenzoic acid as an oxidant. Indeed, the same results were found with the stereoselective oxidation of the thiazolidine sulfur

atom achieved in high yield with only one diastereomer detected. A crystal structure of the stereoselectively formed trimer 'Pro-Thz(O)-Gly' was obtained and studied. The crystal structure for the 'Pro-Thz(O)-Gly' possessed structural characteristics very similar to those seen in the native collagen repeat of 'Pro-Hyp-Gly'. Additionally the central amino acid, oxidized thiazolidine-4-carboxylic acid, possessed the same structural characteristics as the analogous monomeric model compound previously studied. This is a very encouraging result as it adds to previous evidence that N-acetyl-prolyl methyl esters are excellent measures for predicting prolyl structure in peptides. It should also be noted that extensive attempts were made to crystallize the unoxidized compound 'Pro-Thz-Gly' with no success just as with the monomeric model compound.

Protecting group manipulation of both the oxidized and unoxidized triads produced the corresponding Fmoc protected compounds for use in peptide synthesis. As yields for the unoxidized triad 'Pro-Thz-Gly' were higher and the unoxidized triad is more thermodynamically stable it was chosen as the compound to use for exploratory synthesis of collagen-mimic peptides. The unoxidized triad was loaded onto a Tentagel S-RAM resin for use in automated peptide synthesis. Subsequently, multiple attempts were made to synthesize a ten triad repeat peptide of the unoxidized triamino acid building block. At best only trace amounts of the desired peptide were observed via mass spectra.

In conclusion, the stereoselective synthesis of a thiazolidine sulfoxide model compounds was accomplished, and their structures were studied for potential suitability as a Red-Ox active switch for peptide self-assembly. The trans sulfoxide diastereomer proved to have structural characteristics similar to native 4-hydroxyproline in both the

monomeric model form as well as in the central amino acid in the triad of ‘Pro-Thz(O)-Gly’. The oxidized form of this thiazolidine amino acid presents a novel method to potentially induce stabilized peptide structures through stereoselective oxidation. This Red-Ox active thiazolidine amino acid has future potential applications as a switch for macroscale peptide and protein self assembly in biomedical engineering.

APPENDIX 1

NMR Data

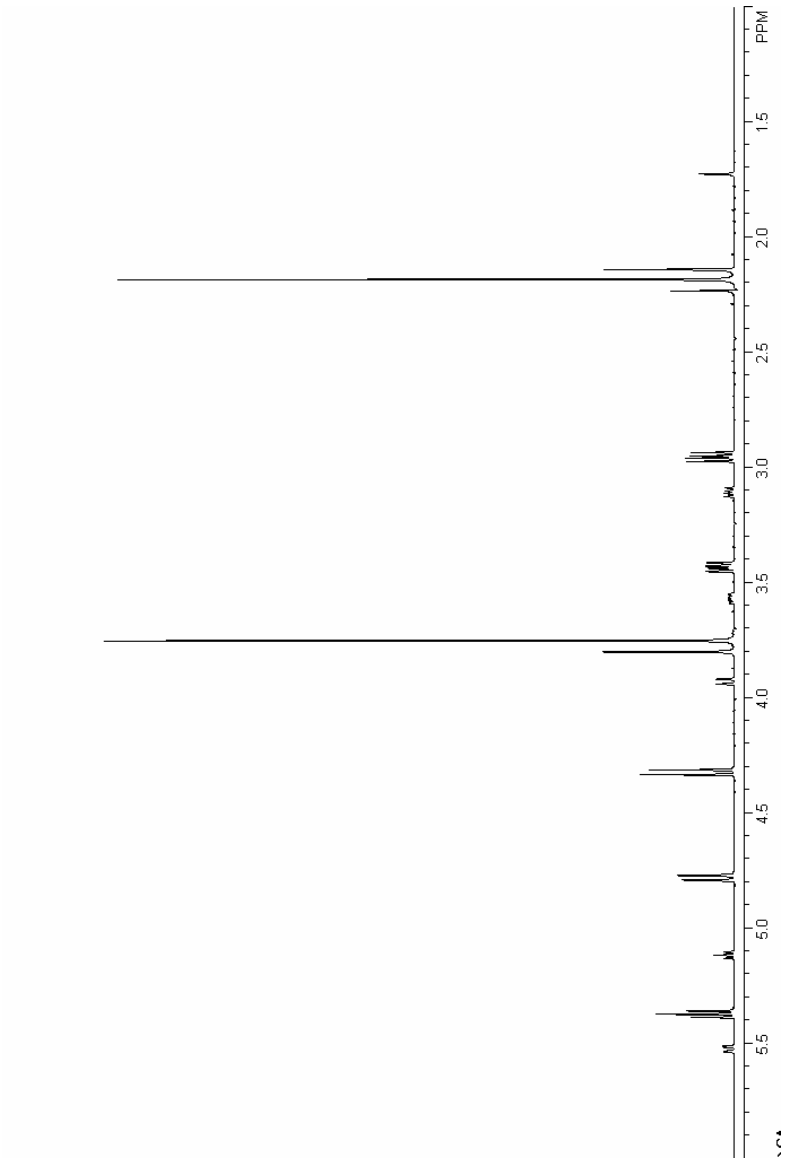

Spectra 1. Full proton spectra of N-Acetyl-1(Rs)-oxo-thiazolidine-4-(R)-carboxylic acid Methyl Ester (Major).

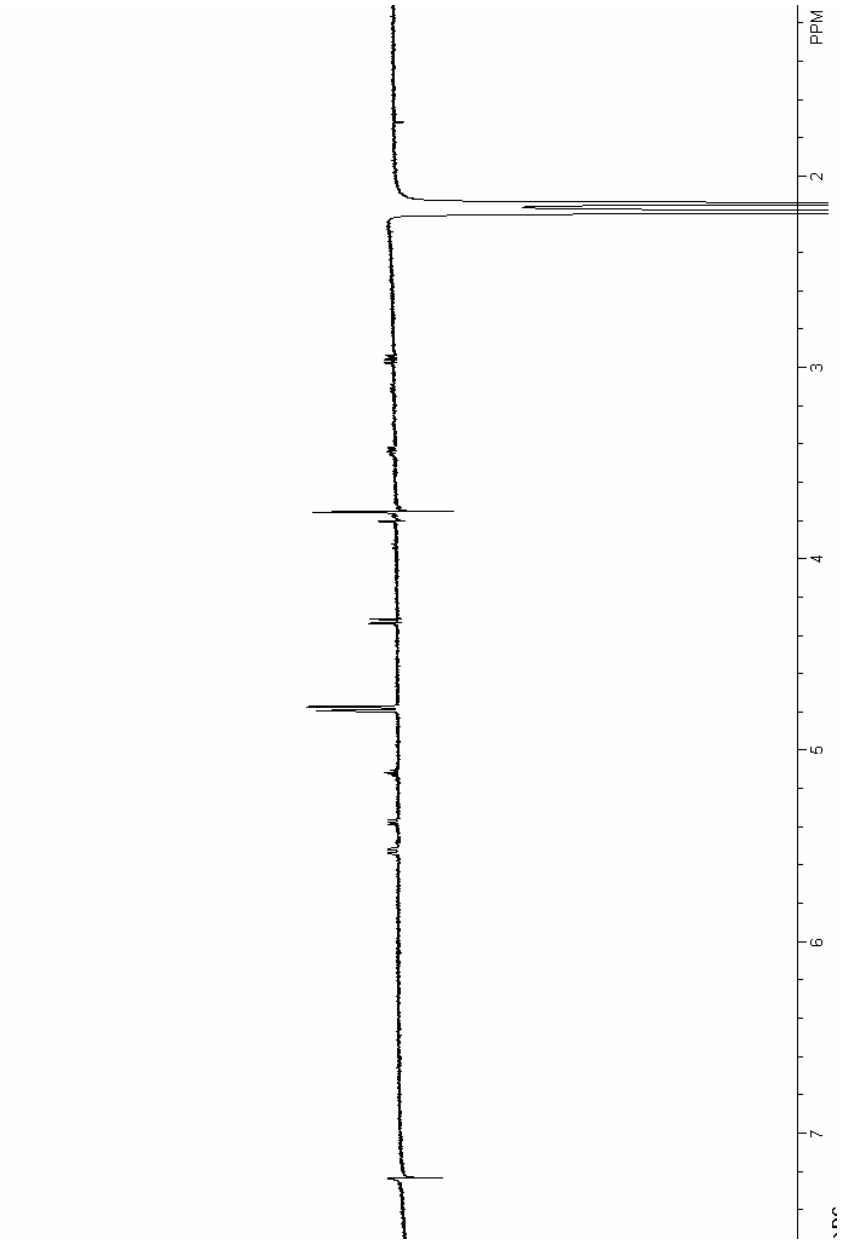

Spectra 2. 1D NOE of N-Acetyl-1(Rs)-oxo-thiazolidine-4-(R)-carboxylic acid Methyl Ester with irradiation at 2.18.

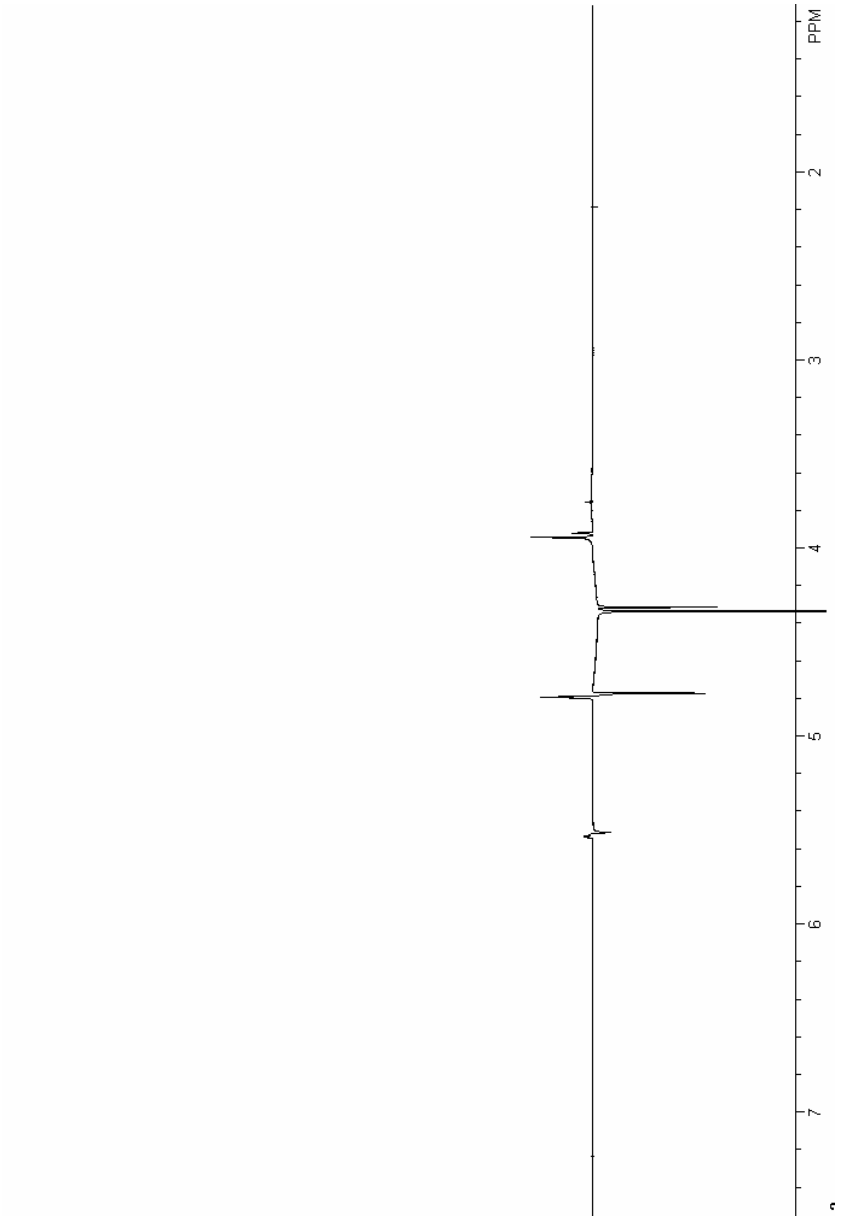

Spectra 3. 1D NOE of N-Acetyl-1(Rs)-oxo-thiazolidine-4-(R)-carboxylic acid Methyl Ester with irradiation at 4.34ppm (398.5).

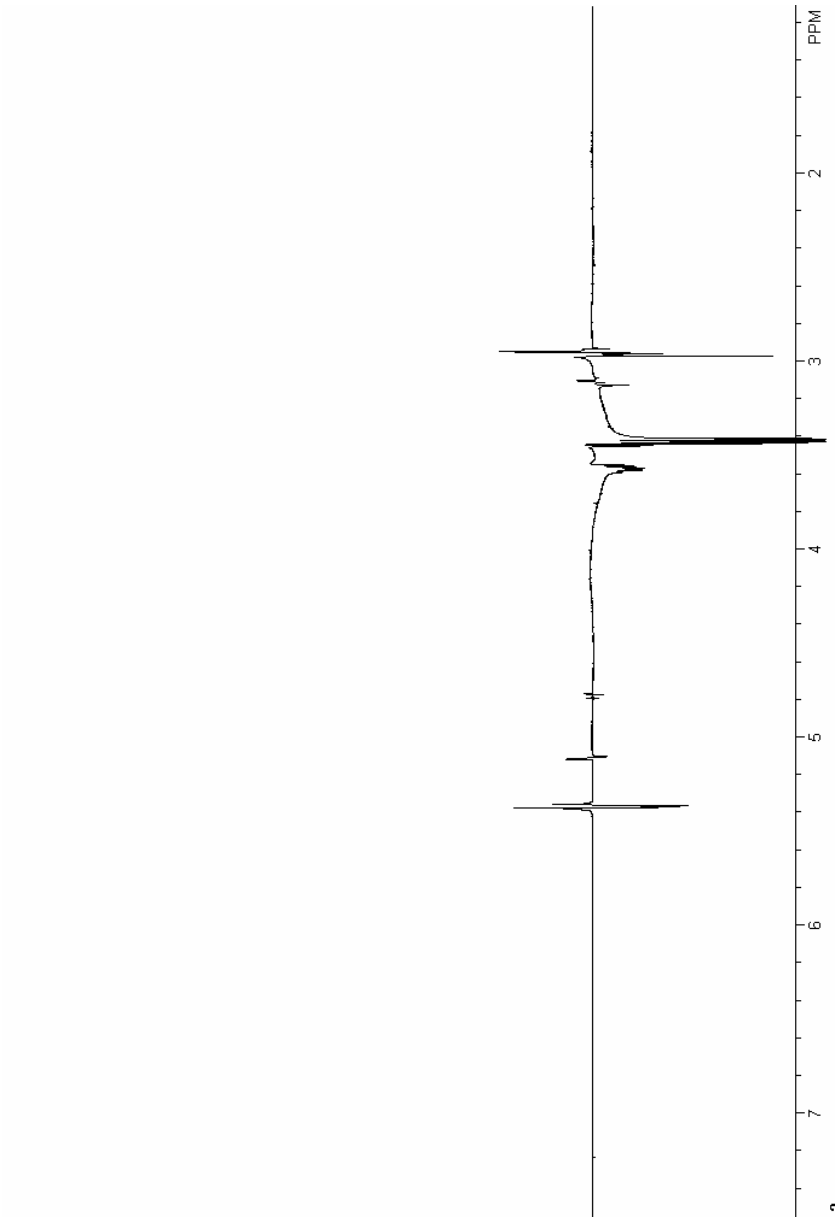

Spectra 4. 1D NOE of N-Acetyl-1(Rs)-oxo-thiazolidine-4-(R)-carboxylic acid Methyl Ester with irradiation at 3.43 ppm (943.4).

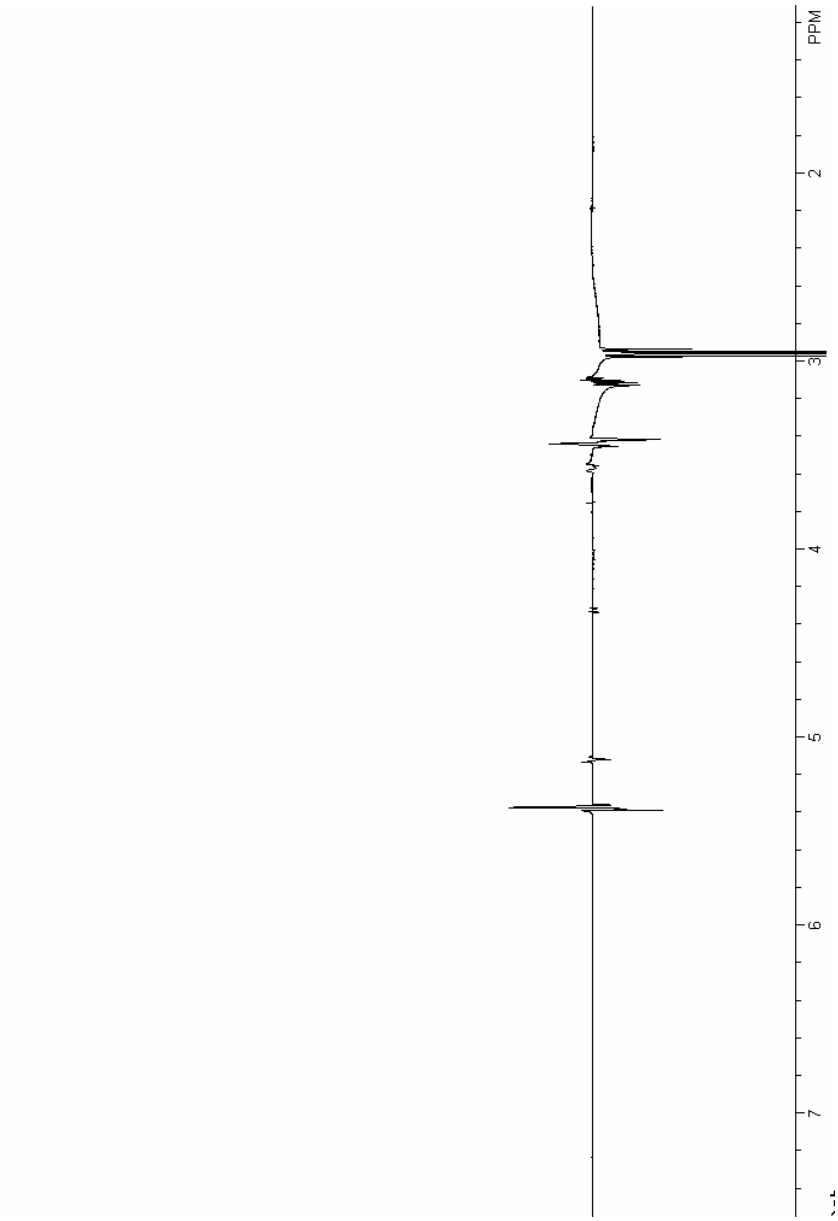

Spectra 5. 1D NOE of N-Acetyl-1(Rs)-oxo-thiazolidine-4-(R)-carboxylic acid Methyl Ester with irradiation at 2.96 ppm (1223.0).

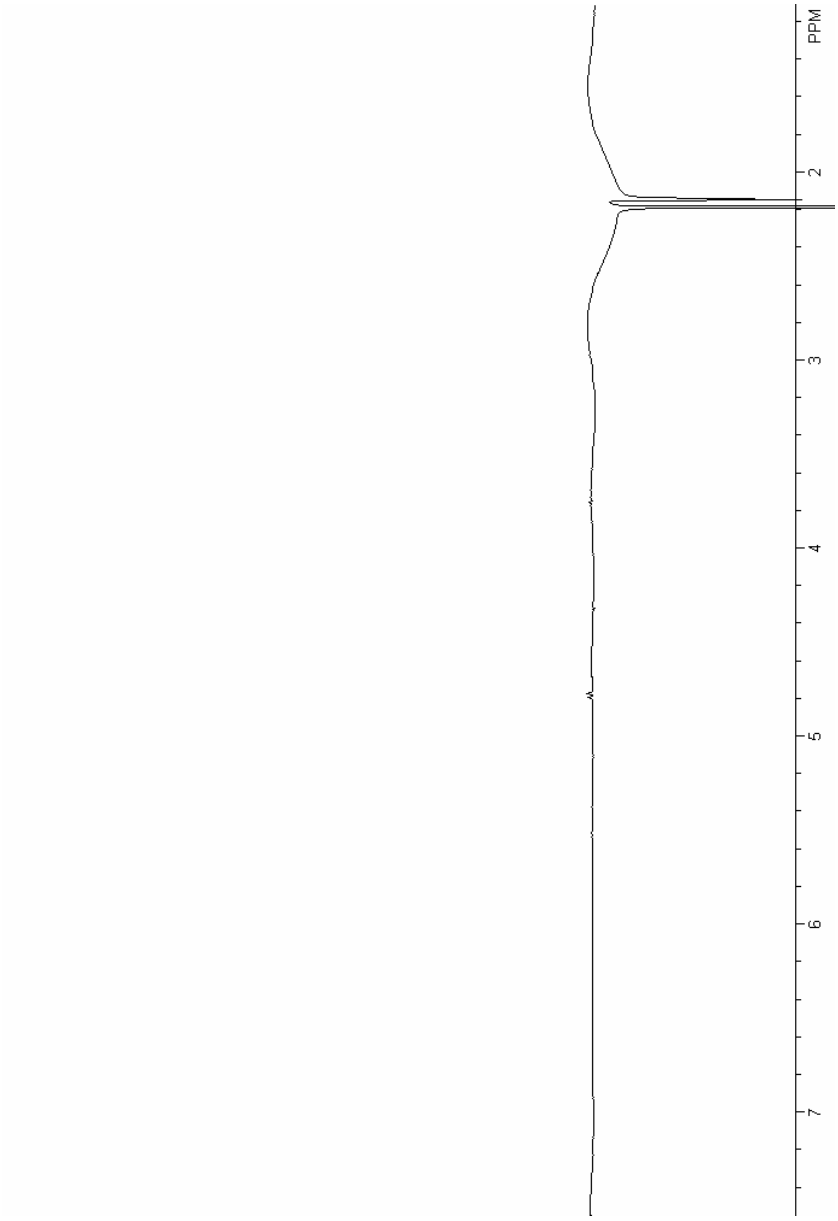

Spectra 6. 1D NOE of N-Acetyl-1(Rs)-oxo-thiazolidine-4-(R)-carboxylic acid Methyl Ester with irradiation at 2.14 ppm (1684.6).

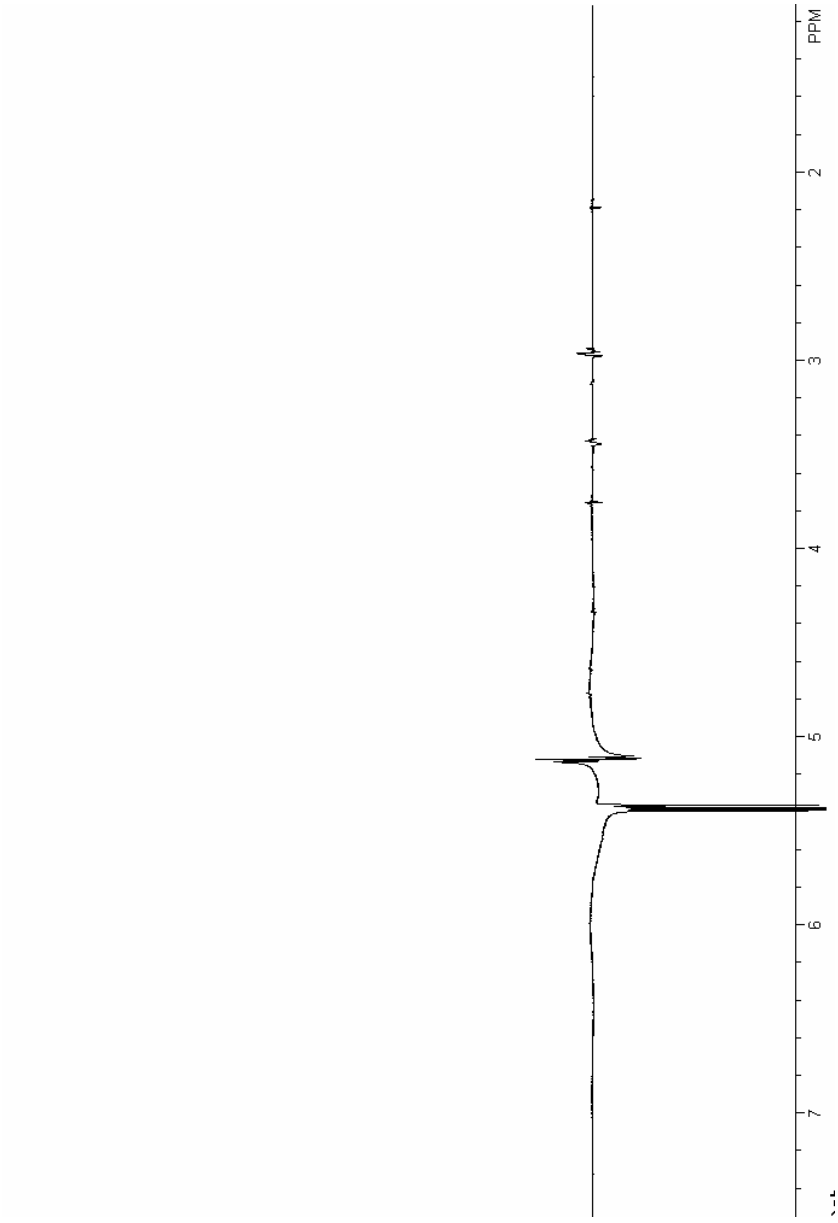

Spectra 7. 1D NOE of N-Acetyl-1(Rs)-oxo-thiazolidine-4-(R)-carboxylic acid Methyl Ester with irradiation at 5.4 ppm (227.6).

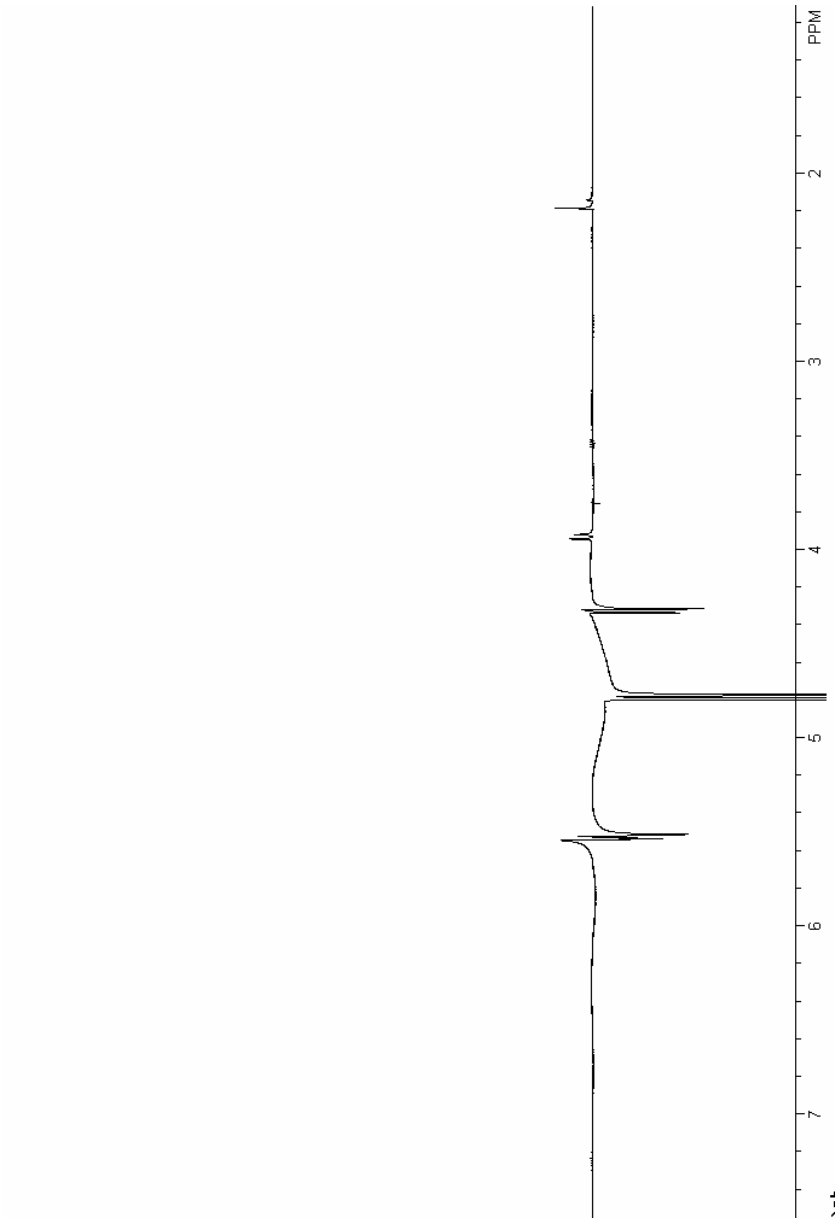

Spectra 8. 1D NOE of N-Acetyl-1(Rs)-oxo-thiazolidine-4-(R)-carboxylic acid Methyl Ester with irradiation at 4.8 ppm (129.0).

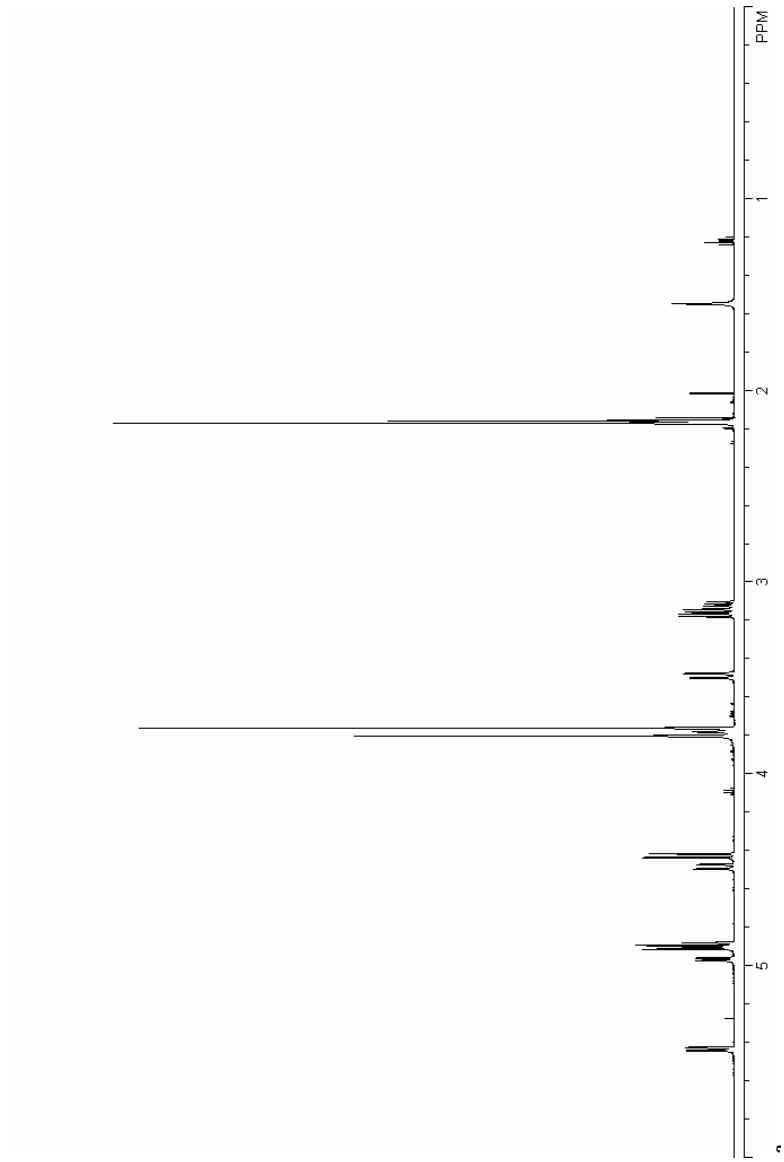

Spectra 9. Full proton spectra of N-Acetyl-1(Ss)-oxo-thiazolidine-4-(R)-carboxylic acid Methyl Ester (cis sulfoxide).

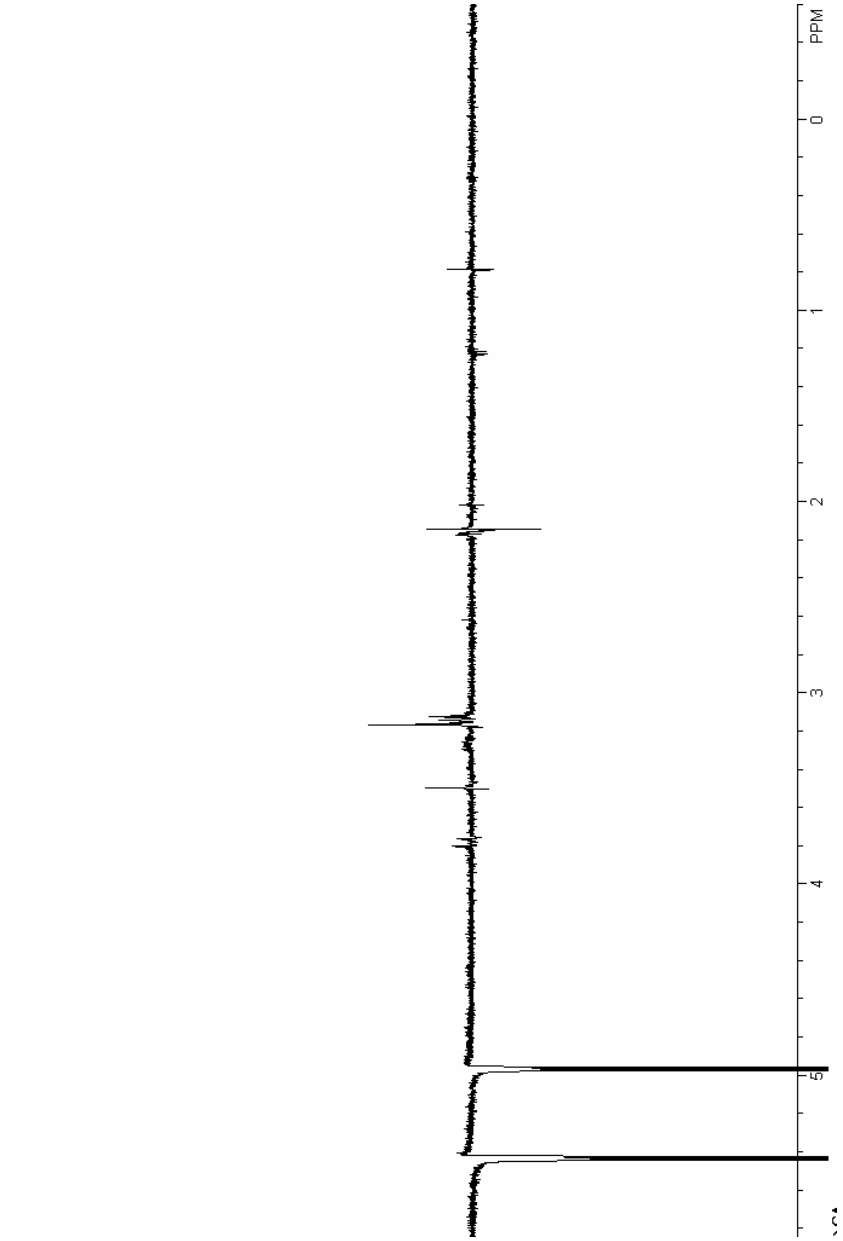

Spectra 10. 1D NOE Spectra of N-Acetyl-1(Ss)-oxo-thiazolidine-4-(R)-carboxylic acid Methyl Ester with irradiation at 5.44 ppm.

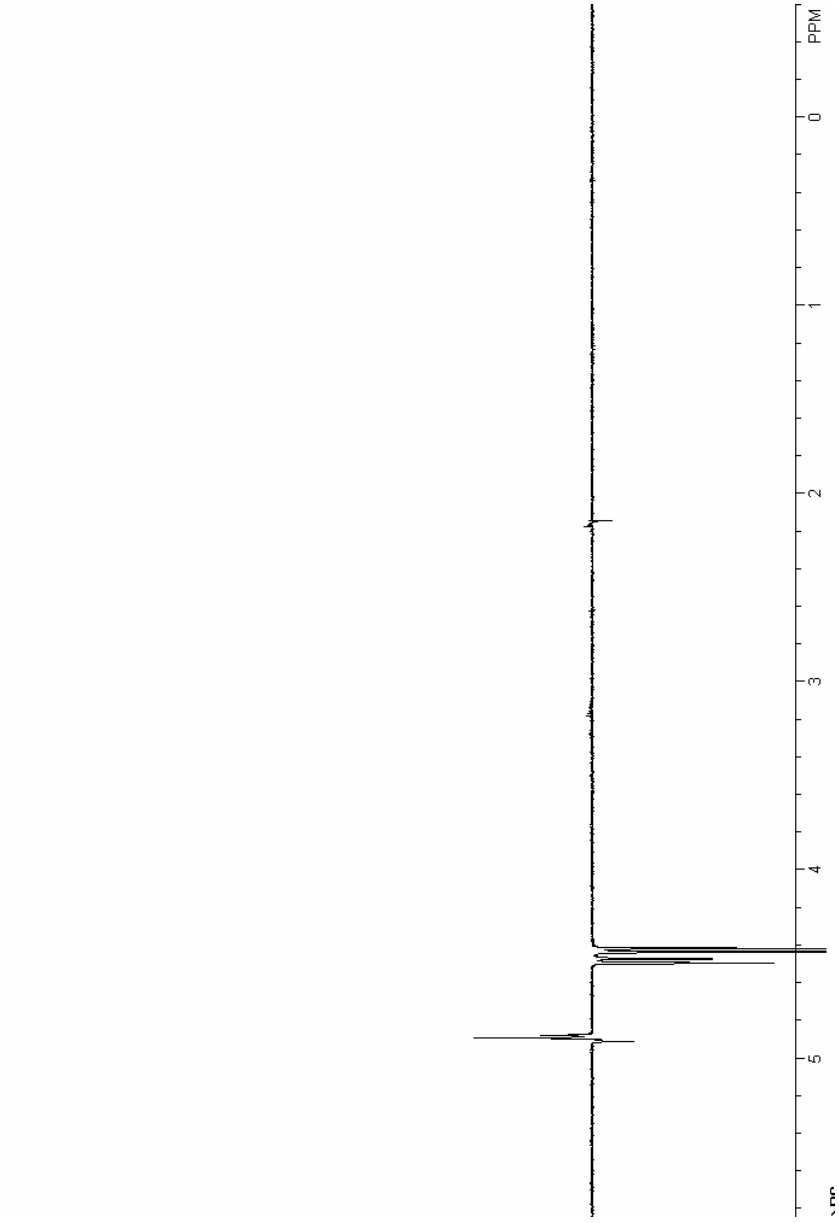

Spectra 11. 1D NOE Spectra of N-Acetyl-1(Ss)-oxo-thiazolidine-4-(R)-carboxylic acid Methyl Ester with irradiation at 4.44 ppm (337.4).

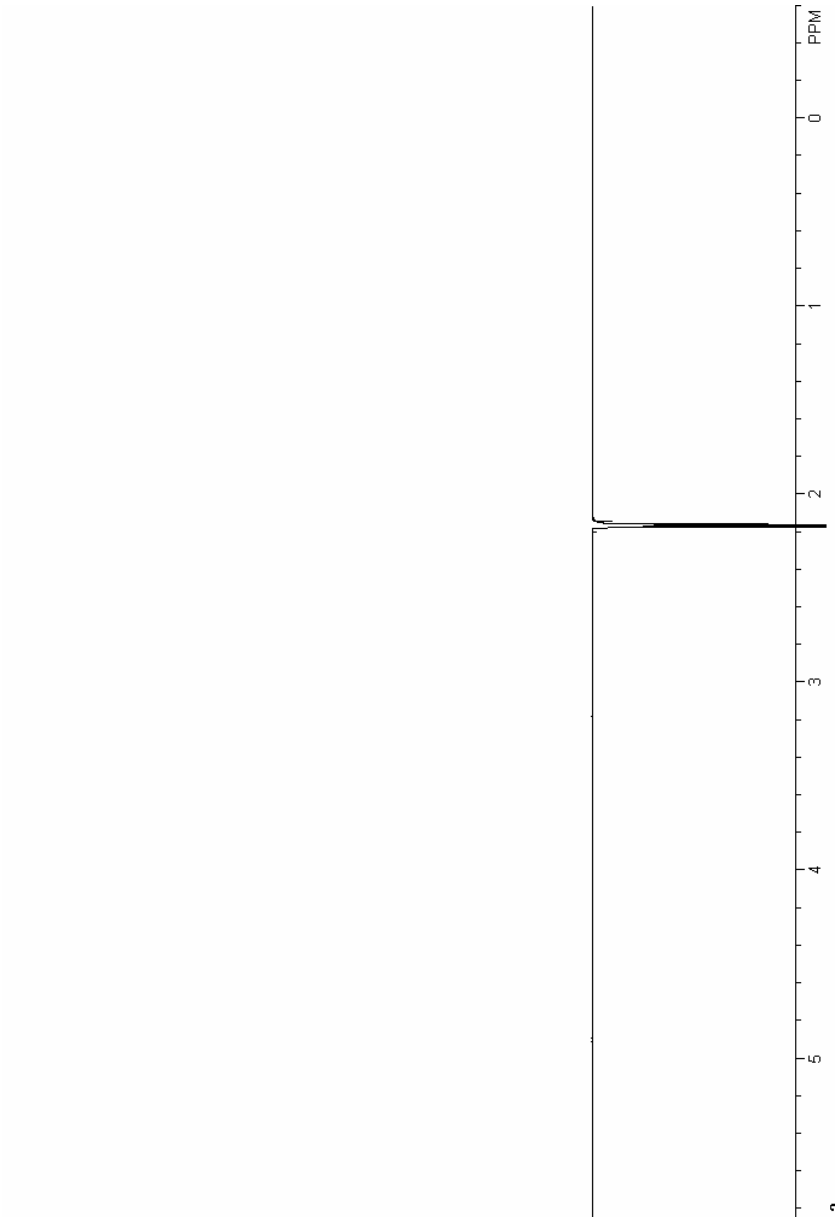

Spectra 12. 1D NOE Spectra of N-Acetyl-1(Ss)-oxo-thiazolidine-4-(R)-carboxylic acid Methyl Ester with irradiation at 2.16 ppm (1702.7).

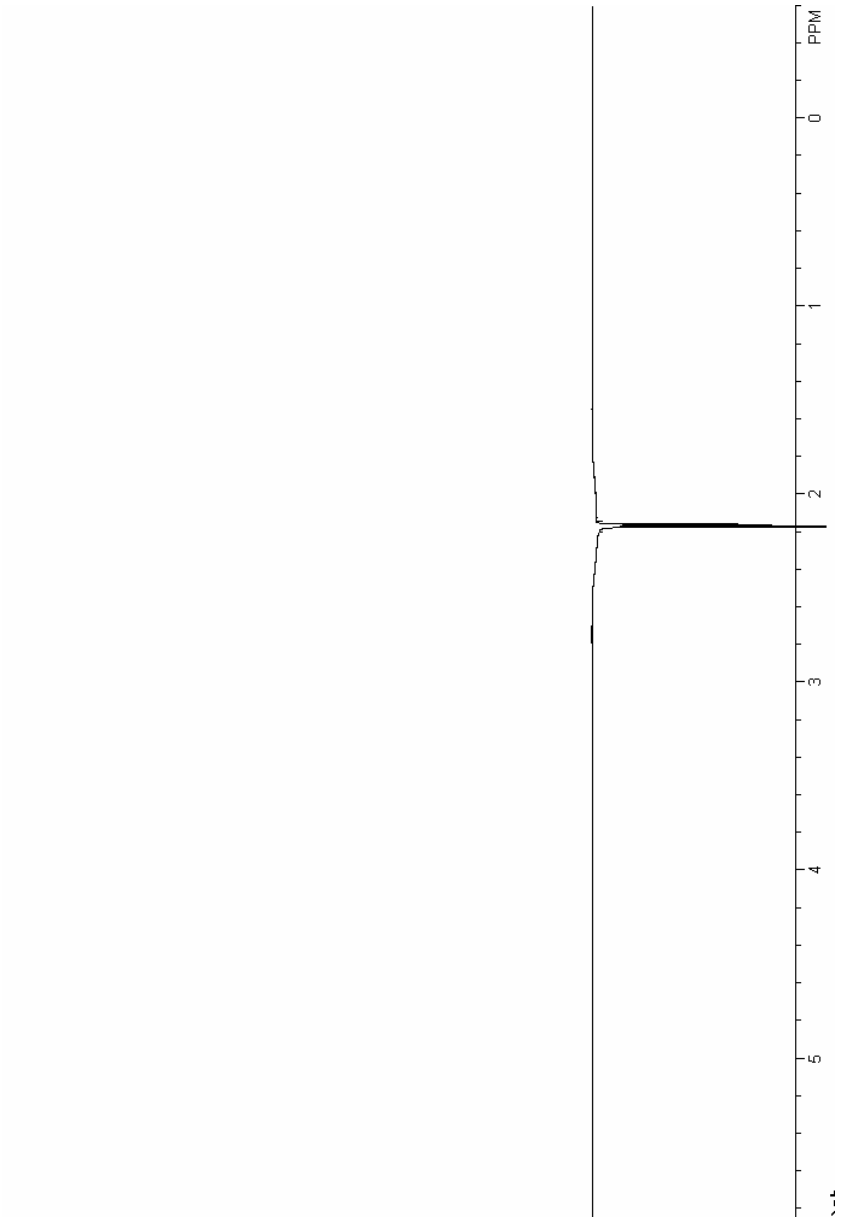

Spectra 13. 1D NOE Spectra of N-Acetyl-1(Ss)-oxo-thiazolidine-4-(R)-carboxylic acid Methyl Ester with irradiation at 2.17 ppm (1695.1).

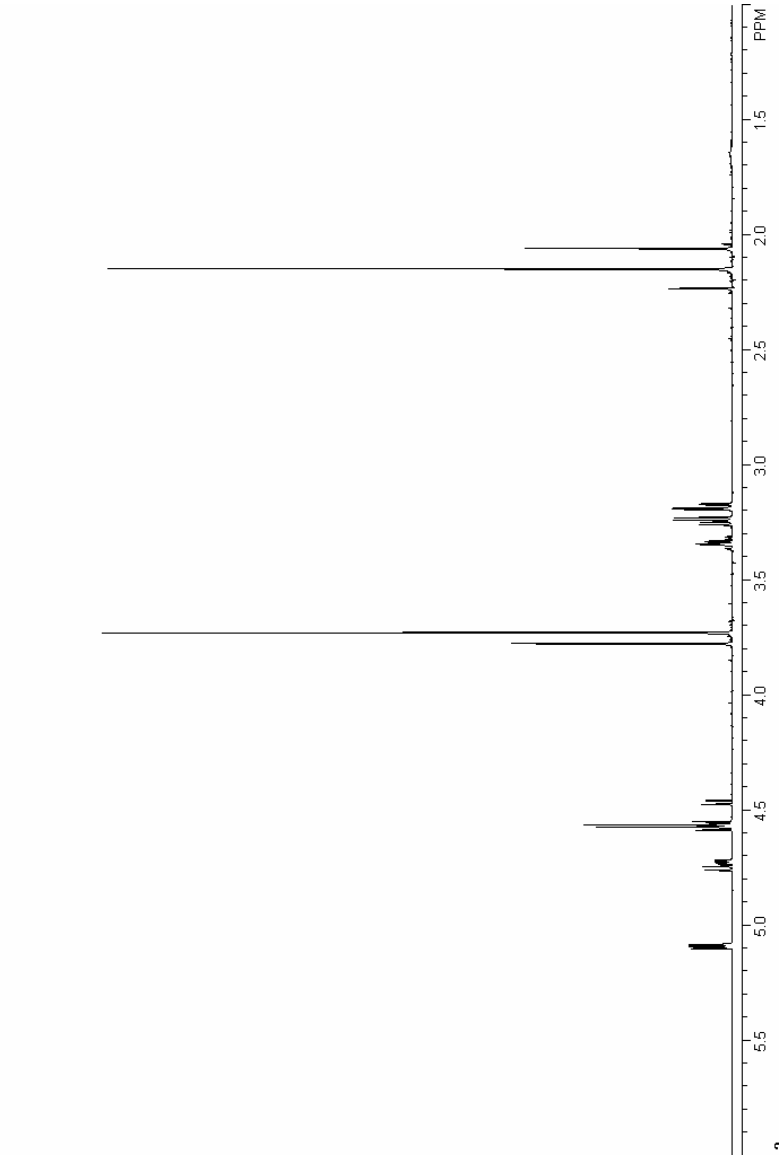

Spectra 14. Full proton Spectra of N-Acetyl-4-Thiazolidine-R-Carboxylic Acid Methyl Ester.

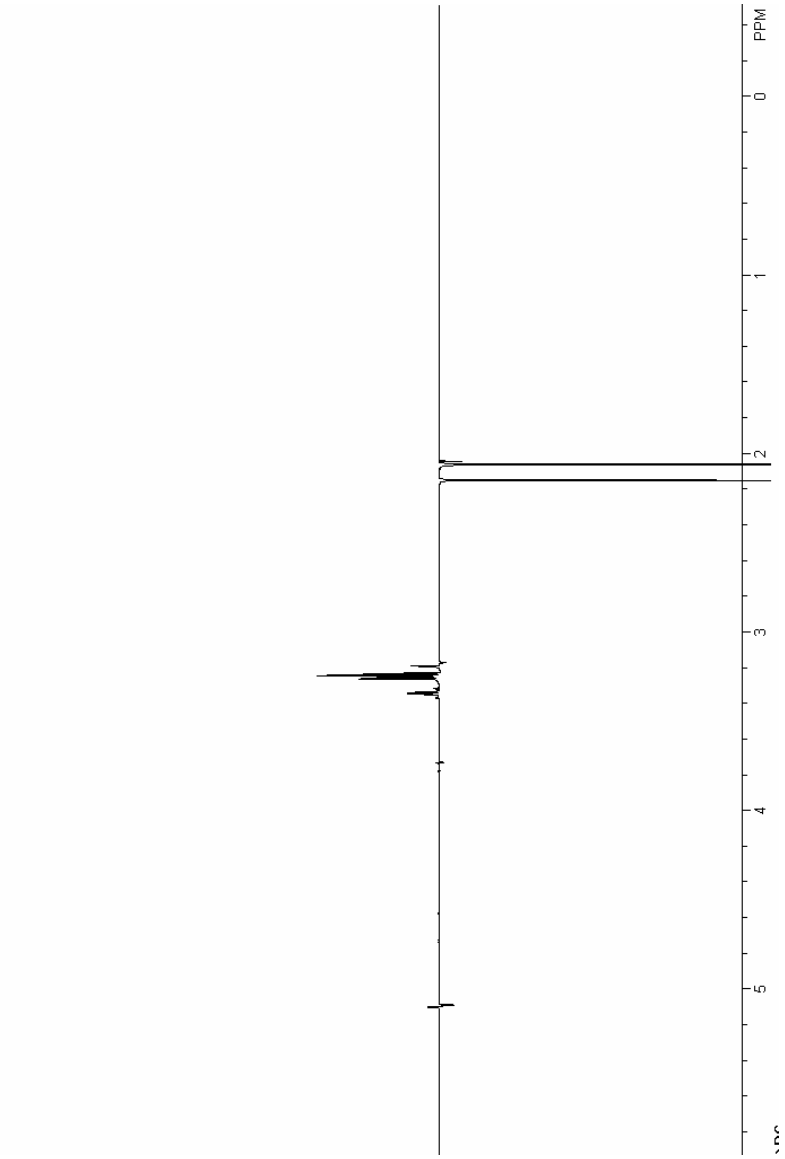

Spectra 15. NOE Spectra of N-Acetyl-4-Thiazolidine-R-Carboxylic Acid Methyl Ester with Irradiation at 2.15 ppm

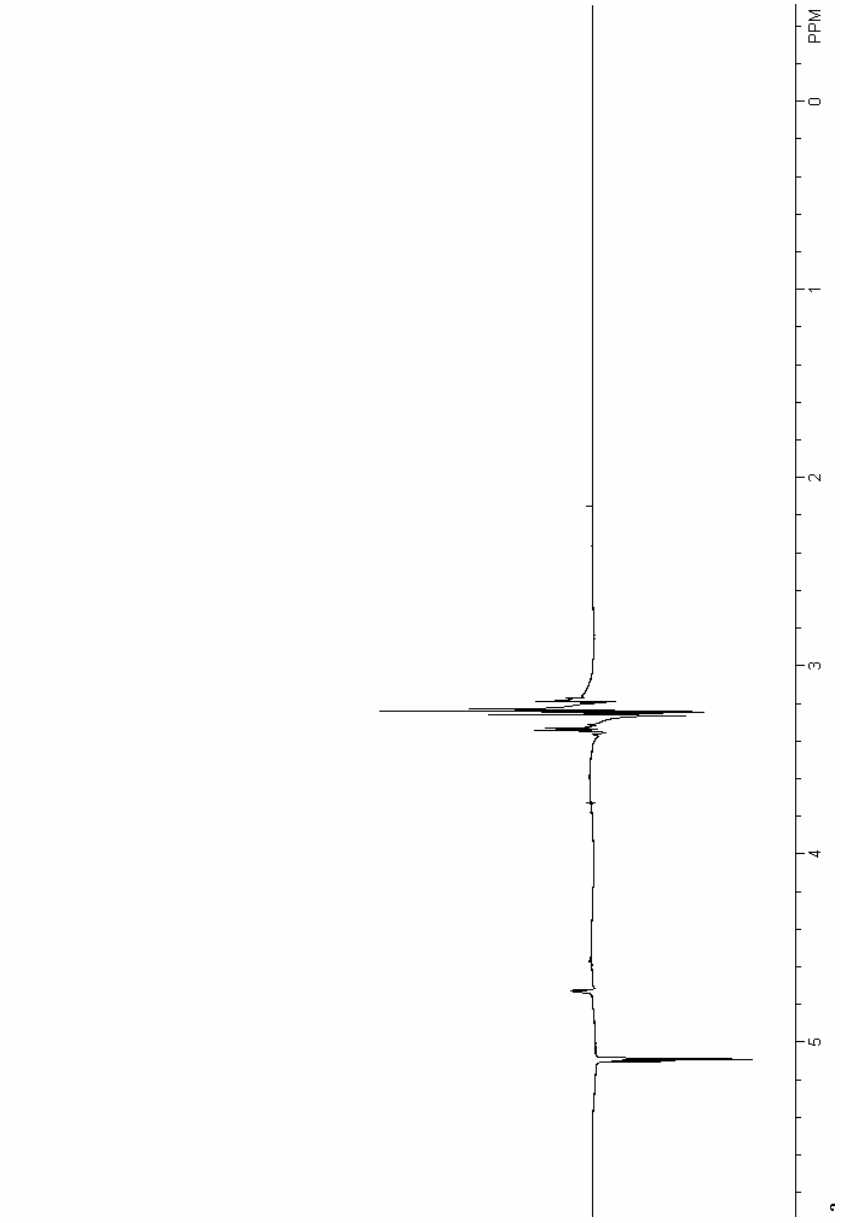

Spectra 16. NOE Spectra of N-Acetyl-4-Thiazolidine-R-Carboxylic Acid Methyl Ester with Irradiation at 5.09 ppm (55).

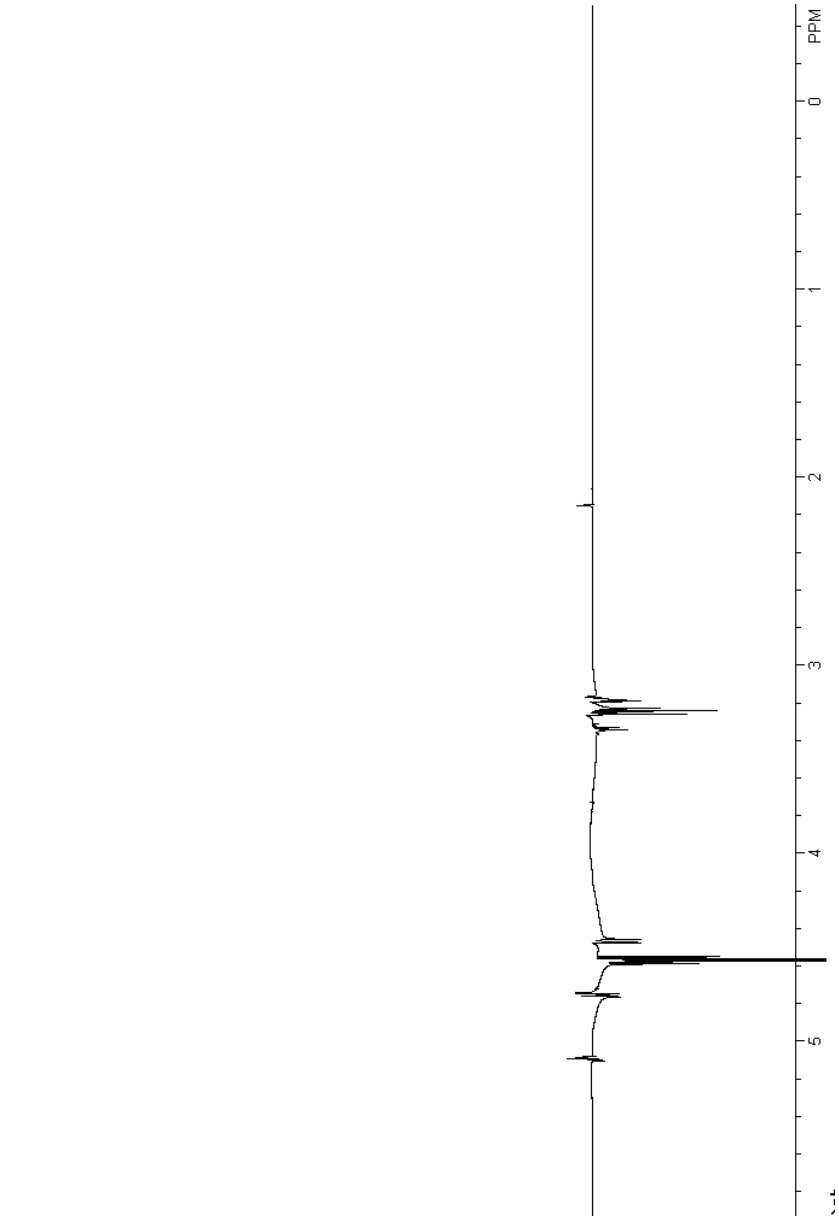

Spectra 17. NOE Spectra of N-Acetyl-4-Thiazolidine-R-Carboxylic Acid Methyl Ester with Irradiation at 4.57 ppm (260.3).

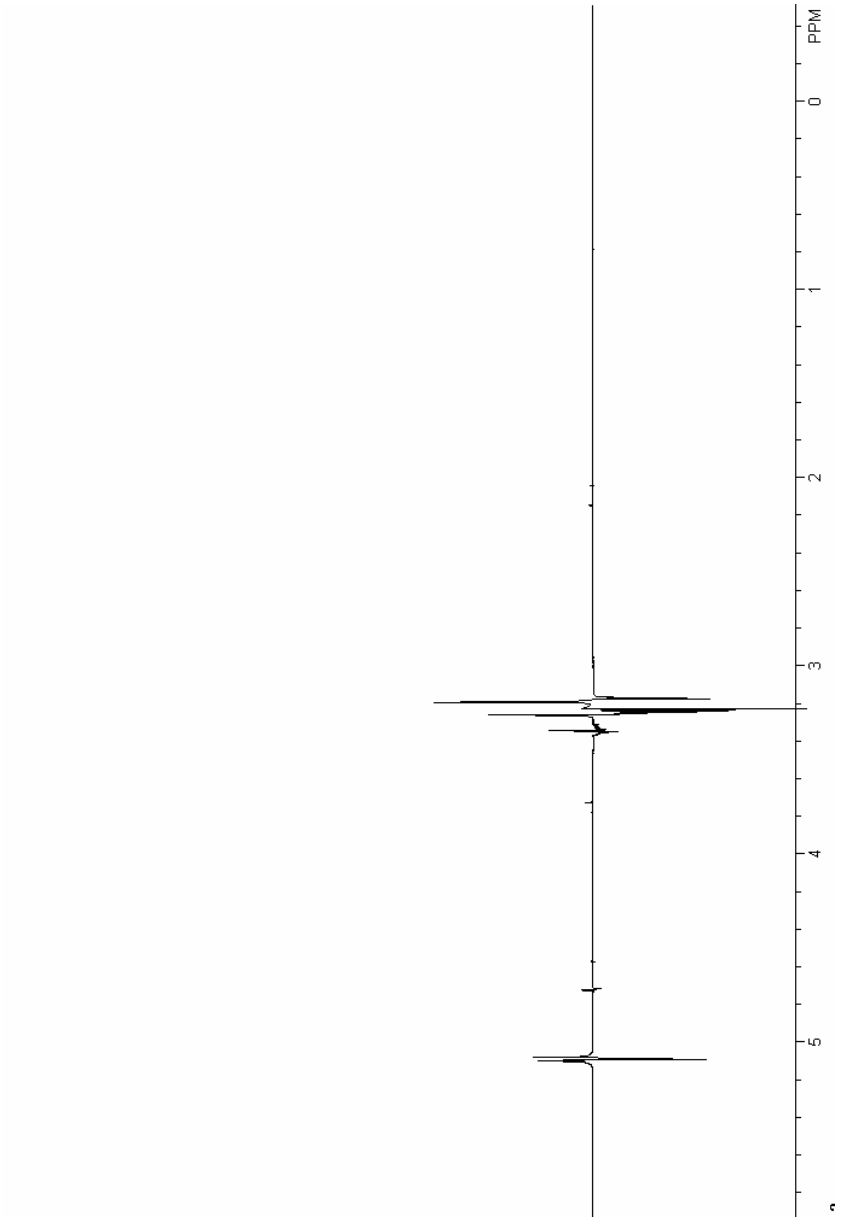

Spectra 18. NOE Spectra of N-Acetyl-4-Thiazolidine-R-Carboxylic Acid Methyl Ester with Irradiation at 3.24 ppm (1054.9).

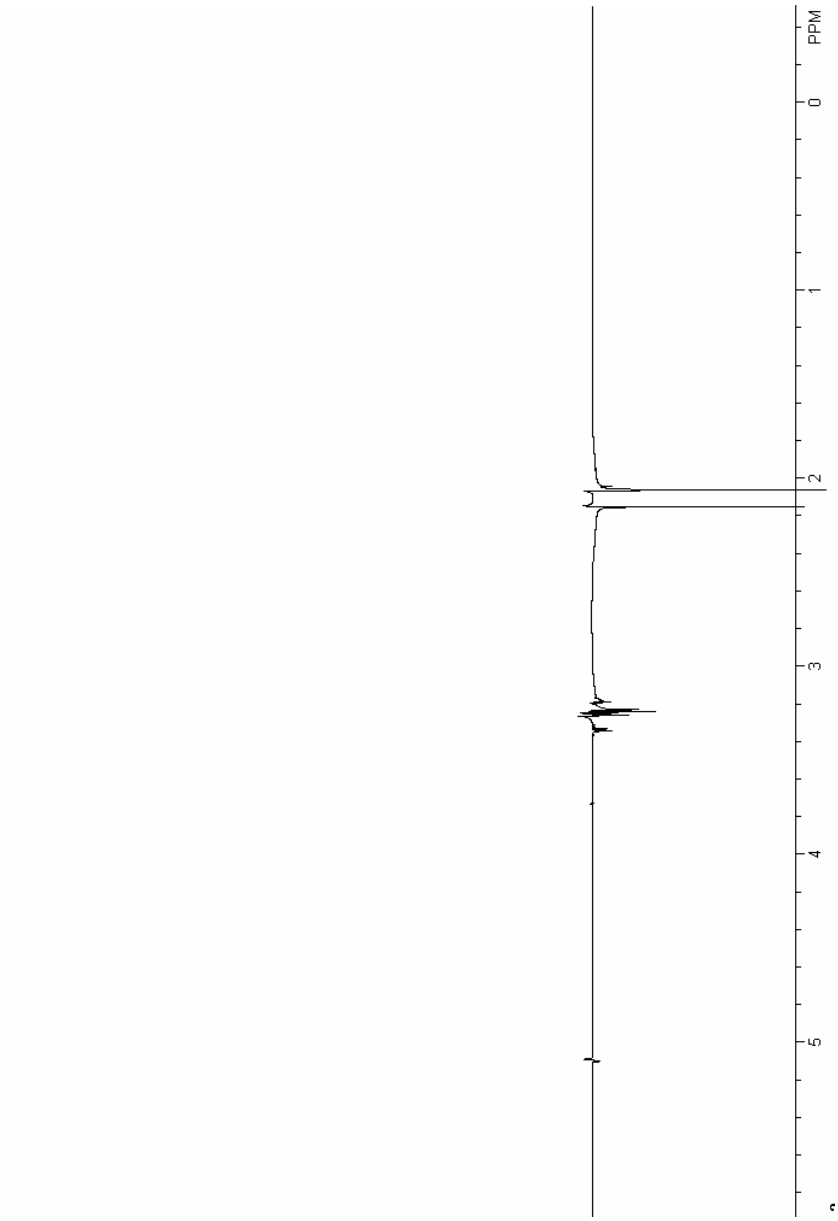

Spectra 19. NOE Spectra of N-Acetyl-4-Thiazolidine-R-Carboxylic Acid Methyl Ester with Irradiation at 2.15 ppm (1708.9).

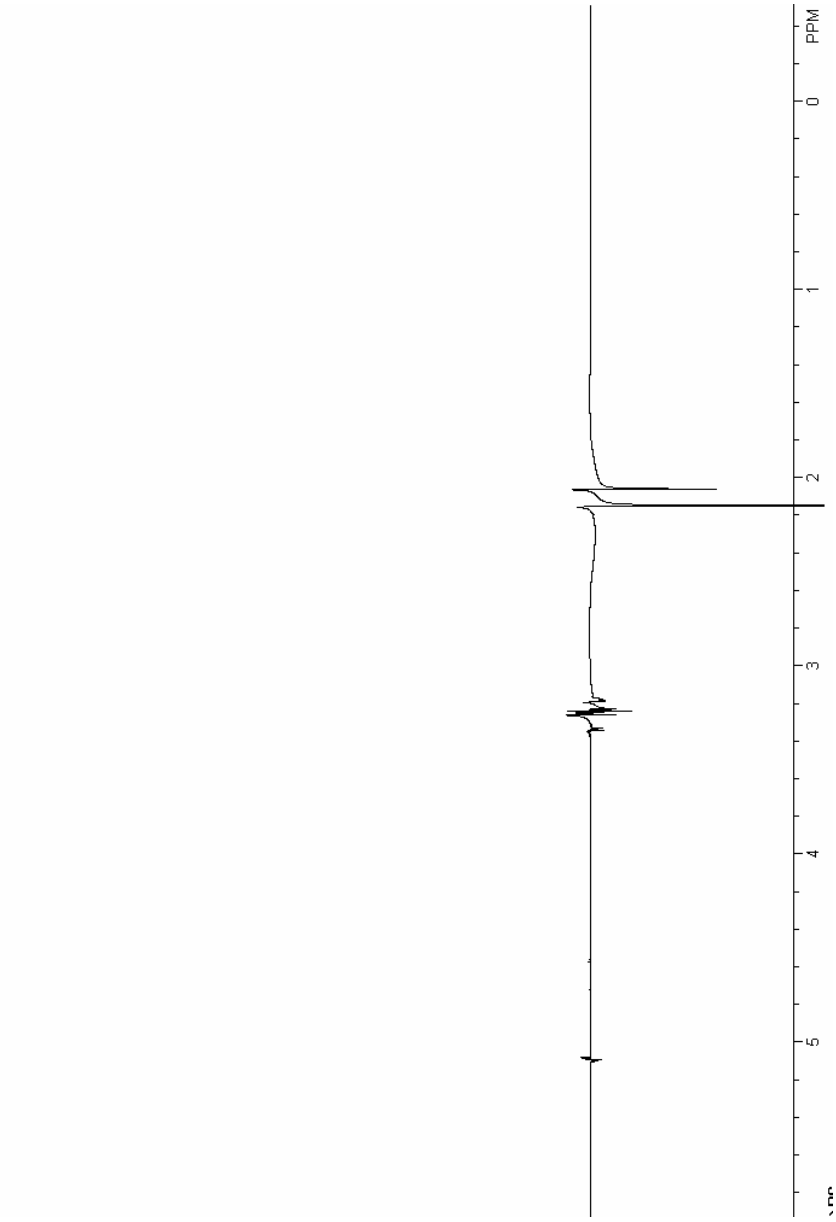

Spectra 20. NOE Spectra of N-Acetyl-4-Thiazolidine-R-Carboxylic Acid Methyl Ester with Irradiation at 2.06 ppm (1761.8).

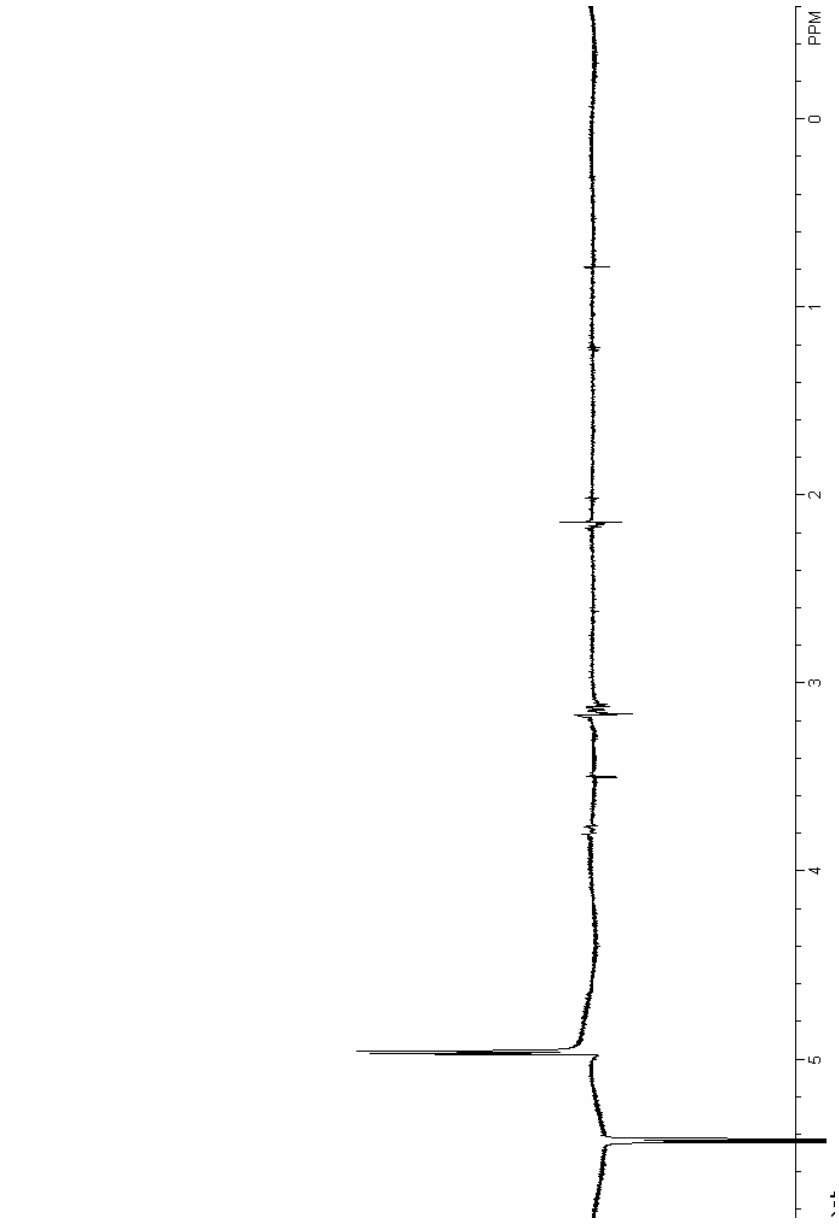

Spectra 21. NOE Spectra of N-Acetyl-4-Thiazolidine-R-Carboxylic Acid Methyl Ester with Irradiation at 5.44 ppm (262.7).

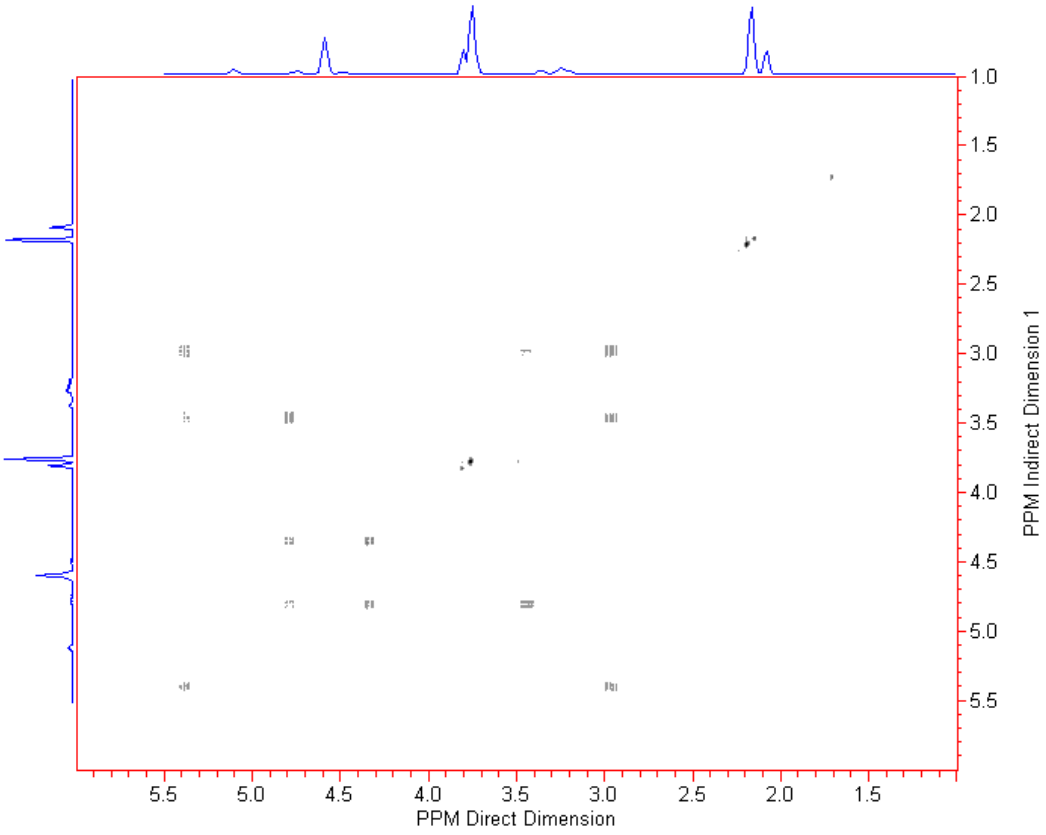

Spectra 21. 2D COSEY Spectra of N-Acetyl-1(Rs)-oxo-thiazolidine-4-(R)-carboxylic acid Methyl Ester.

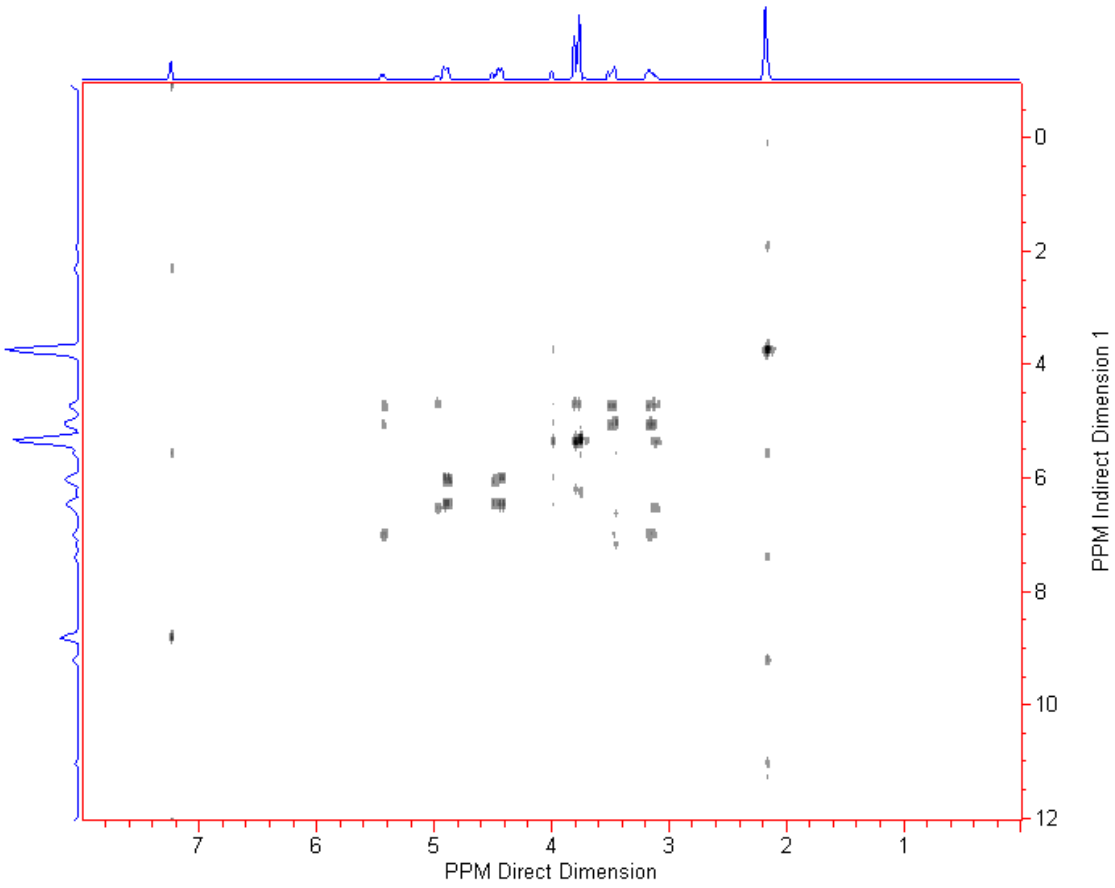

Spectra 22. 2D COSEY Spectra of N-Acetyl-1(Ss)-oxo-thiazolidine-4-(R)-carboxylic acid Methyl Ester.

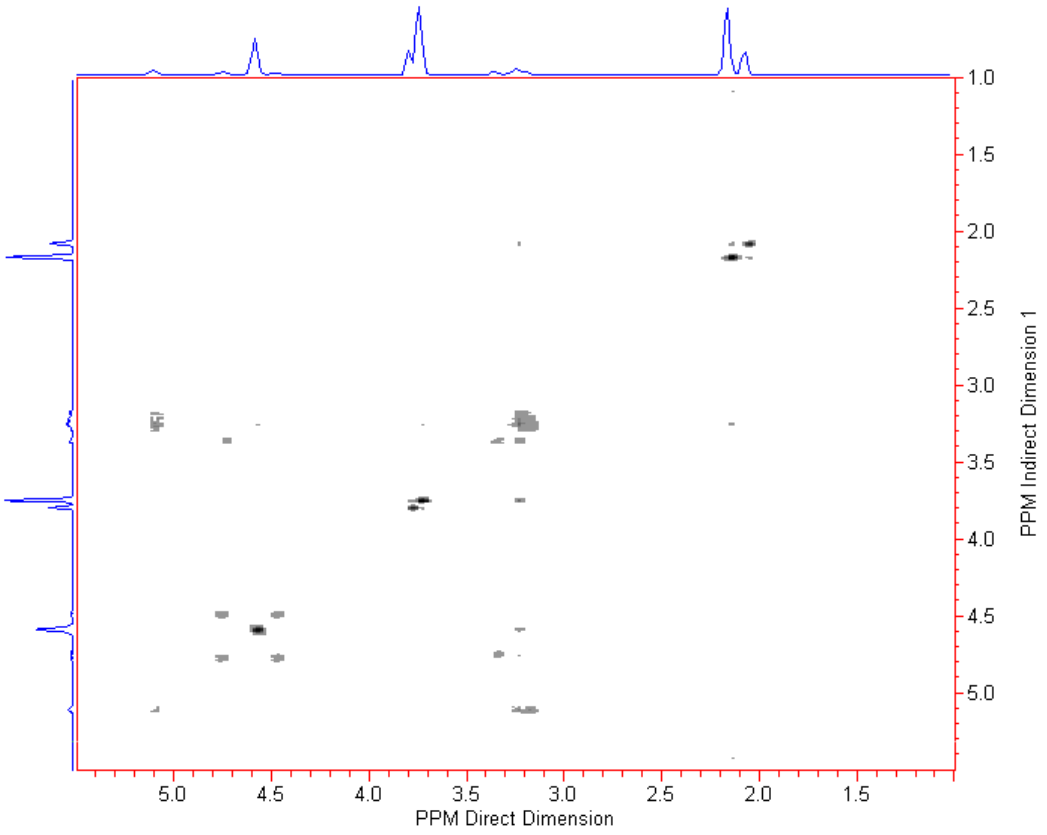

Spectra 23. 2D COSEY Spectra of N-Acetyl-4-Thiazolidine-R-Carboxylic Acid Methyl Ester.

Appendix 2

Synthesis of miscellaneous unnatural amino acids

Materials and Methods

All chemical reagents were purchased from either Fisher Scientific, Inc. (Pittsburgh, PA) or Sigma-Aldrich Chemical Co. (St. Louis, MO) unless otherwise noted. (2*S*,3*S)*-3-hydroxyproline was obtained from Acros Organics, Inc. ^{1}H, ^{19}F and ^{13}C NMR spectra were recorded on a Varian Mercury-300 spectrometer (300MHz for ^{1}H, 75 MHz for ^{13}C), on an Inova-400 spectrometer (400 MHz for ^{1}H, 384 MHz for ^{19}F NMR, 100 MHz for ^{13}C), or an INOVA-600 spectrometer (600 MHz for ^{1}H, 150 MHz for ^{13}C). NMR spectra were recorded on solutions in deuterated chloroform ($CDCl_3$) with residual chloroform (7.26 ppm for ^{1}H NMR and 77.23 ppm for ^{13}C NMR) taken as the internal standard, as well as hexafluorobenzene (-164.9 for ^{19}F NMR) and were reported in parts per million (ppm). Abbreviations for signal coupling are as follows s, singlet; d, doublet; t, triplet; q, quartet; m, multiplet. Electrospray ionization mass spectra were recoded on a JEOL JMS-SX102/SX102A/E mass spectrometer. Analytical Thin Layer Chromatography (TLC) was performed on precoated glass backed plates purchased from Whitman (silica gel 60 F254; 0.25mm thickness). Flash chromatography was carried out with silica gel 60 (230-400 mesh ASTM) from EM Science.

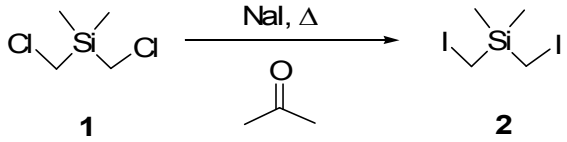

Scheme 1. Synthesis of Bis(iodomethyl)dimethylsilane

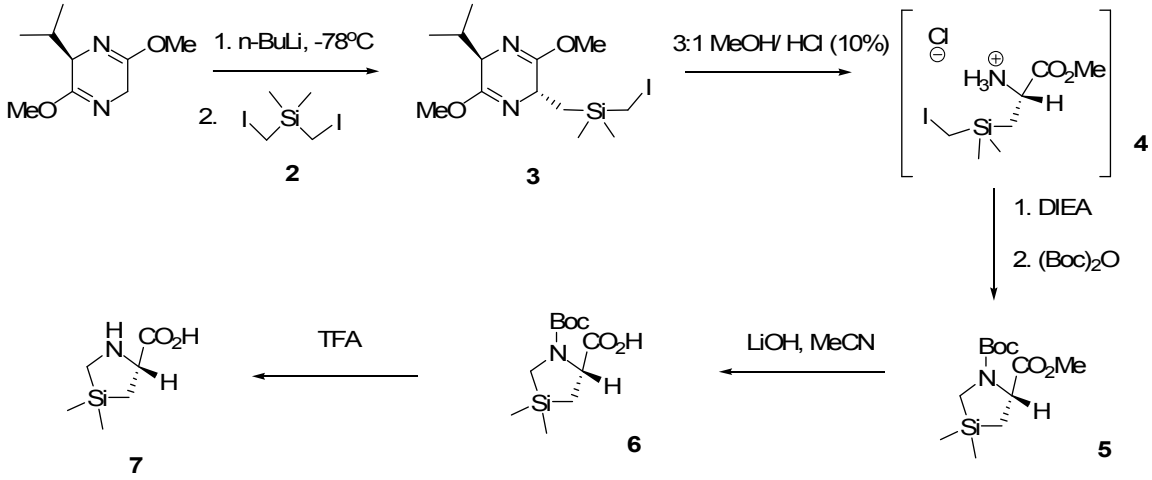

Scheme 2. Synthesis of (R)-silaproline

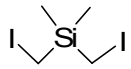

Bis(iodomethyl)dimethylsilane (2). To a dry 250 mL flask fitted with a reflux condenser Bis(chloromethyl)dimethylsilane (**1**, 2.9 g, 18 mmol) was added to the reaction vessel through the reflux condenser followed by 50 mL fresh acetone that had recently been treated with dry calcium carbonate, then sodium iodide (12.2 g, 80 mmol) was added to the mixture followed by an additional 50 mL of fresh acetone. The reaction mixture was then refluxed for 3 hr, and then allowed to cool to room temperature. The crude reaction mixture was then treated with 25 mL of hexanes, and filtered. After initial filtration the solvent was removed by *in vacuo*, and the product redissolved in ether then filtered. This process was repeated until white solid no longer precipitated from the reaction mixture. Finally the ether was removed *in vacuo* to yield the desired product (**2**, 5.7 g 17 mmol) as clear oil that was used without further purification. Rf = 0.8 (4:1 Hexane/EtOAc). ^{1}H NMR (400 MHz, $CDCl_3$) δ 0.35 (s, 6 H), 2.15 (s, 4 H).

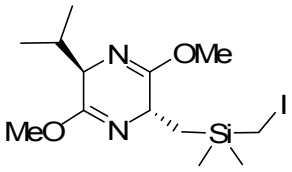

(2*R*,5*R*)-2,5-Dihydro-5-[(iodomethyl)dimethylsilyl]methyl-3,6-dimethoxy-2-isopropylpyrazine (3) {(2*R*,5*S*)-2,5-Dihydro-5-[(iodomethyl)dimethylsilyl]methyl-3,6-dimethoxy-2-isopropylpyrazine (minor isomer)}. To a solution of (*R*)-2,5-dihydro-3,6-dimethoxy-2-isopropylpyrazine (2.16 mL, 11.5 mmol) in THF (40 mL) was slowly added n-BuLi (1.6 M in hexane, 8.2 mL) at –78 °C under argon in a dry flask. The mixture was then stirred for 20 min at this temperature. Then

bis(iodomethyl)dimethylsilane (6.24 g, 18.46 mmol) was added slowly to the reaction so that the reaction temperature did not rise above -70 ^{o}C. The reaction was then allowed to stir under argon at -70^{o}C for 3 hr, and then allowed to warm to room temperature. Upon reaching ambient temperature the reaction was quenched with sat. aq. ammonium chloride (25 mL) extracted with 3 x 40 mL of ethyl acetate and dried over Na_2SO_4 and the solvent evaporated. The oily residue was purified by silica gel chromatography with 5% Et_2O in hexane as eluent. Products were produced in an 8:1 ratio of major isomer **3** to minor isomer with 3.26 g (8.28 mmol) total product isolated for a 69% overall yield, and 2.52 g (6.39 mmol) of the desired product **3** isolated for a 53% yield. **3** (major isomer) Rf = 0.6 (10% Et_2O/ 90% hexane). ^{1}H NMR (400 MHz, $CDCl_3$) δ 0.20 and 0.25 (2 s, 6 H), 0.70 (d, J = 6.84 Hz, 3 H), 0.97–1.07 (dd, , J = 4.17, 10.40 Hz, 1 H), 1.10 (d, J = 6.82 Hz, 3 H), 1.35–1.45 (dd, J = 4.17 Hz, 14.14 Hz, 1 H), 2.15 (s, 2H), 2.20–2.45 (m, 1 H), 3.66 (s, 3 H), 3.76 (s, 3 H), 3.91–4.00 (m, 1 H), 4.02–4.10 (m, 1 H)

Minor Isomer. Oil. Rf = 0.45 (10% Et_2O/ 90% hexane). ^{1}H NMR (400 MHz, $CDCl_3$) δ 0.15 and 0.20 (2s, 6 H), 0.70 (d, J = 6.84 Hz, 3 H), 0.75–0.85 (dd, J = 4.52 Hz, 11.93 Hz, 1 H), 1.00 ([d, J = 6.86 Hz, 3 H], 1.30–1.35 (dd, J = 4.52 Hz, 14.56 Hz, 1 H), 2.10 (s, 2 H), 2.10–2.15 (m, 1 H), 3.55 (s, 3 H), 3.60 (s, 3 H), 3.82–3.90 (m, 1 H), 3.95–4.00 (m, 1 H).

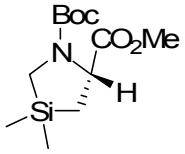

(*R*)-*N*-(*tert*-Butoxycarbonyl)silaproline Methyl Ester (5). **3** (2.5 g, 6.34 mmol) was stirred in a solution of freshly prepared 3M HCl in Methanol (20 mL in a ratio of 1:3) open to air for 4 hr. The solvent was then evaporated off and coevaporated three times with 15 mL portions of methanol. The crude reaction mixture was then dissolved in 20 mL of ether/ methylene chloride (2:3) and treated with 2.4 mL (13.95 mmol) DIEA. After stirring at room temperature open to the air for 4 hr 2.9 g (13.32 mmol) of $(Boc)_2O$ was added and the reaction was allowed to stir overnight. The reaction was then worked up by diluting the reaction with 50 mL of methylene chloride then washing with reaction mixture with 1M $KHSO_4$, water, and sat. aq. NaCl. The organic layer was then dried over Na_2SO_4 and the solvent removed *in vacuo*. The crude oil was then purified via silica gel chromatography using 40% ether/ 60% hexanes to give **5** as an oil in a 45% yield (0.77 g, 2.85 mmol). **5** oil. Rf = 0.4 (2:3 ether/hexanes). ^{1}H NMR (400 MHz, $CDCl_3$): δ 0.20 (s, 6 H), 1.01–1.05 (dd, 1 H, J = 3.31 Hz, 15.14 Hz), 1.10–1.23 (dd, 1 H, J = 10.15 Hz, 15.14 Hz), 1.32 and 1.40 (2s, 9 H), 2.70–2.90 (m, 2 H), 3.60 (s, 3 H), 4.55 and 4.70 (2dd, J = 3.31 Hz, 10.15 Hz); ^{13}C NMR (CDCl3, 100 MHz): δ –2.27 (–1.96), 16.58 (17.53), 28.72 (28.80), 34.60 (34.89), 52.22 (52.36), 59.64 (60.03) , 80.02 (80.27), 156.23 (157.09), 175.14 (175.33).

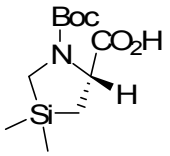

(*R*)-*N*-(*tert*-Butoxycarbonyl)silaproline (6). 5 (0.20 g, 7.3 mmol) was dissolved in 4 mL of a 3:1 methanol/ water mixture. The reaction mixture was then treated with 0.039 g (14 mmol) LiOH for 7 hr until all starting material had disappeared by TLC. The reaction was then worked up by reducing the reaction mixtures volume *in vacuo* followed by the addition of 10 mL water. The aqueous portion was washed with 2 x 5 mL ether, and then the aqueous portion was acidified with 3M HCl to an approximate pH of 3. The acidic layer was then extracted 3 x 10 mL ether, dried over Na_2SO_4 and the solvent removed *in vacuo* to yield 0.19 g (7 mmol) of **6** in a quantitative yield that required no further purification. Oil. Rf = 0.6 (CH_2Cl_2/MeOH/AcOH). ^{1}H NMR (600 MHz, $CDCl_3$): δ 0.20 (s, 6 H), 0.85–1.20 (m, 2 H), 1.30 and 1.40 (2s, 9 H), 2.63–2.90 (m, 2 H), 4.55 and 4.70 (2 dd, J =3.52 Hz, 10.26 Hz, 1 H), 9.50 (s, 1 H). ^{13}C NMR (CDCl3, 150 MHz): 2.23, –2.09, 16.13 (17.39), 28.66 (28.78), 34.61 (34.91), 59.75 (59.86), 80.27 (80.62), 156.38 (157.69), 177.07 (179.06).

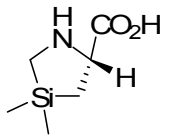

(*R*)-silaproline (7). 6 (0.19 g, 7 mmol) was dissolved in 2 mL of methylene chloride open to air at room temperature. Then 2 mL of TFA was added and the reaction mixture was stirred for 1.5 hr where upon completion of the reaction the solvent was removed *in vacuo*. The reaction mixture was coevaporated 3 x 10 mL methanol to yield **7** (0.10g, 7 mmol) in a 98% yield as a white solid that was used without further purification. **7.** ^{1}H

NMR (600 MHz, D_2O): δ 0.14 (s, 3H), 0.15 (s, 3H), 0.95 (m, 1 H, beta), 1.38 (m, 1 H, beta), 2.30 (m, 1 H, gamma), 2.56 (m, 1 H, gamma), 3.99 (dd, 1 H, J = 7.3Hz and 4.3Hz alpha). ^{13}C NMR (100MHz, D_2O): δ 0.11, 0.26, 18.84, 37.39, 64.45, 177.07. ESI-MS, Calc. for $C_6H_{13}NO_2Si$ [M + H]: 159.072; found 159.075.

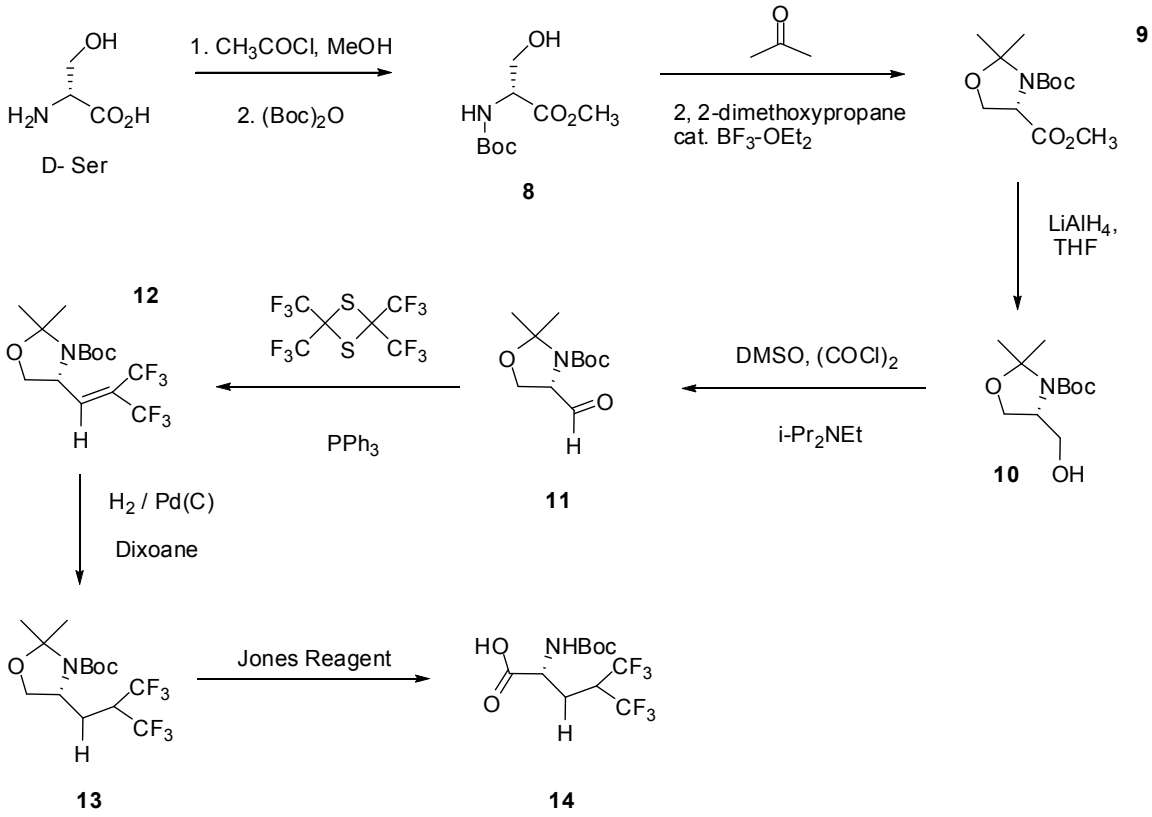

Scheme 3. Synthesis of Hexafluoroleucine

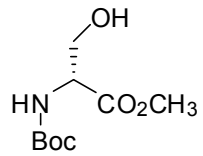

N-[(1,1-Dimethylethoxy)carbonyl]-L-serine methyl ester (8) . A 250 mL round bottomed flask , containing a magnetic stirring bar, is flame dried under an argon purge then charged with 150 mL of fresh methanol. (L)-serine, **1**, (13.16 g, 125 mmol) is added in one portion, and the solution is then cooled to 0 ^{o}C. 23 mL of acetyl chloride is then added slowly to the reaction via syringe, and the reaction allowed to warm with stirring overnight. The reaction is then opened to the atmosphere and the solvent is removed to yield 17.5 g of crude methyl serinate hydrochloride (98-99% yield) as a white crystalline solid that is used without further purification. Subsequently, the flask containing the methyl serinate hydrochloride is charged with 200 mL methylene chloride, and cooled to 0 ^{o}C open to the atmosphere. The resulting white suspension is treated with triethylamine (38 mL, 522 mmol), and allowed to stir for 15 min. Then di-tert-butyl dicarbonate (29.9 g, 137 mmol) is added as a solid in two portions, and the reaction is allowed to warm with stirring overnight. The reaction is then worked up by washing the reaction mixture with 2 x 100 mL 3M HCl, 1 x 100 mL sat. aq. NaCl. The resulting organic layer was then dried over Na_2SO_4 and the solvent removed *in vacuo* to yield 25.55 g (116 mmol, 93% yield) of N-Boc-L-serine methyl ester **(8)** as a colorless oil that is used without further purification. Rf = 0.4 (1:1 hexanes/ ethyl acetate). ^{1}H NMR (400 MHz, $CDCl_3$): δ 1.43 (s, 9 H), 2.19 (bs, 1H), 3.78 (s, 3H), 3.86 (m, 2H), 4.35 (bs, 1H), 5.4 (bs, 1H).

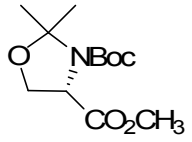

3-(1,1-Dimethylethyl) 4-methyl-(S)-2,2-dimethyloxazolidine-3,4-dicarboxylate (9). In a dry 500 mL flask N-Boc-L-serine methyl ester (25.55 g, 116 mmol) was dissolved in 200 mL fresh acetone (treated with calcium carbonate) and added to the reaction flask under argon. Then 2,2-dimethoxypropane (125 mL mL, 1.4 mol) was also added to the reaction flask followed by boron trifluoride etherate (1.1 mL, 7 mmol). The resulting orange solution is stirred at room temperature for 2.5 hr until TLC analysis indicates all of the starting material is consumed. The reaction mixture was then treated with 2 mL of triethylamine and the solvent is removed under reduced pressure. The residual brown syrup is partitioned between 150 mL methylene chloride and washed with sat. aq. sodium bicarbonate (250 mL). Then the aqueous layer is extracted with methylene chloride (2 × 150 mL) and the combined organic phases are dried over Na_2SO_4 and the solvent removed *in vacuo* to yield **9 (**28.7g, 117 mmol) as a yellow oil in a 97 % yield. **9** was used without further purification. Rf = 0.8 (1:1 hexanes/ ethyl acetate). ^{1}H NMR (400 MHz, $CDCl_3$): δ 1.38 and 1.46 (2s, 9 H), 1.47 and 1.52 (2s, 3 H), 1.62 and 1.66 (2s, 3 H), 3.75 (s, 3 H), 3.98 and 4.09 (m, 2 H), 4.35 and 4.46 (m, 1 H).

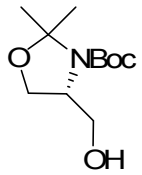

N-[(1,1-Dimethylethoxy)carbonyl]-N,O-isopropylidene-L-serinol (10) . A dry 500 mL three necked round bottomed flask is charged with a high torque magnetic stirring bar, and flame dried under argon. The reaction flask is then charged with 124 mL of 1M lithium aluminum hydride in THF (120 mmol), and an additional 100 mL dry THF is added. The reaction is then cooled to 0 ^{o}C, and two syringes each charged with a solution of the oxazolidine ester **9** (10.01 g, 39 mmol) in dry tetrahydrofuran (50 mL) were added dropwise over 30 min. The reaction is then stirred for an additional 20 min at room temperature. The reaction is the cool to 0 ^{o}C, and opened to the atmosphere. Three drops of water are added to the reaction mixture and it is allowed to stir open to the atmosphere for 30 min at low temperature. 5 g of ice is added to the reaction mixture and the reaction allowed to stir for an additional 1 hr. The reaction is then again cooled to 0 ^{o}C, and 3M KOH is slowly added dropwise to the reaction until all hydrogen evolution has ceased. The reaction mixture is stirred for an addition 30 min, then the white precipitate is removed by filtration through a Celite pad. The filtrate is rinsed with 3 x 50 mL portions of THF. The solvent is removed *in vacuo*, and the residual oil is taken up in 150 mL methylene chloride and washed with 2 x 100 mL of aqueous phosphate buffer (pH 7). The organic phase is dried over Na_2SO_4 and the solvent removed *in vacuo* to yield 17.4 g (75 mmol) of **10** as a clear oil in 80 % yield. The oil was used in subsequent steps without further purification as NMR analysis indicated a purity of > 98%. Rf = 0.25 (1:1 hexanes/ ethyl acetate). ^{1}H NMR (400 MHz, $CDCl_3$): δ 1.42-1.67 (m, 15 H), 3.55 (m, 2H), 3.63 (m, 2H), 3.95 (m, 1H), 4.05 (bs, 1H).

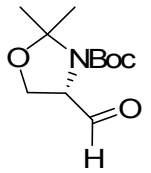

1,1-Dimethylethyl (S)-4-formyl-2,2-dimethyl-3-oxazolidinecarboxylate (11) . A dry 500 mL threenecked round bottomed flask, containing a high torque magnetic stirring bar is equipped with a low-temperature thermometer and flame dried under argon. The flask was then charged with 150 mL of dry methylene chloride followed by oxalyl chloride (9.7 mL, 115 mmol), and the reaction was cooled to –78 °C in a dry ice/ acetone bath. Dry DMSO (16.4 mL, 231 mmol) in a 1:1 mixture with methylene chloride was added slowly to the reaction over 30 min so that the reaction temperature did not exceed –70 °C. The reaction was then allowed to warm to –65 °C over 20 min. In a separate dry round bottom flask **10** (17.9 g, 77 mmol) was dissolved in 80 mL methylene chloride, and cooled to 0 °C under argon. The solution of **10** was then transferred dropwise via cannula to the reaction flask that is cooled to –65 °C. The addition of the solution of **10** should occur slowly, typically taking 1 hr, so that the reaction temperature does not exceed –55 °C. The reaction is then stirred for an additional 30 min at –55 °C, and is then warmed to –45 °C where 32 mL N,N-diisopropylethylamine (182 mmol) of is added to the reaction over a period of 10 min. The reaction is then transferred to an ice bath and allowed to stir for an additional 10 min. The reaction is then quenched with 150 mL of ice-cold 1 M hydrochloric acid solution. The two phases are then partitioned, and the aqueous phase is extracted with methylene chloride (3 × 50 mL). The combined organic phases are washed with pH 7 aqueous phosphate buffer (2 × 100 mL), dried over Na_2SO_4 and the solvent removed *in vacuo*. The product was the chromatographed using silica gel and a 1:1 mixture of hexanes/ ethyl acetate to yield 16.27 g (71 mmol) of **11** as

a clear yellow oil. Rf = 0.5 (1:1 hexanes/ ethyl acetate). ^{1}H NMR (400 MHz, $CDCl_3$): δ 1.24-1.47 and 1.61 (m, 15H), 3.31-3.59 (m, 2H), 3.65 and 3.97 (m, 1H), 9.16 and 9.32 (s, 1H). ^{1}H NMR (400 MHz, C_6D_6, 70°C) δ: 1.34 (s, 9 H), 1.40 (s, 3 H), 1.58 (s, 3 H), 3.57 (d, 1 H, J = 7.6), 3.67 (d, 1 H, J = 7.6), 3.91 (m, 1 H), 9.33 (bs, 1 H); IR (neat) cm−1: 1739, 1710.

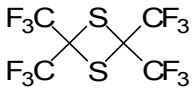

2,2,4,4-Tetrakis(trifluoromethyl)-1,3-dithietane. A dry 500 mL three necked flask was fitted with a high torque magnetic stirring bar, thermometer, reflux condenser, and a gas inlet tube. The flask was then flames dried under argon, and then KF (3 g) was added to the flask followed by 23 g of sulfur. Then 200 mL of dry DMF was added, and the reaction was heated under argon to an internal temperature of 45 °C where a dark blue/green reaction color is observed. Hexafluoropropene is then bubbled through the reaction using a dried pasture pipette. Upon addition of hexafluoropropene the reaction turns bright yellow, and an approximate internal temperature of 55 °C was maintained over 3 hr while hexafluoropropene was bubbled through the reaction. The reaction was stopped when no more solid particulate matter was observed in the reaction vessel. The reaction was then cooled to room temperature with stirring, and was cooled to approximately -30 °C where a white crystalline solid was formed and collected quickly via filtration through a medium glass frit. The filtrate is washed 2 x 50 mL of hexanes, and is then transferred to a round bottom flask where it is allowed to warm to room temperature. The clear liquid is then purified by distillation over sodium sulfate at atmospheric pressure through an air condenser into an ice bath. A clear liquid, with an

EXTREME STENCH, is collected as product, and stored at low temperature under argon where the clear liquid became a white solid in an hour. approximately 94g of compound was isolated for an 80 % yield of product. Additionally all glassware used in these reactions was immediately submerged in a bleach bath to eliminate stench due to residual compound. white solid. bp 109 °C. mp 25 °C. ^{13}C NMR (100 MHz, $CDCl_3$): δ 123. ^{19}F NMR (384 MHz, $CDCl_3$) δ −73.3 (s).

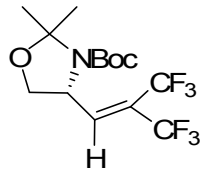

1,1-Dimethylethyl (S)-4- Bis-trifluoromethylene-2,2-dimethyl-3-oxazolidinecarboxylate (12). A 500 mL dry flask is charged with a high torque stir bar, 200 mL of dry diethyl ether, and aldehyde **11** (5.82 g, 25 mmol) under argon. Triphenyl phosphine (46.6 g, 170 mmol) was added in small portions to the vortexing reaction mixture, and then cooled to -78 °C under argon. 2,2,4,4-Tetrakis(trifluoromethyl)-1,3-dithietane (34.1 g, 88 mmol) was dissolved in 100 mL dry ether under argon and placed in an ice bath then was transferred slowly via cannula to the stirring reaction mixture. The reaction was then allowed to warm slowly to room temperature under argon, and stirred for a total of three full days. During this time stirring of the reaction must be maintained. At the end of three days the reaction had obtained an orange color and a large amount of white precipitate. The reaction was worked up by the addition of 100 mL pentane then gravity filtration through a plug of glass wool. The crude reaction mixture was then condensed *in vacuo* and diluted with 300 mL pentane and filtered for a

second time. The crude product was then condensed *in vacuo*, and purified by silica gel chromatography using a mixture of 4:1 hexanes/ Ethyl Acetate to yield 4.44g (12 mmol) of pure product **12** in a 50% yield as a clear oil. After elution of the product the solvent mixture can be changed to neat ethyl acetate to recover a significant remainder of the unreacted Garner aldehyde. ^{1}H NMR (400 MHz, $CDCl_3$): δ 1.43 (s, 9H), 1.56 (s, 3H), 1.64 (s, 3H), 3.85 (dd, 1H, J = 3.9 Hz, 9.3 Hz), 4.17 (dd, 1H, J = 6.9 Hz, 9.3 Hz), 4.81 (4.95, bs, 1H), 6.70 (d, 1H, J = 8.7 Hz). ^{19}F NMR (384 MHz, $CDCl_3$) δ –65.05 (d, 3F, J = 5.9 Hz), –58.50 (d, 3F, J = 5.9 Hz); FT–IR (film): 1714, 1379, 1235, 1164. ESI-MS, Calc. for $C_{14}H_{19}F_6NO_3$ [M + H]: 363.127; found 363.191.

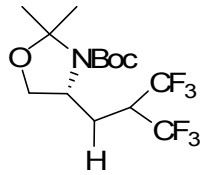

1,1-Dimethylethyl (S)-4- Bis-trifluoromethyl-2,2-dimethyl-3-oxazolidinecarboxylate (13). 4 g (11 mmol) of **12** was dissolved in 75 mL of dioxane in a Parr bomb, and then degassed with argon. 4 g of 10 % Palladium on carbon was then added and the reaction was then set up in a Parr hydrogenator at 55 psi for 24 hours. The reaction was then worked up via filtration through celite and the crude reaction mixture was treated with an additional 4 g of fresh 10 % Palladium on carbon. The reaction was treated at 55 psi in the Parr hydrogenator for another 24 hours. The reaction was worked up via filtration through celite, and then condensed *in vacuo* to yield **13** in 90 % yield (3.61 g, 9.9 mmol) as a clear oil. ^{1}H NMR (400MHz, $CDCl_3$): δ 1.48 (br. s, 12H), 1.62 (s, 3H), 2.18 (2.01, m, 2H), 3.55 (3.00, m, 1H), 3.77 (d, 1H, J = 9.3 Hz), 3.97 (dd, 1H, J = 5.4 Hz, 9.3 Hz), 4.20 (4.12, m, 1H); ^{13}C NMR (100 MHz, $CDCl_3$): δ 153.22 (151.51),

123.89 (q, 2 × CF_3, J = 284.0), 94.47 (94.03), 80.85 (80.73), 67.26 (66.65), 55.58 (55.12), 45.44 (45.12) (quintet, CH, J = 27.2 Hz), 28.98 (28.00), 28.25, 27.58 (26.90), 24.15 (22.86); ^{19}F NMR (384 MHz, $CDCl_3$): δ – 67.56, – 67.97 (m); FT–IR (film): 1707, 1395, 1255, 1169. ESI-MS, Calc. for $C_{14}H_{20}F_6NO_3$ [M + H]: 365.1437; found 365.0992 (266.0960)

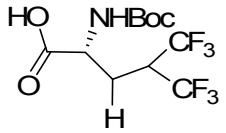

***N*–Boc-5,5,5,5',5',5'-(S)-hexafluoroleucine (14). 13,** 1,1-Dimethylethyl (S)-4- Bis-trifluoromethyl-2,2-dimethyl-3-oxazolidinecarboxylate (0.24 g, 0.6 mmol) was dissolved in 6 mL acetone then cooled to 0 °C open to atmosphere. Then 1.2 mL of 1 Molar Jones reagent was added dropwise to the reaction, and allowed to warm to room temperature over 2 hours. The reaction was then cooled back to 0 °C and quenched with 2-propanol. The reaction was then diluted with 30 mL of sat. aq. ammonium chloride, and extracted with 2 x 30 mL of methylene chloride. The methylene chloride was washed with sat. aq. ammonium chloride and dried over sodium sulfate. The solvent was removed *in vacuo* to yield **14** as a white solid in 55 % yield (0.11g, 33 mmol). Rf = 0.5 (ethyl acetate). ^{1}H NMR (400MHz, $CDCl_3$): δ 1.50 (s, 9H); 2.41-2.12 (br. m, 2H), 3.35 (m, 1H), 4.40 (m, 1H), 7.35 (5.20, d, 1H, *J* = 6.3 Hz). ^{19}F NMR (384 MHz, $CDCl_3$): δ – 67.87, –68.23 (m). FT–IR: 3360-2500m (br.), 3255, 2990, 1723, 1710, 1667, 1487, 1460, 1407, 1298, 1252. ESI-MS, Calc. for $C_{11}H_{15}F_6NO_4$ [M + H]: 340.0978; found 340.0979.

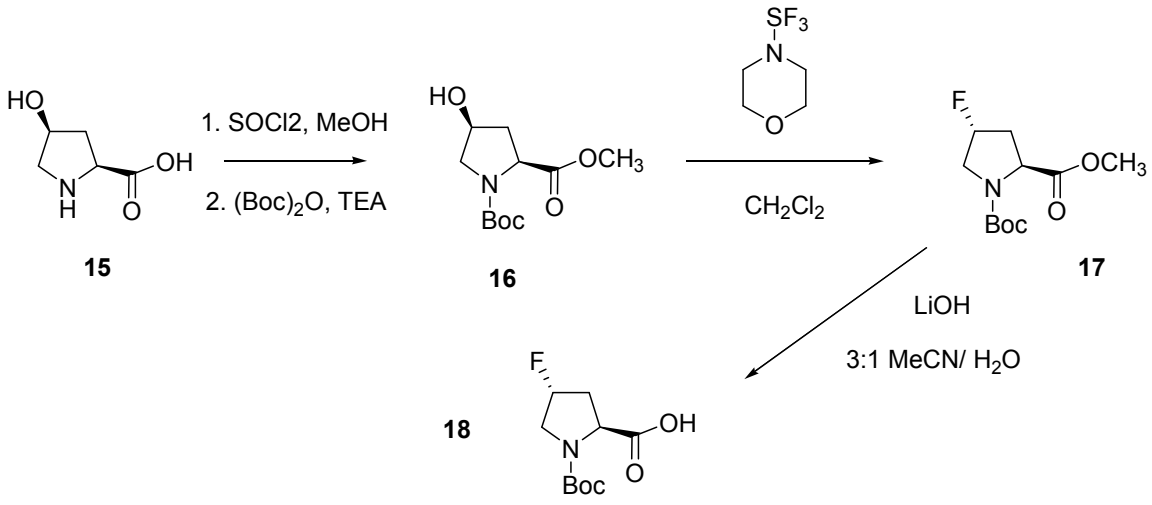

Scheme 4. Synthesis of N-tert-butoxycarbonyl-trans-(2S, 4R)-4-fluoroproline

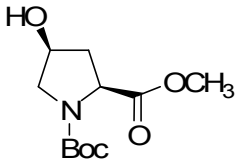

N-Boc-cis-(2S, 4S)-4-Hydroxyproline methyl ester (16). 4-hydroxyproline (10 g, 40 mmol) was dissolved in 150 mL of fresh methanol, and cooled to 0 ^{o}C under argon. Thionyl chloride (3.2 mL) was then added slowly via syringe to the stirring mixture, and allowed to warm to room temperature overnight. Reaction was then worked up by the removal of solvent to yield a white solid in the form of hydroxylproline methyl ester hydrochloride. The white solid was used without further purification and was dissolved in 150 mL methylene chloride and cooled to 0 ^{o}C open to the atmosphere. The reaction was then treated with 5.8 mL triethyl amine (41 mmol) followed by 9 g (42 mmol) of $(Boc)_2O$. The reaction mixture was allowed to warm with stirring overnight, and then was worked up by washing the reaction mixture with 2 x 150 mL 3M HCl followed by 150 mL sat. aq. ammonium chloride. The solution was then dried over sodium sulfate, and the solvent was removed *in vacuo*. to yield **16** as a white solid in 94 % yield (9.2 g, 37 mmol). ^{1}H NMR (400MHz, $CDCl_3$): δ 1.38 and 1.45 (s, 9H), 2.25 (m, 1H), 2.52 (m, 1H), 3.32 (m, 1H), 3.54 (m, 1H), 3.68 (s, 3H), 4.23 (m, 1H), 4.62 (m, 1H).

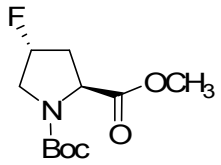

N-Boc-trans-(2S, 4R)-4-fluoroproline methyl ester (17). 5g (20 mmol) of 4-Hydroxyproline methyl ester (16) was dissolved in 100 mL of dry methylene chloride in a dry 250 mL two neck round bottom flask under argon, and the reaction mixture was then cool to -78 ^{o}C. 6.4 mL (51 mmol) of morpholinosulfur trifluoride was carefully added dropwise over five minutes via syringe to the reaction mixture. The reaction mixture was allowed to stir at -78 ^{o}C for one hour, and then warmed to room temperature and allowed to stir for an additional 24 hours. The reaction was then opened to the atmosphere and quenched by the dropwise addition of 1M aqueous sodium bicarbonate (be cautious of the evolution of HF gas). The aqueous phase was then extracted with 25 mL methylene chloride and combined with the methylene chloride reaction solution. The combined solutions were then washed with 100 mL of 10% aqueous citric acid solution followed by 100 mL sat. aq. ammonium chloride. The extract was then dried over sodium sulfate and the solvent removed *in vacuo* to yield the crude product which was purified via silica gel chromatography using a mixture of 4:1 hexane-ethyl acetate. The desired product was isolated in an 84% yield (4.15 g, 16 mmol). Rf = 0.5 (4 hexane/ 1 ethyl acetate). ^{1}H NMR (400MHz, $CDCl_3$): δ 1.40 and 1.45 (s, 9H), 2.00 (m, 1H), 2.61 (m, 1H), 3.65-3.72 (m, 1H), 3.74 (s, 3H), 3.78-3.3.98 (m, 1H), 4.48-4.54 (m, 1H), 5.07 and 5.12 (2s, 1H). ^{19}F NMR (384 MHz, $CDCl_3$): δ - 177.0 (-177.6, m).

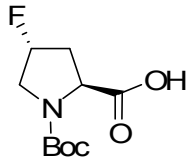

N-tert-butoxycarbonyl-trans-(2S, 4R)-4-fluoroproline (18). 4-Fluoroproline methyl ester (4.15 g, 16 mmol) was dissolved in 75 mL of a 3:1 mixture of acetonitrile and water open to atmosphere at room temperature. 0.77 g (35 mmol) of solid lithium hydroxide was then added to the reaction, and was allowed to stir for three hours until all starting material had disappeared via TLC (1:1 hexane/ethyl acetate). The reaction was then worked up by removing the solvent *in vacuo* and dissolving the reaction mixture in 50 mL water and extracting with 1:1 mixture of hexane-ethyl acetate. The aqueous layer was then acidified using solid potassium bisulfite then extracted with 3 x 75 mL methylene chloride. The extract was then dried over sodium sulfate, and the solvent removed *in vacuo* to yield the free acid in 90 % yield (3.35g, 14 mmol). Rf = 0.5 (ethyl acetate). ^{1}H NMR (400MHz, $CDCl_3$): δ 1.42 and 1.48 (s, 9H), 2.12-2.67 (m, 2H), 3.40-3.72 (m, 1H), 3.86 (m, 1H), 4.38 and 4.48 (m, 1H), 5.05 and 5.12 (2s, 1H). ^{19}F NMR (384 MHz, $CDCl_3$): δ - 177.67 (m).

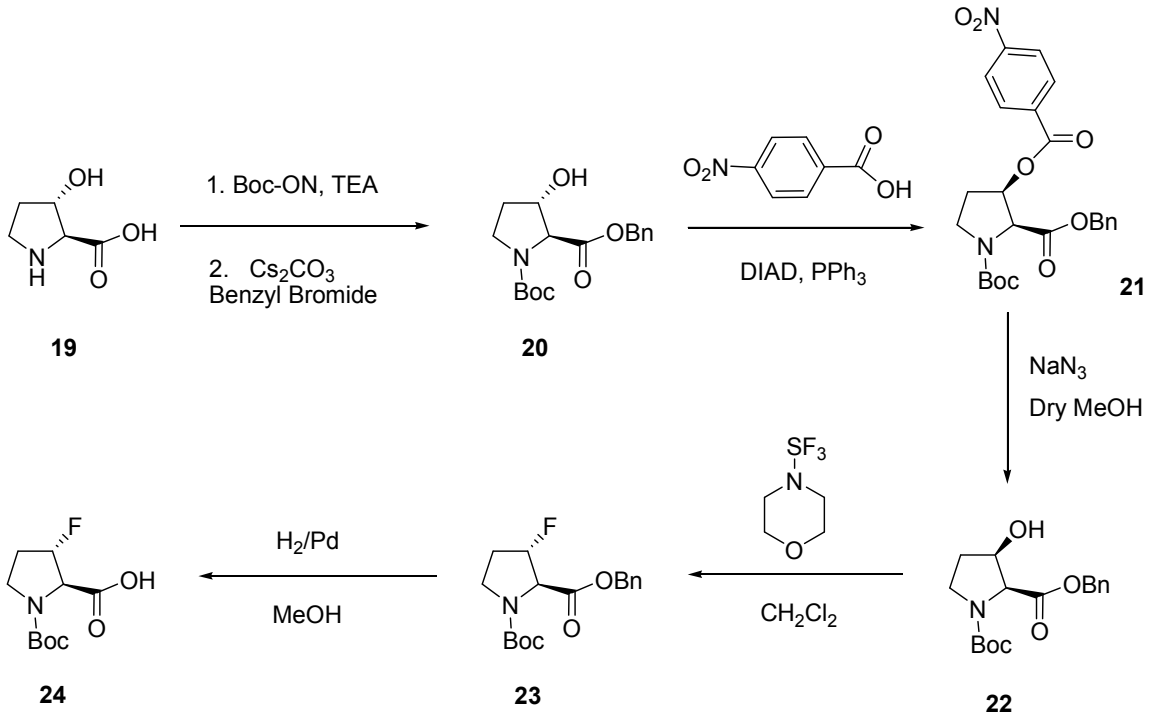

Scheme 5. Synthesis of N-tert-Butoxycarbonyl-trans-(2S, 3S)-3-fluoroproline

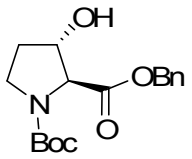

N-Boc-trans-(2S, 3S)-3-Hydroxyproline benzyl ester (20). (2S, 3R)-trans-3-hydroxyproline (10g, 76 mmol) was dissolved in a 1:1 mixture of dioxane-water (50 mL) then triethylamine (11.7 mL, 84 mmol) was added. To the stirring reaction Boc-ON (20.5 g, 75 mmol) in dioxane (50 mL) was added and the reaction was allowed to stir at room temperature for 4 hours. The solvent was then removed *in vacuo*. The resulting residue was then suspended in 100 mL water and extracted with toluene 2 x 75 mL. The aqueous layer was then acidified with solid potassium bisulfate to a pH of 4, and then extracted with ethyl acetate 3 x 100 mL. The combined organic extracts were then washed with sat. aq. ammonium chloride, dried over sodium sulfate, and the solvent removed *in vacuo* to yield the boc-protected product as a white solid (16.7g, 72 mmol) with a crude yield of 95%. ^{1}H NMR (400MHz, $CDCl_3$): δ 1.25 and 1.30 (2s, 9H), 1.72 (m, 1H), 1.88 (m, 1H), 3.41 (m, 2H), 3.97 and 4.08 (s, 1H), 4.27 (m, 1H).

The crude white solid was then dissolved in 150 mL acetonitrile and cooled in an ice bath open to air with a high torque stirring bar. Cesium carbonate was then added (12.5 g, 38 mmol) slowly to the stirring reaction mixture as a solid and the reaction was allowed to warm to room temperature with stirring for 1 hour. Benzyl bromide (9.5 mL, 77 mmol) was added to the reaction and stirred for 20 hours. Once acid was no longer observed via TLC the reaction was worked up by removing the solvent *in vacuo*, and the crude residue was taken up in 100 mL water and adjusted to a pH of 9. The reaction mixture was then extracted with 3 x 75 mL methylene chloride, dried over sodium sulfate,

and the solvent removed *in vacuo*. The crude product was then purified via silica gel chromatography with 1:1 hexanes-ethyl acetate to yield **20** in 87% overall yield (21.3g, 66mmol). ^{1}H NMR (400 MHz, $CDCl_3$): δ 1.34 and 1.48 (2s, 9H), 1.87-2.10 (m, 2H), 3.56-3.70 (m, 2H), 4.22 and 4.35 (2s, 1H), 4.40 (bs, 1H), 5.20 (q, 2H), 7.30-7.45 (m, 5H).

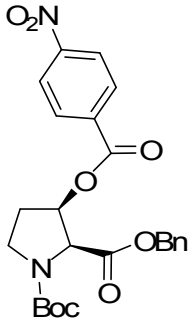

N-Boc-cis-(2S, 3R)-3-p-nitrophenoxyproline benzyl ester (21). 20 (4 g, 12 mmol) was dissolved in 100 mL dry THF under argon and cool in an ice bath. Then 4.89 g (18 mmol) triphenylphosphine and 2.71 g (16 mmol) p-nitrobenzoic acid were added to the stirring reaction mixture. Diisopropyl azodicarboxylate (3.6 mL, 18 mmol) was added slowly to the reaction mixture via syringe, and the reaction was allowed to stir for 2 hours under argon. The reaction was then worked up by the removal of solvent *in vacuo* to yield a yellow oil. The oil was then chromatographed on silica gel using 4:1 hexane-ethyl acetate to yield the product in 92% (5.1g, 11 mmol). Rf = 0.25 (4:1 hexane-ethyl acetate). This reaction proved not to be scaleable beyond the 4 g (12mmol) amount used for this reaction, thus the reaction was run three separate times to generate the material needed for the next step in the synthesis. ^{1}H NMR (400 MHz, $CDCl_3$): δ 1.4 and 1.5 (2s, 9H), 2.20-2.35 (m, 2H), 3.6-3.8 (m, 2H), 4.7 and 4.8 (2d, 1H), 5.20 (q, 2H), 5.70-5.76 (m, 1H), 7.30-7.45 (m, 5H), 7.91-8.0 (dd, 2H), 8.12-8.20 (dd, 2H).

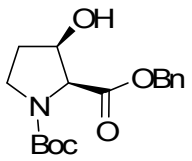

N-Boc-cis-(2S, 3R)-3-hydroxyproline benzyl ester (22). 19.02 g (40 mmol) of **21** was transferred to a 500 mL flask and dissolved in 200 mL of fresh methanol. 8 g (120 mmol) of sodium azide was then added to the reaction mixture then the reaction vessel was fitted with a reflux condenser and heated to 40 ^{o}C for 3 hours open to air. The reaction was allowed to cool and then worked up by removing the solvent *in vacuo*. The crude product was then purified via silica gel chromatography using a 1:1 mixture of hexane-ethyl acetate as elulent to yield 12.19 g (38 mmol) of **22** as a clear oil in 95% yield. ^{1}H NMR (400MHz, $CDCl_3$): δ 1.35 and 1.46 (2s, 9H), 2.00-2.20 (m, 2H), 3.43-3.56 and 3.58-3.70 (2m, 2H), 4.40 and 4.48 (2d, 1H), 4.57-4.65 (m, 1H), 5.20 (q, 2H), 7.30-7.45 (m, 5H).

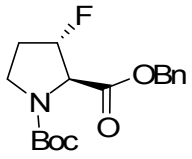

N-Boc-trans-(2S, 3S)-3-fluoroproline benzyl ester (23). N-Boc-cis-(2S, 3R)-3-hydroxyproline benzyl ester (**22,** 5.36 g, 16 mmol) was dissolved in dry methylene chloride under argon, and the solution was cooled to -78 ^{o}C. Morpholinosulfur trifluoride (morph-DAST, 5.21 mL, 41 mmol) was added slowly in a dropwise fashion to the stirring reaction. The reaction was allowed to stir for 1 hour at -78 ^{o}C and then removed for the dry ice-acetone bath and was slowly allowed to warm to room temperature with stirring under argon for 24 hours. The reaction was then slowly quenched with 1M sodium bicarbonate with caution. The aqueous phase was extracted 2 x 50 mL methylene

chloride, and the combined organic phases were washed with 1M potassium bisulfate then sat. aq. ammonium chloride. The extract was dried over sodium sulfate, and the solvent removed *in vacuo*. The crude extract was then purified by silica gel chromatography using 4:1 hexanes-ethyl acetate to give 4.0 g (12 mmol) of the desired product as a colorless oil in a 77% yield. Rf = 0.8 (1:1 hexanes-ethyl acetate). ^{1}H NMR (400 MHz, $CDCl_3$): δ 1.34 and 1.46 (2s, 9H), 2.00-2.25 (m, 2H), 3.50-3.60 and 3.63-3.76 (2m, 2H), 4.48-4.67 (4s, 1H), 5.08-5.11 (m, 1H), 5.20 (m, 2H), 7.30-7.45 (m, 5H). ^{19}F NMR (384 MHz, $CDCl_3$): δ - 174.6 (-175.4 , m).

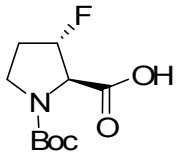

N-*tert*-Butoxycarbonyl-trans-(2S, 3S)-3-fluoroproline (24). 3-fluoroproline benzyl ester (4.77 g, 14 mmol) was dissolved in fresh methanol (150 mL) in a 250 mL round bottom flask. 10% Pd on carbon (2.32 g) was added to the reaction mixture with a gentle flow of argon gas. The reaction mixture was then fitted with a balloon containing H_2 (gas), and allowed to stir overnight at room temperature. The H_2 (gas) was refilled as needed until the reaction was shown to be complete by TLC. The reaction was then worked up by the addition of celite to the crude reaction mixture followed by filtration through a celite pad. The solvent was then removed *in vacuo* to yield a white solid which was recrystallized from methanol/pentane to yield 3.39 g (13.6 mmol) of product as a white solid in 97 % yield. ^{1}H NMR (400 MHz, $CDCl_3$): δ 1.39 and 1.42 (s, 9H), 2.00-2.15 (m, 2H), 3.52-3.62 (m, 2H), 4.45 (m, 1H), 5.19 and 5.40 (4s, 1H). ^{19}F NMR (384 MHz, $CDCl_3$): δ - 174.8 (-181.9, m).

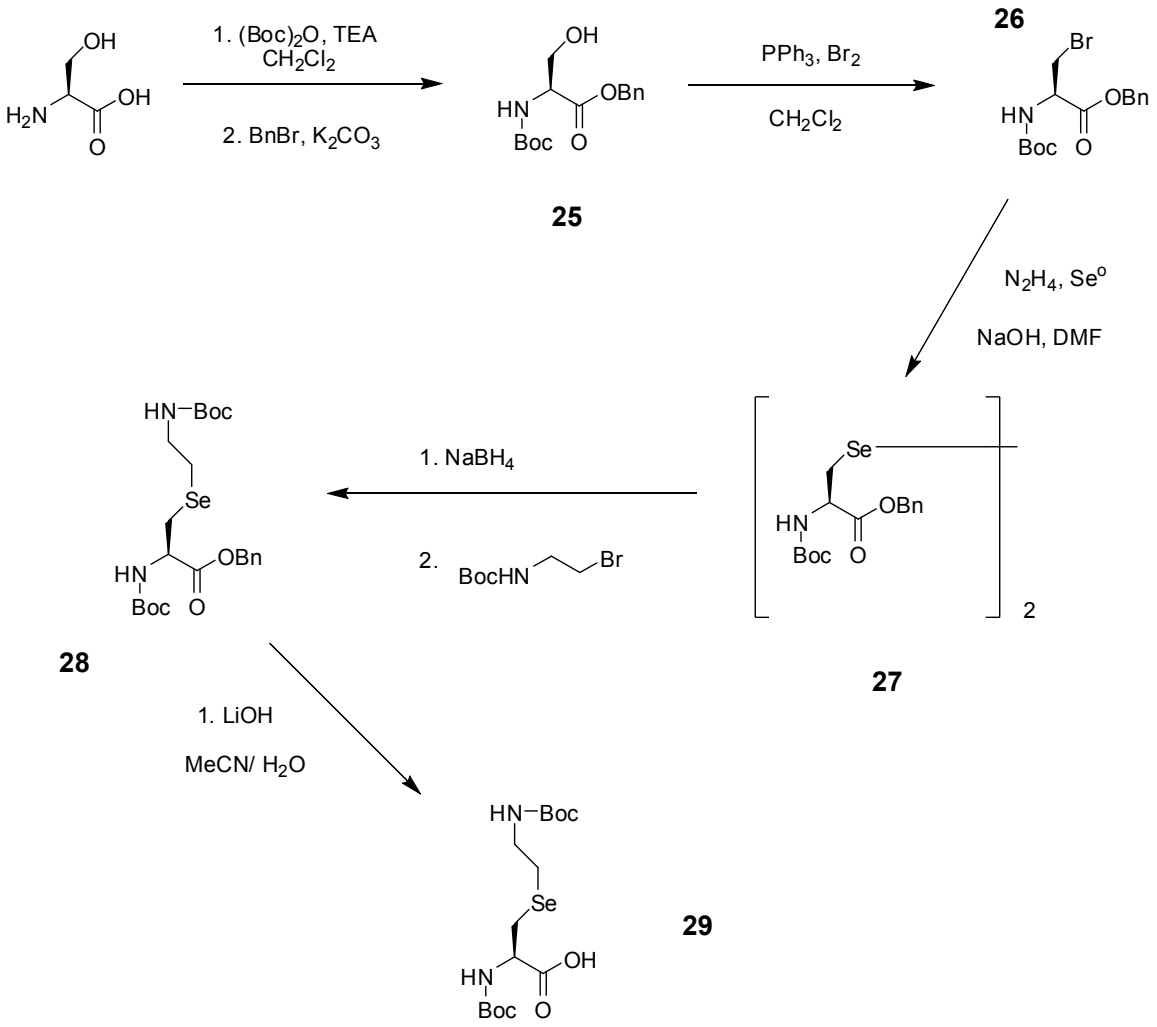

Scheme 6. Synthesis of γ-Selenolysine.

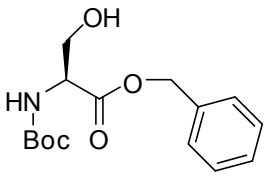

***N-tert*-Butoxycarbonyl-Serine-benzyl ester (25).** Serine (7.31 g, 70 mmol) was dissolved in 75 mL methylene chloride and cooled to 0 ^{o}C and 10 mL triethylamine was added followed by di-*tert*-butyl dicarbonate (15.2 g, 71 mmol). The reaction was allowed to warm to room temperature with stirring overnight. The reaction was then worked up by washing the crude reaction mixture 3 x 100 mL 1M potassium bisulfite. The organic extract was dried over sodium sulfate and the solvent removed *in vacuo* to produce a clear viscous oil. The oil was then dissolved in 60 mL acetonitrile along with potassium carbonate (5 g, 35 mmol), and the reaction was allowed to stir for 20 minuets. Benzyl bromide (8.5 mL, 71 mmol) was then added to the mixture, and the reaction was allowed to stir for 6 hours at room temperature. The reaction was then worked up by removing most of the solvent *in vacuo* then redissolving the crude reaction mixture in methylene chloride. The reaction was then washed 2 x 100 mL sat. aq. sodium bicarbonate, and the organic phase was then dried over sodium sulfate and the solvent removed *in vacuo* to yield a white solid **25** (18.5 g, 62 mmol) in 90 % yield. Rf = 0.4 (1:1 hexanes/ ethyl acetate). ^{1}H NMR (400 MHz, $CDCl_3$): δ 1.45 (s, 9H), 3.26 (m, 1H), 3.70 (m, 1H), 4.25 (m, 1H), 5.15 (m, 2H), 7.34 (m, 5 H).

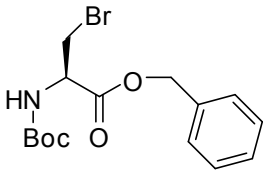

Benzyl *N-tert*-Butoxycarbonyl-β-bromo-(R)-alaninate (26). In a dry round bottom flask triphenylphosphene (1.8 g, 7 mmol) was dissolved in 20 mL of dry methylene chloride under argon gas and cool in an ice bath. Liquid bromine (0.36 mL, 7mmol) was then added slowly to the reaction and allowed to stir for 20 minuets. Then a mixture of serine **25** (1 g, 3.5 mmol) and imidazole (0.47 g, 7 mmol) was dissolved in 10 mL dry methylene chloride then slowly added to the stirring reaction mixture. The reaction was then allowed to stir for 2 hours during which time a white precipitate formed. The reaction was then worked up by filtering the crude mixture with subsequent purification via silica gel chromatography using 5:1 hexanes/ ethyl acetate to produce **26** (1.11 g, 3.1 mmol) as a clear oil in an 87 % yield. Rf = 0.6 (5:1 hexanes/ ethyl acetate. ^{1}H NMR (400 MHz, $CDCl_3$): δ 1.45 (s, 9H), 3.70 (dd, J = 10.5, 3.5 Hz, 1H), 3.85 (dd, J = 10.5, 3.1 Hz, 1H), 4.79 (m, 1H), 5.15 (m, 2H), 7.34 (m, 5 H). ^{13}C NMR (100MHz, $CDCl_3$): δ 27.8, 33.5, 53.8, 67.3, 79.7, 127.9, 128.3, 134.6, 154.3, 168.8.

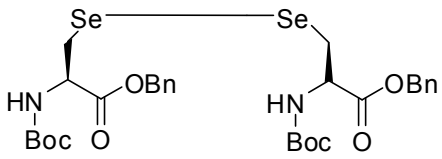

***N-tert*-Butoxycarbonyl-homoselenocystine Benzyl Ester (27).**[1] Pulverized elemental selenium (0.15 g, 1.8 mmol) and solid sodium hydroxide (0.1 g, 2.5 mmol) were mixed in 25 mL round bottomed flask under argon in 3 mL of DMF. Then 3 drops of N_2H_4–H_2O was added to the reaction and then was heated 60 ^oC for 3 hours to a red-black color. The reaction was then cool to room temperature and **26** (0.6 g, 1.6 mmol) in 1.5 mL DMF was added to the stirring reaction. The reaction was allowed to stir for 1 hour under argon. The reaction was then worked up by pouring the crude reaction mixture into 20 mL 1M HCl, some gas and heat evolved from the quenched reaction. The crude reaction mixture was then extracted with 3 x 10 mL 1:1 diethyl ether/ hexanes, and dried over sodium sulfate then the solvent removed *in vacuo*. The produced the desired product **27** (0.23 g, 0.65 mmol) in an 39 % yield that required no further purification. Rf = 0.6 (5:1 hexanes/ ethyl acetate). ^{1}H NMR (400 MHz, $CDCl_3$): δ 1.48 (s, 18H), 1.97-2.34 (m, 4H), 2.89 (m, 4H), 4.19 (m, 2H,), 5.14 (m, 4H) 7.23 (m, 10H).

[1]It should be noted that this synthesis of Seleno-Lysine has a fatal flaw that is responsible for the low yield going from bromide (**26**) to the diselenide (**27**). The carboxylate benzyl protecting group should be replaced with a tert-butyl protecting group in order to resist decomposition during the highly basic conditions needed for the installation of the selenium moiety.

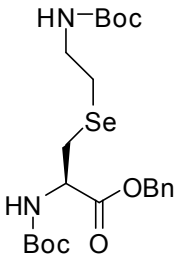

N, N'-*tert*-Butoxycarbonyl-Selenolysine Benzyl Ester (28). Diselenide **27** (0.16 g, 0.2 mmol) was dissolved in 3 mL of degassed ethanol under argon in an ice bath. Sodium borohydride was then added in one portion and the reaction turned immediately brown. After 10 minutes N-tert-butoxycarbonyl-1-bromo-2-ethylamine (0.16 g, 0.7 mmol) in 1 mL of degassed ethanol was added to the reaction mixture. The reaction mixture was allowed to stir for 2 hours under argon while warming to room temperature. The crude product was the purified via silica gel chromatography using 4:1 hexane/ ethyl acetate to produce the desired product **28** (0.07 g, 0.14 mmol) in a 70 % yield. Rf = 0.5 (4:1 hexanes/ ethyl acetate). ^{1}H NMR (400 MHz, $CDCl_3$): δ 1.35 (s, 18H), 3.23 (m, 2H), 3.41 (m, 4H), 4.95 (m, 1H), 5.09 (m, 2H), 7.22 (m, 5H). ^{13}C NMR (100MHz, $CDCl_3$): δ 28.2, 28.3, 40.2, 54.0, 65.4, 67.9, 79.5, 80.5, 127.2, 127.9, 129.0, 135.1, 155.1, 155.4, 171.0. ESI-MS, Calc. for $C_{22}H_{34}N_2O_6Se$ [M + H]: 503.1654; found 503.1655.

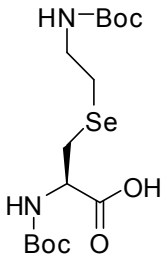

N, N'-*tert*-Butoxycarbonyl-γ-Selenolysine Benzyl Ester (29). The protected selenolysine **28** (0.067g, 0.16 mmol) was dissolved in 2 mL of degassed dioxane followed by 12 mL of degassed 1M lithium hydroxide at room temperature open to atmosphere. The reaction was allowed to proceed until it was complete by TLC. The reaction was then worked up by extracting the reaction mixture with 5 mL hexanes then separated. The aqueous layer was then acidified with 6 M HCl and extracted with 2 x 10 mL ethyl acetate. The solvent was then removed *in vacuo* to produce a white solid (**29**, 0.059 g, 0.14 mmol) without need of further purification in a 90 % yield. ^{1}H NMR (400 MHz, $CDCl_3$): δ 1.25 (s, 18H), 3.18 (m, 2H), 3.40 (m, 4H), 4.93 (m, 1H), 5.05 (m, 2H). ^{13}C NMR (100MHz, $CDCl_3$): δ 28.1, 28.4, 40.4, 54.2, 65.8, 68.2, 79.5, 80.5, 155.1, 155.4, 175.4. ESI-MS, Calc. for $C_{15}H_{28}N_2O_6Se$ [M - H]: 411.1034; found 411.088.

APPENDIX 3

Crystallographic data

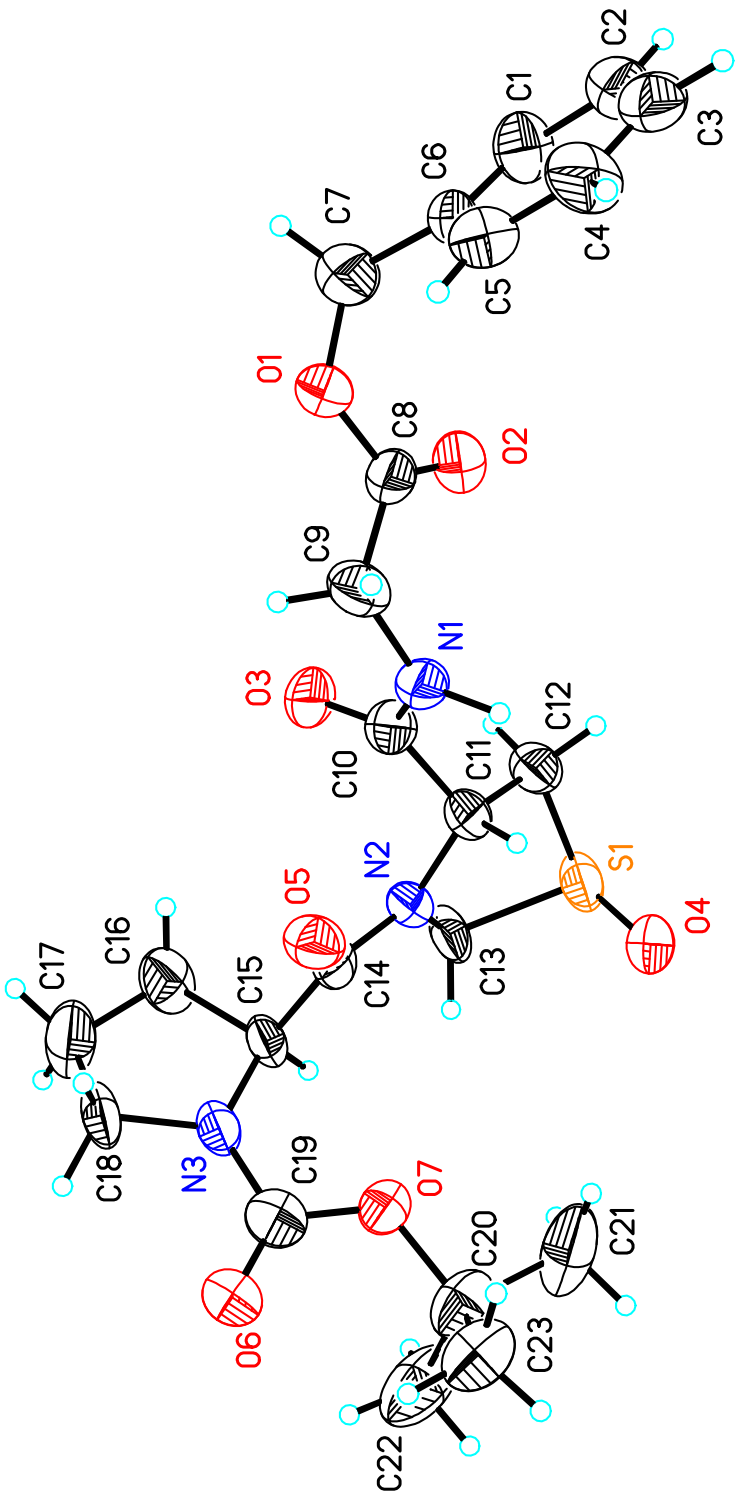

Figure 1. Crystallographically determined structure of N-tert-butoxycarbonyl-prolyl-1(R_s)-oxo-thiazolidine-4-(R)-carboxylic acid-glycine benzyl ester.

Table A1-1. Crystal data and structure refinement for JS_SOBs.

Identification code	JS_SO	
Empirical formula	C23 H31 N3 O7 S	
Formula weight	493.57	
Temperature	173(2) K	
Wavelength	1.54178 Å	
Crystal system	Orthorhombic	
Space group	P2(1)2(1)2(1)	
Unit cell dimensions	a = 6.1056(10) Å	α= 90°.
	b = 17.130(3) Å	β= 90°.
	c = 23.522(4) Å	γ = 90°.
Volume	2460.2(7) $Å^3$	
Z	4	
Density (calculated)	1.333 Mg/m^3	
Absorption coefficient	1.578 mm^{-1}	
F(000)	1048	
Crystal size	0.21 x 0.03 x 0.02 mm^3	
Theta range for data collection	5.50 to 64.50°.	
Index ranges	-6<=h<=7, -14<=k<=18, -26<=l<=26	
Reflections collected	8173	
Independent reflections	3482 [R(int) = 0.1330]	
Completeness to theta = 64.50°	89.2 %	
Absorption correction	Semi-empirical from equivalents	
Max. and min. transmission	0.9691 and 0.7329	
Refinement method	Full-matrix least-squares on F^2	
Data / restraints / parameters	3482 / 0 / 315	
Goodness-of-fit on F^2	1.007	
Final R indices [I>2sigma(I)]	R1 = 0.0632, wR2 = 0.0990	
R indices (all data)	R1 = 0.1473, wR2 = 0.1263	
Absolute structure parameter	0.04(5)	
Extinction coefficient	0.00122(15)	
Largest diff. peak and hole	0.221 and -0.278 $e.Å^{-3}$	

Table A1-2. Atomic coordinates (x 10^4) and equivalent isotropic displacement parameters ($Å^2$x 10^3) for JS_SOBs. U(eq) is defined as one third of the trace of the orthogonalized U^{ij} tensor.

	x	y	z	U(eq)
C(1)	8725(14)	1854(4)	3590(3)	57(2)
C(2)	8433(16)	1075(5)	3720(3)	62(2)
C(3)	6435(16)	725(5)	3628(3)	63(2)
C(4)	4749(15)	1162(5)	3413(3)	66(3)
C(5)	5029(15)	1939(5)	3289(3)	61(2)
C(6)	7022(14)	2303(4)	3396(3)	46(2)
C(7)	7293(15)	3162(4)	3283(3)	68(3)
C(8)	6869(15)	3276(4)	2275(3)	52(2)
C(9)	5281(13)	3558(4)	1841(3)	58(2)
C(10)	7414(12)	3935(5)	1023(3)	45(2)
C(11)	8157(12)	3691(4)	433(3)	44(2)
C(12)	10490(11)	3367(4)	448(3)	49(2)
C(13)	10249(11)	4384(4)	-307(3)	48(2)
C(14)	6453(14)	4793(4)	-45(3)	41(2)
C(15)	6698(11)	5526(3)	-391(3)	39(2)
C(16)	7267(12)	6205(4)	19(3)	60(2)
C(17)	5591(14)	6808(5)	-50(4)	78(3)
C(18)	3699(12)	6452(4)	-348(3)	53(2)
C(19)	3621(15)	5433(4)	-1086(3)	49(2)
C(20)	4403(15)	4430(5)	-1820(3)	62(2)
C(21)	5997(14)	3757(5)	-1804(4)	91(3)
C(22)	4948(16)	5035(5)	-2263(3)	96(3)
C(23)	2122(14)	4119(5)	-1868(3)	71(3)
N(1)	5991(10)	3436(4)	1264(2)	49(2)
N(2)	8271(10)	4347(3)	35(2)	39(1)
N(3)	4630(10)	5782(3)	-632(2)	43(2)
O(1)	6062(8)	3437(3)	2800(2)	56(1)
O(2)	8616(10)	2976(3)	2191(2)	60(1)
O(3)	8116(9)	4535(3)	1251(2)	56(2)
O(4)	9842(9)	2888(3)	-597(2)	57(1)
O(5)	4722(8)	4633(3)	198(2)	50(1)

O(6)	1895(9)	5667(3)	-1289(2)	59(2)
O(7)	4783(8)	4803(3)	-1255(2)	50(1)
S(1)	11384(3)	3412(1)	-278(1)	51(1)

Table A1-3. Bond lengths [Å] and angles [°] for JS_SOBs.

C(1)-C(6)	1.372(10)
C(1)-C(2)	1.381(9)
C(2)-C(3)	1.376(11)
C(3)-C(4)	1.369(11)
C(4)-C(5)	1.372(9)
C(5)-C(6)	1.391(10)
C(6)-C(7)	1.504(9)
C(7)-O(1)	1.441(8)
C(8)-O(2)	1.200(9)
C(8)-O(1)	1.357(8)
C(8)-C(9)	1.490(10)
C(9)-N(1)	1.438(8)
C(10)-O(3)	1.236(8)
C(10)-N(1)	1.346(9)
C(10)-C(11)	1.518(9)
C(11)-N(2)	1.463(7)
C(11)-C(12)	1.529(9)
C(12)-S(1)	1.793(6)
C(13)-N(2)	1.454(7)
C(13)-S(1)	1.805(6)
C(14)-O(5)	1.233(8)
C(14)-N(2)	1.361(8)
C(14)-C(15)	1.502(8)
C(15)-N(3)	1.452(8)
C(15)-C(16)	1.550(9)
C(16)-C(17)	1.464(9)
C(17)-C(18)	1.483(9)
C(18)-N(3)	1.445(8)
C(19)-O(6)	1.224(9)
C(19)-O(7)	1.351(9)
C(19)-N(3)	1.370(9)
C(20)-O(7)	1.491(8)

C(20)-C(23)	1.495(10)
C(20)-C(22)	1.508(10)
C(20)-C(21)	1.509(11)
O(4)-S(1)	1.501(5)
C(6)-C(1)-C(2)	121.2(8)
C(3)-C(2)-C(1)	120.0(9)
C(4)-C(3)-C(2)	119.1(8)
C(3)-C(4)-C(5)	121.0(9)
C(4)-C(5)-C(6)	120.4(9)
C(1)-C(6)-C(5)	118.1(7)
C(1)-C(6)-C(7)	121.6(8)
C(5)-C(6)-C(7)	120.2(7)
O(1)-C(7)-C(6)	113.7(6)
O(2)-C(8)-O(1)	124.0(7)
O(2)-C(8)-C(9)	127.2(7)
O(1)-C(8)-C(9)	108.8(7)
N(1)-C(9)-C(8)	113.8(6)
O(3)-C(10)-N(1)	124.7(7)
O(3)-C(10)-C(11)	121.5(7)
N(1)-C(10)-C(11)	113.8(6)
N(2)-C(11)-C(10)	112.8(6)
N(2)-C(11)-C(12)	104.4(5)
C(10)-C(11)-C(12)	111.0(6)
C(11)-C(12)-S(1)	104.3(4)
N(2)-C(13)-S(1)	104.9(4)
O(5)-C(14)-N(2)	120.6(6)
O(5)-C(14)-C(15)	121.5(7)
N(2)-C(14)-C(15)	117.6(7)
N(3)-C(15)-C(14)	112.1(6)
N(3)-C(15)-C(16)	102.2(5)
C(14)-C(15)-C(16)	108.2(6)
C(17)-C(16)-C(15)	107.7(6)
C(16)-C(17)-C(18)	107.9(6)
N(3)-C(18)-C(17)	103.8(6)
O(6)-C(19)-O(7)	126.8(7)

O(6)-C(19)-N(3)	123.2(8)
O(7)-C(19)-N(3)	109.9(7)
O(7)-C(20)-C(23)	111.5(6)
O(7)-C(20)-C(22)	106.7(6)
C(23)-C(20)-C(22)	113.4(8)
O(7)-C(20)-C(21)	101.8(6)
C(23)-C(20)-C(21)	109.3(7)
C(22)-C(20)-C(21)	113.5(8)
C(10)-N(1)-C(9)	120.0(6)
C(14)-N(2)-C(13)	125.1(5)
C(14)-N(2)-C(11)	118.8(6)
C(13)-N(2)-C(11)	115.3(5)
C(19)-N(3)-C(18)	122.0(6)
C(19)-N(3)-C(15)	124.4(6)
C(18)-N(3)-C(15)	113.6(6)
C(8)-O(1)-C(7)	117.5(6)
C(19)-O(7)-C(20)	121.5(6)
O(4)-S(1)-C(12)	105.0(3)
O(4)-S(1)-C(13)	107.0(3)
C(12)-S(1)-C(13)	87.7(3)

Symmetry transformations used to generate equivalent atoms:

Table A1-4. Anisotropic displacement parameters ($Å^2 x\ 10^3$)for JS_SOBs. The anisotropic displacement factor exponent takes the form: $-2\pi^2[\ h^2a^{*2}U^{11} + ... + 2\ h\ k\ a^*\ b^*\ U^{12}\ ]$

	U^{11}	U^{22}	U^{33}	U^{23}	U^{13}	U^{12}
C(1)	51(5)	48(6)	72(6)	-4(4)	-1(5)	-7(5)
C(2)	72(7)	57(6)	57(6)	5(4)	-1(5)	-3(5)
C(3)	87(7)	59(6)	43(5)	2(4)	10(5)	-7(6)
C(4)	75(7)	51(6)	72(6)	14(4)	-7(5)	-30(5)
C(5)	71(7)	66(7)	47(5)	1(4)	-3(5)	3(5)
C(6)	68(6)	30(5)	40(5)	-3(3)	-4(4)	-3(4)
C(7)	95(8)	52(7)	57(6)	2(4)	-8(5)	0(5)
C(8)	79(7)	36(5)	39(5)	-4(3)	4(5)	0(5)
C(9)	71(6)	53(6)	48(5)	15(3)	7(5)	10(4)
C(10)	51(5)	37(6)	46(5)	-1(4)	-4(4)	-5(4)
C(11)	61(6)	29(5)	42(5)	6(3)	1(4)	0(4)
C(12)	58(5)	40(5)	50(5)	4(3)	-11(4)	-1(4)
C(13)	61(5)	25(4)	59(5)	9(3)	7(4)	8(4)
C(14)	57(5)	23(4)	43(4)	1(3)	3(4)	-8(4)
C(15)	43(4)	24(4)	51(5)	2(3)	-4(4)	6(3)
C(16)	61(6)	34(6)	86(6)	-1(4)	-17(5)	-11(4)
C(17)	62(6)	65(7)	106(8)	-40(5)	-22(5)	18(5)
C(18)	58(5)	32(5)	68(5)	-2(4)	10(5)	19(4)
C(19)	49(5)	48(6)	50(5)	12(4)	7(5)	-8(5)
C(20)	71(6)	62(6)	53(6)	-10(4)	14(4)	-18(5)
C(21)	71(7)	79(8)	122(8)	-53(6)	3(6)	4(6)
C(22)	149(10)	82(8)	57(6)	-11(4)	26(7)	-47(7)
C(23)	70(7)	81(7)	62(6)	-14(4)	4(5)	-15(5)
N(1)	76(5)	37(4)	34(4)	3(3)	1(3)	-2(4)
N(2)	46(4)	34(4)	36(3)	5(2)	-1(3)	6(3)
N(3)	46(4)	31(4)	53(4)	-1(3)	-5(3)	9(3)
O(1)	83(4)	45(3)	41(3)	7(2)	3(3)	8(3)
O(2)	77(4)	46(4)	56(4)	-1(2)	4(3)	10(3)
O(3)	80(4)	32(3)	56(3)	-9(2)	-8(3)	-10(3)
O(4)	75(4)	37(3)	57(3)	-6(2)	-7(3)	2(3)
O(5)	51(3)	56(4)	44(3)	8(2)	2(3)	5(3)

O(6)	64(4)	55(4)	57(3)	2(2)	-11(3)	13(3)
O(7)	54(3)	50(4)	45(3)	-9(2)	-5(3)	7(3)
S(1)	60(1)	33(1)	61(1)	2(1)	6(1)	11(1)

Table A1-5. Hydrogen coordinates (x 10^4) and isotropic displacement parameters ($Å^2$x 10^3) for JS_SOBs.

	x	y	z	U(eq)
H(1)	10101	2078	3636	69
H(2)	9587	786	3869	74
H(3)	6232	199	3710	76
H(4)	3394	929	3350	79
H(5)	3879	2223	3133	74
H(7A)	6836	3450	3618	81
H(7B)	8833	3271	3220	81
H(9A)	3895	3292	1897	69
H(9B)	5032	4111	1899	69
H(11)	7160	3293	283	53
H(12A)	10503	2834	586	59
H(12B)	11422	3683	690	59
H(13A)	11270	4762	-152	58
H(13B)	9907	4529	-696	58
H(15)	7820	5465	-685	47
H(16A)	7285	6019	409	72
H(16B)	8702	6415	-71	72
H(17A)	6169	7240	-271	93
H(17B)	5141	7005	318	93
H(18A)	2575	6295	-80	63
H(18B)	3068	6813	-620	63
H(21A)	7454	3954	-1750	136
H(21B)	5924	3475	-2156	136
H(21C)	5625	3414	-1496	136
H(22A)	3930	5460	-2237	144
H(22B)	4854	4804	-2635	144
H(22C)	6408	5225	-2202	144
H(23A)	1793	3804	-1542	106
H(23B)	2002	3807	-2206	106
H(23C)	1107	4546	-1889	106

H(24)	5440(100)	2910(40)	1050(20)	50(20)

Table A1-6. Torsion angles [°] for JS_SOBs.

C(6)-C(1)-C(2)-C(3)	3.3(11)
C(1)-C(2)-C(3)-C(4)	-0.7(11)
C(2)-C(3)-C(4)-C(5)	0.1(12)
C(3)-C(4)-C(5)-C(6)	-2.0(12)
C(2)-C(1)-C(6)-C(5)	-5.1(11)
C(2)-C(1)-C(6)-C(7)	176.8(7)
C(4)-C(5)-C(6)-C(1)	4.4(11)
C(4)-C(5)-C(6)-C(7)	-177.4(7)
C(1)-C(6)-C(7)-O(1)	143.9(7)
C(5)-C(6)-C(7)-O(1)	-34.2(10)
O(2)-C(8)-C(9)-N(1)	0.7(12)
O(1)-C(8)-C(9)-N(1)	178.5(6)
O(3)-C(10)-C(11)-N(2)	-42.6(10)
N(1)-C(10)-C(11)-N(2)	138.6(6)
O(3)-C(10)-C(11)-C(12)	74.1(9)
N(1)-C(10)-C(11)-C(12)	-104.7(7)
N(2)-C(11)-C(12)-S(1)	-40.2(6)
C(10)-C(11)-C(12)-S(1)	-162.0(5)
O(5)-C(14)-C(15)-N(3)	-28.6(9)
N(2)-C(14)-C(15)-N(3)	157.5(6)
O(5)-C(14)-C(15)-C(16)	83.4(8)
N(2)-C(14)-C(15)-C(16)	-90.5(7)
N(3)-C(15)-C(16)-C(17)	-4.0(8)
C(14)-C(15)-C(16)-C(17)	-122.5(7)
C(15)-C(16)-C(17)-C(18)	16.3(9)
C(16)-C(17)-C(18)-N(3)	-21.9(9)
O(3)-C(10)-N(1)-C(9)	-3.8(11)
C(11)-C(10)-N(1)-C(9)	175.0(6)
C(8)-C(9)-N(1)-C(10)	-80.9(8)
O(5)-C(14)-N(2)-C(13)	167.4(6)
C(15)-C(14)-N(2)-C(13)	-18.7(10)
O(5)-C(14)-N(2)-C(11)	-2.3(10)
C(15)-C(14)-N(2)-C(11)	171.6(6)
S(1)-C(13)-N(2)-C(14)	-150.6(6)

S(1)-C(13)-N(2)-C(11)	19.4(7)
C(10)-C(11)-N(2)-C(14)	-55.5(9)
C(12)-C(11)-N(2)-C(14)	-176.1(5)
C(10)-C(11)-N(2)-C(13)	133.8(6)
C(12)-C(11)-N(2)-C(13)	13.3(8)
O(6)-C(19)-N(3)-C(18)	1.2(11)
O(7)-C(19)-N(3)-C(18)	-177.4(6)
O(6)-C(19)-N(3)-C(15)	-178.7(6)
O(7)-C(19)-N(3)-C(15)	2.7(9)
C(17)-C(18)-N(3)-C(19)	-159.5(7)
C(17)-C(18)-N(3)-C(15)	20.4(8)
C(14)-C(15)-N(3)-C(19)	-74.8(8)
C(16)-C(15)-N(3)-C(19)	169.5(7)
C(14)-C(15)-N(3)-C(18)	105.3(7)
C(16)-C(15)-N(3)-C(18)	-10.4(8)
O(2)-C(8)-O(1)-C(7)	-6.2(11)
C(9)-C(8)-O(1)-C(7)	175.9(6)
C(6)-C(7)-O(1)-C(8)	-77.0(8)
O(6)-C(19)-O(7)-C(20)	16.9(11)
N(3)-C(19)-O(7)-C(20)	-164.5(6)
C(23)-C(20)-O(7)-C(19)	-62.0(9)
C(22)-C(20)-O(7)-C(19)	62.4(9)
C(21)-C(20)-O(7)-C(19)	-178.4(6)
C(11)-C(12)-S(1)-O(4)	-61.8(5)
C(11)-C(12)-S(1)-C(13)	45.1(5)
N(2)-C(13)-S(1)-O(4)	68.1(5)
N(2)-C(13)-S(1)-C(12)	-36.9(5)

Symmetry transformations used to generate equivalent atoms:

Table A1-7. Hydrogen bonds for JS_SOBs [Å and °].

D-H...A	d(D-H)	d(H...A)	d(D...A)	<(DHA)
N(1)-H(24)...O(4)#1	1.09(6)	1.77(6)	2.847(7)	170(5)
N(1)-H(24)...S(1)#1	1.09(6)	2.96(6)	3.932(6)	150(4)

Symmetry transformations used to generate equivalent atoms:

#1 x-1/2,-y+1/2,-z

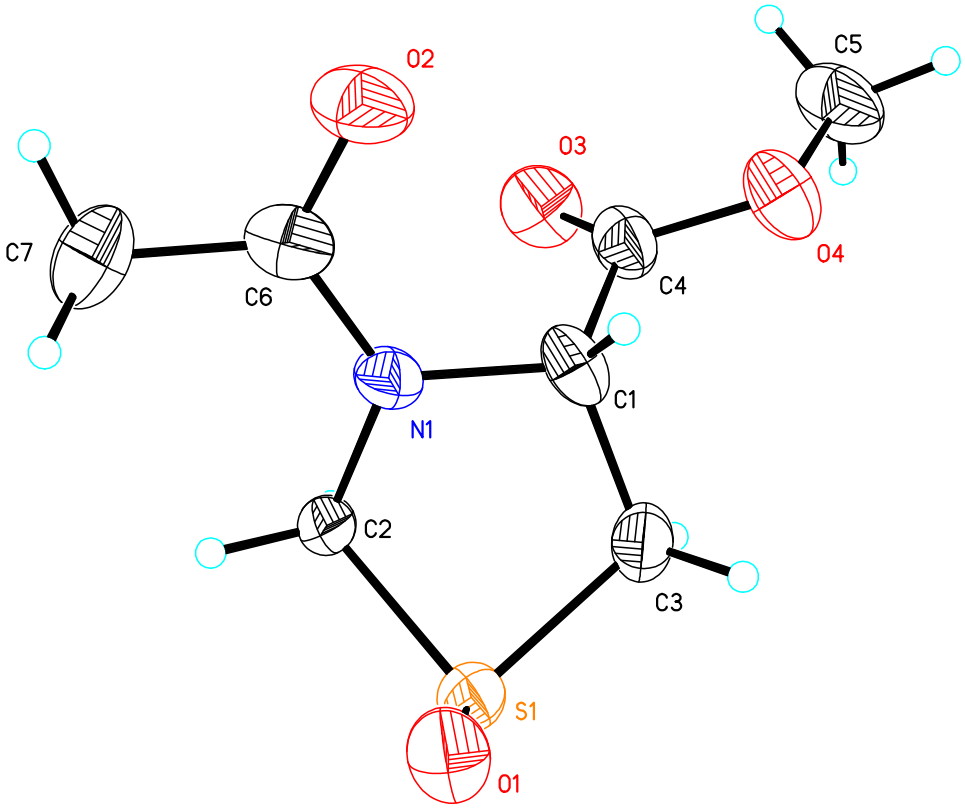

Figure 2. X-Ray crystal structure of N-Acetyl-4(R)-oxide-Thiazolidine-(R)-Carboxylic Acid Methyl Ester (trans/ major product)

Table A2-1. Crystal data and structure refinement for S256s.

Identification code	S256s	
Empirical formula	C7 H11 N O4 S	
Formula weight	205.23	
Temperature	173(2) K	
Wavelength	1.54178 Å	
Crystal system	Monoclinic	
Space group	P2(1)	
Unit cell dimensions	a = 6.2724(8) Å	α= 90°.
	b = 5.5820(7) Å	β= 92.165(9)°.
	c = 13.7387(15) Å	γ = 90°.
Volume	480.68(10) $Å^3$	
Z	2	
Density (calculated)	1.418 Mg/m^3	
Absorption coefficient	2.911 mm^{-1}	
F(000)	216	
Crystal size	0.30 x 0.22 x 0.15 mm^3	
Theta range for data collection	3.22 to 67.09°.	
Index ranges	-7<=h<=7, -6<=k<=5, -15<=l<=16	
Reflections collected	3037	
Independent reflections	1305 [R(int) = 0.1504]	
Completeness to theta = 67.09°	94.2 %	
Absorption correction	Semi-empirical from equivalents	
Max. and min. transmission	0.6693 and 0.4755	
Refinement method	Full-matrix least-squares on F^2	
Data / restraints / parameters	1305 / 1 / 121	
Goodness-of-fit on F^2	1.045	
Final R indices [I>2sigma(I)]	R1 = 0.0585, wR2 = 0.1277	
R indices (all data)	R1 = 0.1340, wR2 = 0.1769	
Absolute structure parameter	0.05(5)	
Extinction coefficient	0.019(4)	
Largest diff. peak and hole	0.672 and -0.687 $e.Å^{-3}$	

Table A2-2. Atomic coordinates (x 10^4) and equivalent isotropic displacement parameters ($Å^2$x 10^3) for S256s. U(eq) is defined as one third of the trace of the orthogonalized U^{ij} tensor.

	x	y	z	U(eq)
S(1)	5162(3)	9518(2)	3705(1)	34(1)
N(1)	1895(9)	7134(9)	3019(4)	33(1)
O(1)	3829(9)	11227(8)	4266(3)	42(1)
O(2)	-1472(8)	6519(10)	2469(4)	50(1)
O(3)	2781(9)	5130(8)	1233(4)	48(1)
O(4)	2157(9)	8673(9)	490(3)	47(1)
C(1)	2306(12)	8690(11)	2196(4)	35(2)
C(2)	3760(11)	6668(11)	3637(4)	31(2)
C(3)	4474(12)	9935(11)	2415(5)	37(2)
C(4)	2413(12)	7229(13)	1264(5)	35(2)
C(5)	2483(15)	7555(16)	-450(5)	54(2)
C(6)	-62(12)	6111(13)	3097(5)	37(2)
C(7)	-424(12)	4476(18)	3938(6)	52(2)

Table A2-3. Bond lengths [Å] and angles [°] for S256s.

S(1)-O(1)	1.501(5)	C(4)-C(1)-C(3)	109.8(5)
S(1)-C(2)	1.819(6)	N(1)-C(1)-H(1)	109.8
S(1)-C(3)	1.823(7)	C(4)-C(1)-H(1)	109.8
N(1)-C(6)	1.362(9)	C(3)-C(1)-H(1)	109.8
N(1)-C(2)	1.442(9)	N(1)-C(2)-S(1)	104.6(4)
N(1)-C(1)	1.456(8)	N(1)-C(2)-H(2A)	110.8
O(2)-C(6)	1.233(9)	S(1)-C(2)-H(2A)	110.8
O(3)-C(4)	1.195(9)	N(1)-C(2)-H(2B)	110.8
O(4)-C(4)	1.340(8)	S(1)-C(2)-H(2B)	110.8
O(4)-C(5)	1.455(8)	H(2A)-C(2)-H(2B)	108.9
C(1)-C(4)	1.522(9)	C(1)-C(3)-S(1)	107.8(4)
C(1)-C(3)	1.546(10)	C(1)-C(3)-H(3A)	110.1
C(1)-H(1)	1.0000	S(1)-C(3)-H(3A)	110.1
C(2)-H(2A)	0.9900	C(1)-C(3)-H(3B)	110.1
C(2)-H(2B)	0.9900	S(1)-C(3)-H(3B)	110.1
C(3)-H(3A)	0.9900	H(3A)-C(3)-H(3B)	108.5
C(3)-H(3B)	0.9900	O(3)-C(4)-O(4)	125.3(6)
C(5)-H(5A)	0.9800	O(3)-C(4)-C(1)	124.8(6)
C(5)-H(5B)	0.9800	O(4)-C(4)-C(1)	109.8(6)
C(5)-H(5C)	0.9800	O(4)-C(5)-H(5A)	109.5
C(6)-C(7)	1.497(11)	O(4)-C(5)-H(5B)	109.5
C(7)-H(7A)	0.9800	H(5A)-C(5)-H(5B)	109.5
C(7)-H(7B)	0.9800	O(4)-C(5)-H(5C)	109.5
C(7)-H(7C)	0.9800	H(5A)-C(5)-H(5C)	109.5
		H(5B)-C(5)-H(5C)	109.5
O(1)-S(1)-C(2)	107.7(3)	O(2)-C(6)-N(1)	119.5(7)
O(1)-S(1)-C(3)	107.6(3)	O(2)-C(6)-C(7)	121.8(7)
C(2)-S(1)-C(3)	88.0(3)	N(1)-C(6)-C(7)	118.6(7)
C(6)-N(1)-C(2)	126.3(6)	C(6)-C(7)-H(7A)	109.5
C(6)-N(1)-C(1)	119.8(6)	C(6)-C(7)-H(7B)	109.5
C(2)-N(1)-C(1)	113.6(5)	H(7A)-C(7)-H(7B)	109.5
C(4)-O(4)-C(5)	115.5(6)	C(6)-C(7)-H(7C)	109.5
N(1)-C(1)-C(4)	110.4(5)	H(7A)-C(7)-H(7C)	109.5
N(1)-C(1)-C(3)	107.3(5)	H(7B)-C(7)-H(7C)	109.5

Table A2-4. Anisotropic displacement parameters ($Å^2 x\ 10^3$)for S256s. The anisotropic displacement factor exponent takes the form: $-2\pi^2[\ h^2 a^{*2} U^{11} + ... + 2\ h\ k\ a^*\ b^*\ U^{12}\ ]$

	U^{11}	U^{22}	U^{33}	U^{23}	U^{13}	U^{12}
S(1)	42(1)	27(1)	32(1)	-1(1)	1(1)	-3(1)
N(1)	25(3)	43(3)	29(3)	5(2)	-5(3)	-3(3)
O(1)	63(4)	30(2)	35(3)	-6(2)	11(3)	9(2)
O(2)	33(3)	71(4)	46(3)	-7(3)	-2(3)	2(3)
O(3)	56(3)	42(3)	44(3)	-5(2)	2(3)	7(3)
O(4)	57(3)	56(3)	28(2)	2(2)	5(2)	9(3)
C(1)	45(5)	41(4)	21(3)	2(2)	3(3)	8(3)
C(2)	30(4)	33(3)	30(3)	9(3)	-6(3)	-9(3)
C(3)	49(4)	31(3)	31(3)	4(3)	6(3)	-4(3)
C(4)	36(4)	43(4)	27(3)	5(3)	3(3)	2(3)
C(5)	56(6)	80(6)	26(4)	-5(4)	2(4)	0(5)
C(6)	32(4)	45(4)	35(4)	-10(3)	1(4)	7(3)
C(7)	46(4)	48(4)	63(5)	4(5)	21(4)	-3(5)

Table A2-5. Hydrogen coordinates (x 10^4) and isotropic displacement parameters ($Å^2$x 10^3) for S256s.

	x	y	z	U(eq)
H(1)	1152	9920	2124	42
H(2A)	4661	5416	3350	37
H(2B)	3349	6140	4291	37
H(3A)	4366	11664	2261	44
H(3B)	5587	9221	2013	44
H(5A)	3993	7144	-501	81
H(5B)	2057	8672	-972	81
H(5C)	1617	6097	-508	81
H(7A)	-1857	3783	3871	77
H(7B)	-291	5386	4547	77
H(7C)	640	3190	3947	77

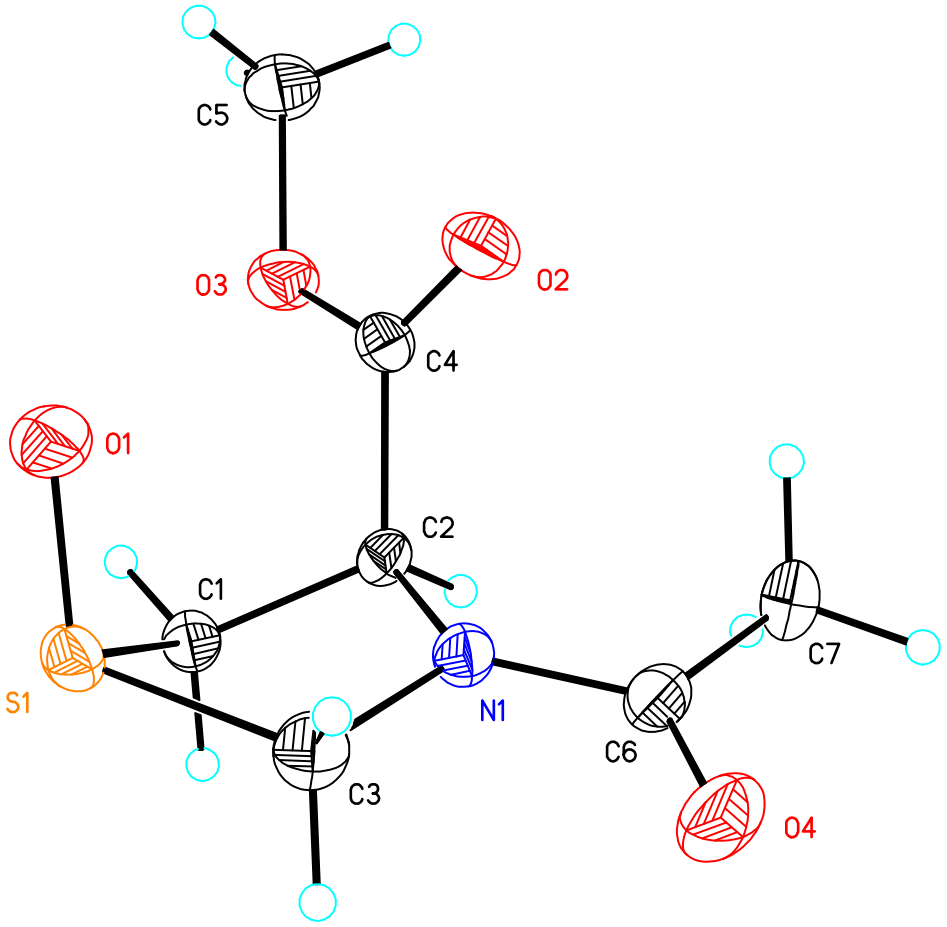

Figure 3. X-Ray crystal structure of N-Acetyl-4(S)-oxide-Thiazolidine-(R)-Carboxylic Acid Methyl Ester (cis/ minor product)

Table A3-1. Crystal data and structure refinement for S284s.

Identification code	s284s	
Empirical formula	C7 H11 N O4 S	
Formula weight	205.23	
Temperature	173(2) K	
Wavelength	0.71073 Å	
Crystal system	Monoclinic	
Space group	P2(1)	
Unit cell dimensions	a = 6.7924(10) Å	α= 90°.
	b = 6.1910(10) Å	β= 90.640(3)°.
	c = 10.5527(16) Å	γ = 90°.
Volume	443.73(12) $Å^3$	
Z	2	
Density (calculated)	1.536 Mg/m^3	
Absorption coefficient	0.347 mm^{-1}	
F(000)	216	
Crystal size	0.29 x 0.11 x 0.10 mm^3	
Theta range for data collection	1.93 to 28.40°.	
Index ranges	-9<=h<=9, -8<=k<=8, -14<=l<=14	
Reflections collected	6573	
Independent reflections	2184 [R(int) = 0.0345]	
Completeness to theta = 28.40°	99.6 %	
Absorption correction	Semi-empirical from equivalents	
Max. and min. transmission	0.9662 and 0.9062	
Refinement method	Full-matrix least-squares on F^2	
Data / restraints / parameters	2184 / 1 / 120	
Goodness-of-fit on F^2	1.043	
Final R indices [I>2sigma(I)]	R1 = 0.0384, wR2 = 0.0945	
R indices (all data)	R1 = 0.0404, wR2 = 0.0957	
Absolute structure parameter	0.04(8)	
Largest diff. peak and hole	0.442 and -0.211 $e.Å^{-3}$	

Table A3-2. Atomic coordinates (x 10^4) and equivalent isotropic displacement parameters ($Å^2$x 10^3) for S284s. U(eq) is defined as one third of the trace of the orthogonalized U^{ij} tensor.

	x	y	z	U(eq)
C(1)	10440(3)	4758(4)	2825(2)	20(1)
C(2)	8582(3)	5248(3)	2061(2)	17(1)
C(3)	10014(3)	8742(4)	2612(2)	26(1)
C(4)	6668(3)	4649(4)	2736(2)	19(1)
C(6)	7983(3)	8522(4)	722(2)	23(1)
C(7)	6626(3)	7217(4)	-114(2)	30(1)
N(1)	8700(2)	7540(3)	1773(2)	19(1)
O(1)	8897(2)	6828(3)	4731(1)	30(1)
O(2)	5212(2)	5731(3)	2746(2)	28(1)
O(3)	6834(2)	2661(3)	3210(2)	27(1)
O(4)	8402(3)	10409(3)	486(2)	36(1)
S(1)	10669(1)	6984(1)	3908(1)	22(1)
C(5)	5095(3)	1736(5)	3782(2)	34(1)

Table A3-3. Bond lengths [Å] and angles [°] for S284s.

C(1)-C(2)	1.521(3)	N(1)-C(2)-H(2)	108.4
C(1)-S(1)	1.797(2)	C(1)-C(2)-H(2)	108.4
C(1)-H(1A)	0.9900	C(4)-C(2)-H(2)	108.4
C(1)-H(1B)	0.9900	N(1)-C(3)-S(1)	107.34(16)
C(2)-N(1)	1.454(3)	N(1)-C(3)-H(3A)	110.2
C(2)-C(4)	1.535(2)	S(1)-C(3)-H(3A)	110.2
C(2)-H(2)	1.0000	N(1)-C(3)-H(3B)	110.2
C(3)-N(1)	1.455(3)	S(1)-C(3)-H(3B)	110.2
C(3)-S(1)	1.800(2)	H(3A)-C(3)-H(3B)	108.5
C(3)-H(3A)	0.9900	O(2)-C(4)-O(3)	125.54(19)
C(3)-H(3B)	0.9900	O(2)-C(4)-C(2)	125.0(2)
C(4)-O(2)	1.194(3)	O(3)-C(4)-C(2)	109.19(17)
C(4)-O(3)	1.333(3)	O(4)-C(6)-N(1)	120.8(2)
C(6)-O(4)	1.228(3)	O(4)-C(6)-C(7)	122.2(2)
C(6)-N(1)	1.351(3)	N(1)-C(6)-C(7)	116.90(19)
C(6)-C(7)	1.505(3)	C(6)-C(7)-H(7A)	109.5
C(7)-H(7A)	0.9800	C(6)-C(7)-H(7B)	109.5
C(7)-H(7B)	0.9800	H(7A)-C(7)-H(7B)	109.5
C(7)-H(7C)	0.9800	C(6)-C(7)-H(7C)	109.5
O(1)-S(1)	1.4949(14)	H(7A)-C(7)-H(7C)	109.5
O(3)-C(5)	1.451(2)	H(7B)-C(7)-H(7C)	109.5
C(5)-H(5A)	0.9800	C(6)-N(1)-C(2)	126.21(18)
C(5)-H(5B)	0.9800	C(6)-N(1)-C(3)	118.85(18)
C(5)-H(5C)	0.9800	C(2)-N(1)-C(3)	114.02(17)
		C(4)-O(3)-C(5)	117.07(17)
C(2)-C(1)-S(1)	104.45(14)	O(1)-S(1)-C(1)	104.79(9)
C(2)-C(1)-H(1A)	110.9	O(1)-S(1)-C(3)	106.66(11)
S(1)-C(1)-H(1A)	110.9	C(1)-S(1)-C(3)	87.79(11)
C(2)-C(1)-H(1B)	110.9	O(3)-C(5)-H(5A)	109.5
S(1)-C(1)-H(1B)	110.9	O(3)-C(5)-H(5B)	109.5
H(1A)-C(1)-H(1B)	108.9	H(5A)-C(5)-H(5B)	109.5
N(1)-C(2)-C(1)	104.97(16)	O(3)-C(5)-H(5C)	109.5
N(1)-C(2)-C(4)	112.44(16)	H(5A)-C(5)-H(5C)	109.5
C(1)-C(2)-C(4)	114.04(16)	H(5B)-C(5)-H(5C)	109.5

Table A3-4. Anisotropic displacement parameters ($Å^2 x\ 10^3$)for S284s. The anisotropic displacement factor exponent takes the form: $-2\pi^2[\ h^2 a^{*2} U^{11} + ... + 2\ h\ k\ a^*\ b^*\ U^{12}\ ]$

	U^{11}	U^{22}	U^{33}	U^{23}	U^{13}	U^{12}
C(1)	19(1)	22(1)	18(1)	-2(1)	0(1)	2(1)
C(2)	19(1)	19(1)	14(1)	0(1)	1(1)	0(1)
C(3)	31(1)	20(1)	28(1)	2(1)	-3(1)	-5(1)
C(4)	18(1)	21(1)	18(1)	-3(1)	-2(1)	-5(1)
C(6)	24(1)	25(1)	22(1)	5(1)	4(1)	4(1)
C(7)	32(1)	36(1)	23(1)	7(1)	-5(1)	2(1)
N(1)	21(1)	18(1)	20(1)	2(1)	-2(1)	-2(1)
O(1)	27(1)	40(1)	22(1)	-7(1)	5(1)	-3(1)
O(2)	20(1)	31(1)	35(1)	3(1)	1(1)	1(1)
O(3)	23(1)	25(1)	32(1)	7(1)	2(1)	-4(1)
O(4)	44(1)	28(1)	38(1)	13(1)	3(1)	0(1)
S(1)	19(1)	28(1)	20(1)	-4(1)	-2(1)	-3(1)
C(5)	29(1)	36(2)	38(1)	13(1)	-1(1)	-13(1)

Table A3-5. Hydrogen coordinates (x 10^4) and isotropic displacement parameters ($Å^2$x 10^3) for S284s.

	x	y	z	U(eq)
H(1A)	11599	4672	2267	23
H(1B)	10309	3376	3289	23
H(2)	8636	4425	1246	20
H(3A)	9346	10051	2932	31
H(3B)	11208	9192	2152	31
H(7A)	6272	8060	-869	45
H(7B)	5431	6855	352	45
H(7C)	7290	5884	-371	45
H(5A)	4922	2349	4630	52
H(5B)	5251	166	3848	52
H(5C)	3937	2067	3255	52

Table A3-6. Torsion angles [°] for S284s.

S(1)-C(1)-C(2)-N(1)	42.90(17)
S(1)-C(1)-C(2)-C(4)	-80.60(18)
N(1)-C(2)-C(4)-O(2)	18.7(3)
C(1)-C(2)-C(4)-O(2)	138.0(2)
N(1)-C(2)-C(4)-O(3)	-166.81(17)
C(1)-C(2)-C(4)-O(3)	-47.5(2)
O(4)-C(6)-N(1)-C(2)	-169.53(19)
C(7)-C(6)-N(1)-C(2)	11.9(3)
O(4)-C(6)-N(1)-C(3)	-1.2(3)
C(7)-C(6)-N(1)-C(3)	-179.83(18)
C(1)-C(2)-N(1)-C(6)	148.12(19)
C(4)-C(2)-N(1)-C(6)	-87.4(2)
C(1)-C(2)-N(1)-C(3)	-20.7(2)
C(4)-C(2)-N(1)-C(3)	103.9(2)
S(1)-C(3)-N(1)-C(6)	179.56(15)
S(1)-C(3)-N(1)-C(2)	-10.8(2)
O(2)-C(4)-O(3)-C(5)	0.1(3)
C(2)-C(4)-O(3)-C(5)	-174.38(18)
C(2)-C(1)-S(1)-O(1)	63.91(15)
C(2)-C(1)-S(1)-C(3)	-42.74(13)
N(1)-C(3)-S(1)-O(1)	-73.63(17)
N(1)-C(3)-S(1)-C(1)	31.15(15)

Symmetry transformations used to generate equivalent atoms: